

The  
University  
Of  
Sheffield.

# **Developmental regulation of dental regeneration and morphogenesis in Fishes**

**By:**

Alexandre Pierre Thiery

A thesis submitted in partial fulfilment of the requirements for the degree of  
Doctor of Philosophy

The University of Sheffield  
Faculty of Science  
Department of Animal and Plant Sciences

Submission date  
August 2018



## Summary

The study of odontogenesis has been limited by the lack of established developmental models which regenerate their teeth continuously throughout life. Furthermore, our understanding of dental morphogenesis is primarily based on research on the mouse. Evolutionary developmental biology seeks to comparatively study natural morphological diversity in order to identify the developmental mechanisms which underpin their evolution. Throughout this thesis, I investigate the process of dental morphogenesis and successional regeneration in both cartilaginous fishes (Chondrichthyes) and bony fishes (Osteichthyes), in order to provide a more detailed picture of the evolution of odontogenesis, and a reference point for the comparative study of dental regeneration in humans.

I show that odontogenesis is widely conserved from sharks through to mammals, and that the most usual vertebrate dentitions develop from only subtle modification of the ancestral bauplan. Furthermore, the process of dental regeneration appears to be important, not only for the replacement of lost or damaged dentition, but also in the evolution of dental morphological diversification. Given that successional dental regeneration is an ancestral gnathostome characteristic, I also investigate the regulation of dental regeneration in a basal gnathostome lineage. Our *de novo* transcriptome sequencing and predictive gene regulatory network analysis reveals novel candidate markers involved in the regulation of successional dental regeneration, previously undescribed during odontogenesis. This thesis lays the groundwork for the comparative study of these novel markers in mammalian models.



## Acknowledgements

I would like to express my deepest gratitude to Dr Gareth Fraser for his support, guidance and positive outlook, throughout my entire time in higher education. He has served as not only a supervisor, but a close friend. His approach centres primarily around the development of his students, providing them with responsibility and freedom to question, whilst also affording reassurance in times of need. It has been a pleasure to be a member of his lab and I look forward to collaborating in the future.

I would also like to thank all past and present members of the Fraser lab, in particular Dr Kyle Martin and Rory Cooper. Kyle's expert knowledge has helped guide the direction of my research throughout the course of my project, whilst Rory has been a trusted friend and co-worker, generously offering his time and bolstering me during the difficult periods. This thesis is a reflection of both their professional and personal support and I am eternally grateful for their help.

Throughout my PhD, I have had the pleasure of working with a number of collaborators, to whom I owe an enormous debt. I would particularly like to thank Dr Zerina Johanson, who has selflessly dedicated her time to hosting me at the Natural History museum in London. She has supported me throughout my project and lent her expert knowledge and advice on multiple occasions.

This project would not have been accomplished without the help of a number of people in the APS department. This list is by no means exhaustive, but includes: staff of the

molecular ecology laboratory, notably my friend and lab manager Rachel Tucker; staff of the animal facility who have helped care for my study organisms; administrative staff who have willingly fulfilled many last minute requests; and academic staff, notably Jon Slate for his professional guidance and advice. I would also like to thank my funding body, NERC, without whom this work would not have been possible, and my committee members, Abigail Tucker and Keith Hunter, who have given their time to reading and examining my work.

Finally, I would like to thank friends and family, who have supported me tirelessly without complaint. The help and support that they have provided is not limited to the last four years, and therefore this thesis is equally theirs as it is my own. Special thanks to my mother, who instilled within me a thirst for knowledge and the freedom to question without restriction from a young age. Lastly, my fiancée Harriet, for her positive outlook on life, her unconditional love and support, and her endless supply of delicious food.

## Statement of intellectual contribution

### *Chapter 2*

This chapter is published in PNAS (Thiery *et al.*, 2017) and is presented in the published format. Permission to include this work has been obtained from the publisher who have provided the following statement of confirmation ‘Permission is granted for your use of the material as described in your request. Please include a full citation for the original PNAS article when reusing the material. Because this material published after 2008, a copyright note is not needed. There is no charge for this material, either. Let us know if you have any questions. Sincerely, Kay McLaughlin for Diane Sullenberger, PNAS Executive Editor’. Methods have been expanded upon to provide further description of the undertaken research. The research project was designed by myself, Takanori Shono and Gareth Fraser. The data presented is a combination of my own research efforts, as well as those of Takanori Shono. I conducted CT scanning, immunohistochemistry and BrdU pulse chase experiments. Section *in situ* hybridisation was carried out by myself and Takanori Shono. Takanori Shono conducted the small molecule Notch manipulations, whole mount *in situ* hybridisation and DiI cell tracking experiments. Figures 1, 2, 3 and 5 were made by myself, whilst figure 4 was made by Takanori Shono. I wrote the manuscript. Takanori Shono and Gareth Fraser helped write sections specifically describing the results of experiments conducted by Takanori Shono. All authors edited and approved the final manuscript draft for publication.


### Chapter 3

This research was designed by myself and Gareth Fraser. Kyle Martin carried out initial tissue sub-dissections, RNA sequencing, *de novo* transcriptome assembly and k-means clustering. Cameron Howitt ran the RNEA analysis for his 3<sup>rd</sup> year undergraduate project under my supervision. All other work presented is my own, including: CT scan rendering, manual segmentation of CT scans, histology, Pearson correlation of differentially expressed RNAseq markers, GO enrichment analysis, GRN reconstruction and subsetting, *in situ* hybridisation, immunohistochemistry, phylogenetic analysis of RNAseq candidates and RNAseq fold change expression change. All of the data was analysed and presented by myself. I wrote the manuscript, with feedback provided by Gareth Fraser and Rory Cooper.


### Chapter 4

All of the work presented in this chapter is my own, apart from whole mount *in situ* hybridisations which were carried out by Rory Cooper and imaged by myself. Rory Cooper and Gareth Fraser provided feedback on the manuscript.

#### Certified approval of major contributory co-authors

Dr Takanori Shono: 

Date: 09 / 08 / 18

Dr Gareth Fraser: 

Date: 08/08/2018







# Table of Contents

## Chapter 1

<b>General introduction .....</b>	<b>15</b>
<i>Regeneration .....</i>	<i>15</i>
<i>Ectodermal appendages .....</i>	<i>18</i>
<i>Evolution of ‘true’ teeth.....</i>	<i>21</i>
<i>Dental development .....</i>	<i>24</i>
<i>Dental development in fishes .....</i>	<i>27</i>
Thesis rationale .....	29
Research summary .....	31
<i>Chapter 2 summary .....</i>	<i>31</i>
<i>Chapter 3 summary .....</i>	<i>32</i>
<i>Chapter 4 summary .....</i>	<i>33</i>

## Chapter 2

<b>Spatially restricted dental regeneration drives pufferfish beak development .....</b>	<b>35</b>
Abstract .....	35
Significance Statement.....	36
Introduction .....	37
Results.....	40
<i>Source of epithelial dental progenitors in intraosseous pufferfish dental regeneration</i>	<i>43</i>
<i>Canonical Wnt signalling active in dental progenitors .....</i>	<i>48</i>
<i>Initiation of dental regeneration appears conserved during the development of the pufferfish beak .....</i>	<i>50</i>
<i>Restriction in dental replacement takes place between first and second dental generations .....</i>	<i>53</i>
<i>Inhibition of the Notch signalling pathway leads to stunted growth of the elongated banded dentition .....</i>	<i>56</i>
Discussion .....	60
Materials and methods .....	65
<i>Animals .....</i>	<i>65</i>
<i>CT scanning .....</i>	<i>66</i>
<i>Histology and clearing and staining .....</i>	<i>66</i>
<i>Lineage tracing (DiI).....</i>	<i>67</i>

<i>cDNA and riboprobes</i> .....	67
<i>Forward and reverse primer sequences</i> .....	68
<i>Immunohistochemistry</i> .....	69
<i>Section in situ hybridisation</i> .....	71
<i>Whole-mount in situ hybridisation</i> .....	72
<i>Treatment with small molecules</i> .....	72
Acknowledgments .....	73
Supplementary information .....	74

## Chapter 3

### **Small spotted catshark *de novo* transcriptome assembly reveals novel markers of successional dental regeneration .....**

Abstract.....	75
Introduction .....	76
Results .....	80
<i>Histological and morphological analysis of the catshark dentition</i> .....	80
<i>RNAseq analysis of dental sub-regions</i> .....	83
<i>RNEA predicted Gene Regulatory Networks during dental initiation</i> .....	86
<i>Sub-setting GRNs based on prior knowledge of gene interactions</i> .....	88
<i>Gene Ontology (GO) enrichment analysis</i> .....	92
<i>Expression of predictive SL GRN markers</i> .....	92
<i>Expression of SL markers in conjunction with Sox2</i> .....	95
Discussion.....	99
<i>Conclusion</i> .....	102
Materials and Methods .....	103
<i>Animal husbandry</i> .....	103
<i>Paraffin sectioning and histology</i> .....	103
<i>Micro-computed tomography (MicroCT)</i> .....	104
<i>RNAseq and differential expression analysis</i> .....	104
<i>RNEA analysis</i> .....	105
<i>GO enrichment analysis</i> .....	106
<i>RNAseq sequence of interest identity check</i> .....	106
<i>Probe synthesis</i> .....	107
<i>In situ hybridisation</i> .....	107
<i>Double in situ hybridisation/immunohistochemistry</i> .....	108

Supplementary information .....	110
---------------------------------	-----

## Chapter 4

### **Conservation of enamel knot signalling in sharks supports homology of the dental signalling centre ..... 117**

Abstract .....	117
Introduction .....	118
Results .....	122
<i>Histological and morphological analysis of the catshark dentition</i> .....	122
<i>In situ hybridisation of key markers within the developing tooth</i> .....	125
<i>Whole mount in situ hybridisation in first generation teeth</i> .....	132
<i>RT-qPCR following canonical Wnt manipulation</i> .....	136
<i>Geometric morphometric analysis of tooth shape and size following Wnt treatment</i> ..	139
<i>In silico modelling of tooth shape following Wnt manipulation</i> .....	147
Discussion .....	150
<i>Catsharks possess an enamel knot-like signalling centre</i> .....	150
<i>Canonical Wnt signalling as a regulator of natural shark dental variation</i> .....	153
<i>Conclusion</i> .....	156
Methods.....	156
<i>Animal husbandry</i> .....	157
<i>Sectioning and Histology</i> .....	157
<i>Scanning Electron Microscopy (SEM)</i> .....	157
<i>Probe synthesis</i> .....	157
<i>Double in situ hybridisation/immunohistochemistry</i> .....	159
<i>Whole mount in situ hybridisation</i> .....	160
<i>Small molecule treatment</i> .....	160
<i>RT-qPCR</i> .....	161
<i>Geometric morphometric analysis</i> .....	162
<i>ToothMaker modelling of catshark dentition</i> .....	163
Supplementary information .....	165

## Chapter 5

### **General Discussion..... 173**

<i>Research summary</i> .....	173
<i>The bigger picture</i> .....	176

<i>Future project directions</i> .....	181
<i>Limitations</i> .....	183
<i>Conclusion</i> .....	184
<b>Appendix</b> .....	<b>185</b>
Abbreviations .....	185
Solutions .....	187
<b>References</b> .....	<b>189</b>

# Chapter 1

## General introduction

### *Regeneration*

Regeneration is a term widely used in developmental biology, referring to a whole suite of developmental processes through which tissues are renewed, repaired or replaced (Fig 1). It can be used to describe: the repair of single cells (i.e. axon regrowth (Cheng *et al.*, 1996)); tissue repair via cellular proliferation (i.e. epidermal regrowth (Cotsarelis *et al.*, 1999)); whole organ regeneration (i.e. limb regeneration in salamanders (Brockes and Kumar, 2005)); and whole body plan restoration (i.e. planaria fragmentation and subsequent regeneration (Pearson and Alvarado, 2008)). The definition of regeneration is therefore context dependent and inevitably encompasses numerous idiosyncrasies (Tsonis, 2000). In order to avoid ambiguity, I refer to regeneration in the context of *de novo* organ re-development.

Regeneration is widespread throughout the animal kingdom (Bely and Nyberg, 2010). Whole body regeneration occurs in basal protostomes, including the Placozoa, Prolifera and Cnidaria, as well as in early diverging deuterostomes and basal chordates, including the cephalochordates and hemichordates (Bely and Nyberg, 2010). There is extensive variation in regenerative potential, with loss of regeneration observed in several animal lineages (Bely, 2010).

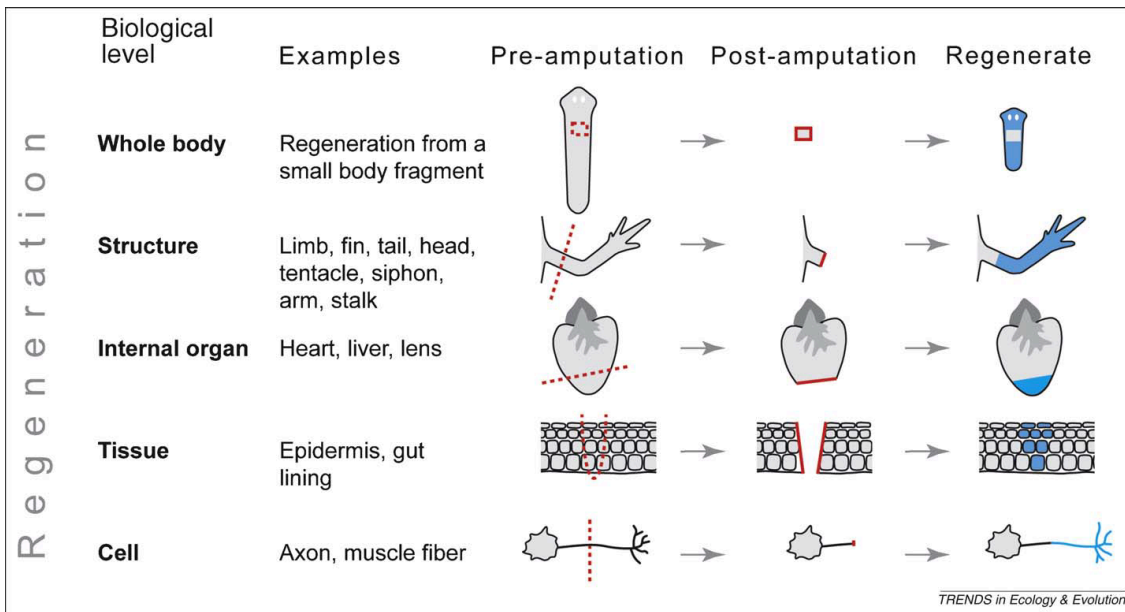


**Figure 1.** Different levels of vertebrate regeneration following tissue damage. A single species may be able to regenerate at multiple different levels. Figure taken from Bely and Nyberg (2010).

Human fascination with regeneration stems back centuries (Dinsmore, 1991) and can be in part attributed to our own lack of regenerative potential (Bely, 2010). As a result, the study of vertebrate regeneration has received research attention due to the potential for clinical application (Mao and Mooney, 2015). However, much of our understanding of development stems from research on chick and mice, which exhibit low levels of regeneration relative to other vertebrate groups (Bely and Nyberg, 2010; Vivien *et al.*, 2016). In order to understand the fundamental requirements for regeneration to take place, it is imperative to study a diverse range of animal models. The study of evolutionary developmental biology (evo-devo) seeks to understand how developmental processes have been modified over evolutionary time, through the comparative study of organismal development. By placing our understanding of animal regeneration into an



evolutionary context, evo-devo is ideally placed to investigate how regenerative potential has been lost.

Tissue regeneration requires a source of stem cells. Stem cells are defined by their ability to both self-renew and differentiate into multiple cell types (Ratajczak *et al.*, 2012). During organ regeneration, one of the ways in which stem cells are recruited is through cell dedifferentiation (Tsonis, 2000). Urodeles exhibit the extraordinary ability to regenerate entirely patterned limbs following amputation. Mesenchymal cells at the site of injury dedifferentiate and form a blastema; these cells then redifferentiate, reforming a limb composed of all associated cell types (Stocum, 1984). In other tissues, stem cells are set aside early in development, forming a defined stem cell niche: an isolated microenvironment whereby stem cells are regulated and maintained (Greco and Guo, 2010). Either in response to injury, or at specific periods in time, activated stem cells give rise to progenitors which then differentiate into the cell types of the given organ (Ohe *et al.*, 2015).

Stem cell niches have been identified in a variety of ectodermal appendages, including: the hair follicle (Cotsarelis *et al.*, 1990); the intestinal crypt (Cheng and Leblond, 1974); the sebaceous gland (Ohe *et al.*, 2015); and the cervical loop of the mouse incisor (Juuri *et al.*, 2012). Two types of stem cells have been identified within epithelial stem cell niches required for ectodermal appendage regeneration. These are slow cycling stem cells, which act as a long term store of regenerative potential and rapid cycling short term stem cells (Greco *et al.*, 2009; Greco and Guo, 2010; Ohe *et al.*, 2015).

## *Ectodermal appendages*

In vertebrates, a range of specialised structures develop from the ectoderm, including hair, feathers, scales, teeth, intestinal villi and sebaceous glands (Pispa and Thesleff, 2003). There is a high degree of similarity during the development of ectodermal appendages. The first histological sign is the formation of an epithelial placode: an epithelial thickening with an associated mesenchymal condensation (Fig 2). The epithelial component is derived from the ectoderm, whereas the mesenchyme is derived from either the neural crest or mesoderm (Pispa and Thesleff, 2003). However, although termed ectodermal, in specific cases these appendages can also form from endodermal epithelium, for example in the formation of the pharyngeal teeth in the Mexican axolotl (Soukup *et al.*, 2008). Reciprocal epithelial-mesenchymal signalling within the placode regulates ectodermal organogenesis from the initial placode stage through to late morphogenesis (Thesleff *et al.*, 1995).

Despite this developmental similarity observed between different ectodermal appendages, there has been debate over their evolutionary relationship (Maderson, 1972; Wu *et al.*, 2004; Musser *et al.*, 2015). Both hair and feathers develop from an invagination of the epithelium, exhibit regenerative cycling of their respective follicles and share extensive similarities in their molecular development (Lin *et al.*, 2006, 2013; Yang and Cotsarelis, 2010); these features are indicative of an ancestral relationship. However, neither feathers nor hair were present in the ancestor of birds and mammals. Reptilian scales were previously thought to develop in the absence of an epithelial placode, supporting the theory that feathers, hair and scales evolved independently from

one another (Dhouailly, 2009). However, research has since revealed anatomical placodes in multiple reptilian lineages, suggesting a shared ancestral homology between amniotic integumentary appendages (Di-Poï and Milinkovitch, 2016). More recent findings have also provided evidence for an anatomical placode in chonrichthyan dermal denticles, as well as conservation of the underlying gene regulatory network regulating the onset of placode development. This reveals deep homology between vertebrate ectodermal appendages dating back 450 million years (Cooper *et al.*, 2017).

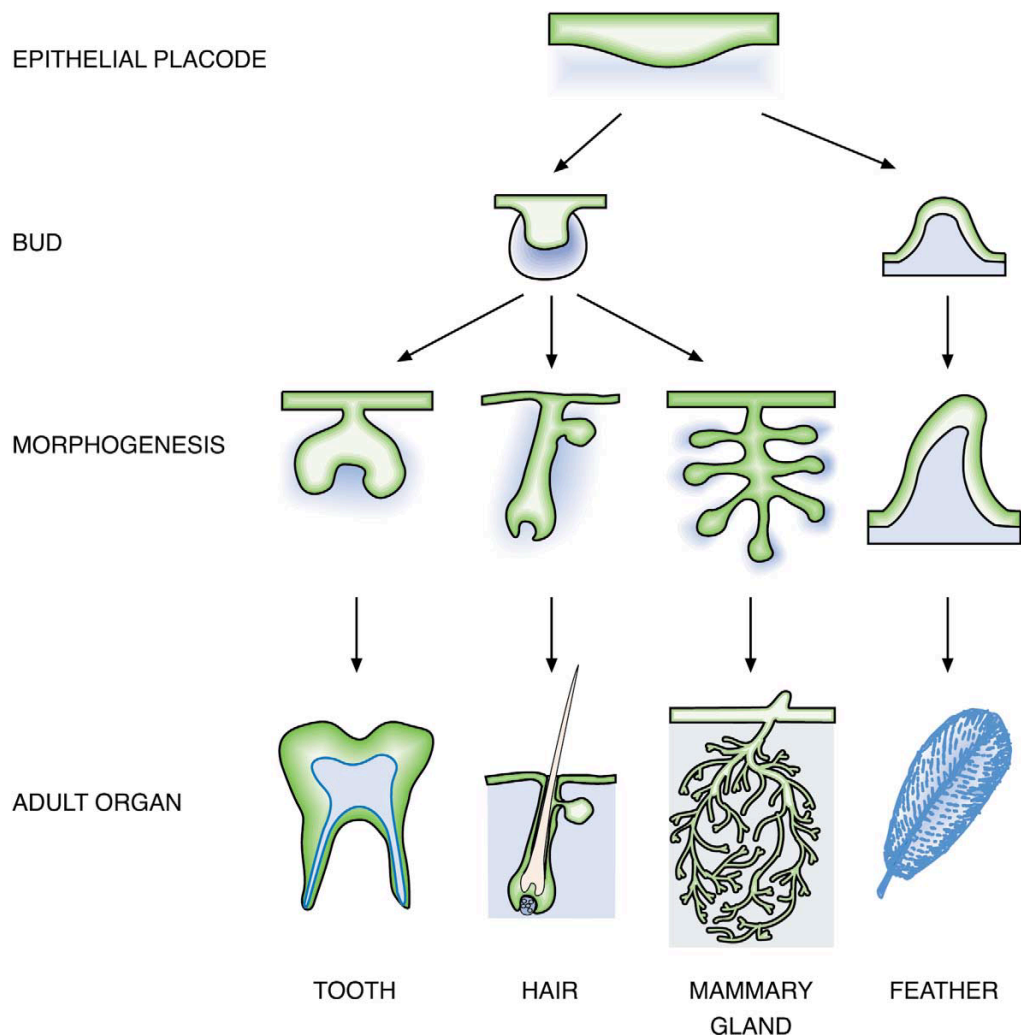


**Figure 1. Schematic representation of vertebrate ectodermal organ development.** This figure illustrates how morphologically disparate organs develop through the formation of a conserved ancestral placode. Figure taken from Pispa and Thesleff (2003).

Despite this shared common ancestry, various lineage specific modifications have taken place leading to divergence of appendage type and regenerative potential. A number of examples illustrate this diversity in regeneration. The intestinal epithelium is replaced every five days (Haegerbarth and Clevers, 2009), enabled by the presence of slow cycling *Bmi1*<sup>+</sup> and fast cycling *Lgr5*<sup>+</sup> stem cells at the crypt of each intestinal villi (Barker *et al.*, 2007; Greco and Guo, 2010), as is the case during regeneration of the acral sweat gland (Fig 3) (Ohe *et al.*, 2015). Hair and feathers both undergo cyclical regeneration, whereby each follicle exhibits distinct periods of growth, followed by regression (hair) or moulting (feathers), and rest phase (Yang and Cotsarelis, 2010; Lin *et al.*, 2013). Periodically, stem cells located at the hair and feather bulge (although not anatomically equivalent) are activated, resulting in regeneration of the follicle (Yue *et al.*, 2005; Yang and Cotsarelis, 2010). Regeneration of the vertebrate dentition varies dramatically dependent upon the lineage in question (Tucker and Fraser, 2014). Finally, scales and dermal denticles do not cyclically regenerate one for one, although *de novo* structures are formed following wounding (Reif, 1978; Wu *et al.*, 2014).

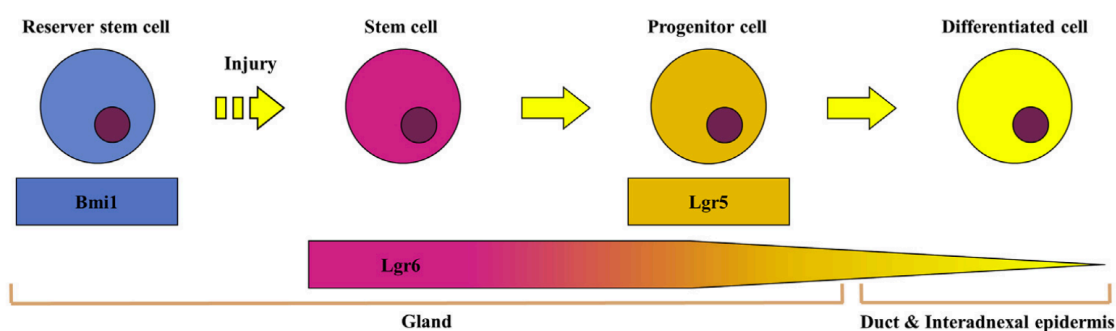


**Figure 3. Illustration of stem cell activation during regeneration of the acral epidermis.** Schematic reveals two distinct stem cell types, identifiable by their expression of *Bmi1* or *Lgr6*. Figure taken from Ohe *et al.* (2015).

### *Evolution of 'true' teeth*

With the exception of birds, which have secondarily lost the ability to form teeth, teeth are found in all major vertebrate lineages. Tooth-like structures composed of a dentine pulp and an enamel or enameloid cap are termed odontodes. They are found both within the oro-pharyngeal cavity (teeth) and on the skin surface (denticles) of extant basal gnathostomes (Reif, 1980; Donoghue and Rücklin, 2016); these differ from the keratinous teeth observed in extant jawless vertebrates (Lethbridge and Potter, 1981; Donoghue and Rücklin, 2016).

The evolution of teeth and denticles has been subject to lively debate, in part fuelled by contrasting fossil evidence (Fraser *et al.*, 2010). Extinct jawless vertebrate fossils have revealed: (1) the presence of oro-pharyngeal odontodes but the absence of dermal denticles in conodonts (the general consensus amongst palaeontologists is that conodonts are vertebrates (Sansom *et al.*, 1992; Donoghue and Sansom, 2002; Murdock *et al.*, 2013), although there remains some controversy (Turner *et al.*, 2010)); (2) the presence of dermal denticles but the absence of oro-pharyngeal odontodes in the ostracoderms; and (3) the presence of both denticle ornamentation and tooth-like whorls in thelodonts (Fig 4) (Purnell, 1995; Smith and Coates, 1998; Donoghue and Sansom, 2002; Fraser *et al.*, 2010). These fossils have driven opposing hypotheses for the evolution of odontodes: the 'outside-in' and 'inside-out' hypotheses, termed based on the predicted directional movement of odontodes between the external dermis and the internal oro-pharyngeal cavity over evolutionary time (Fraser *et al.*, 2010; Donoghue and Rücklin, 2016). It is currently generally thought that odontodes are thought to have

initially evolved outside of the oral cavity, with teeth arising through co-option of the underlying odontode gene regulatory network (Fraser *et al.*, 2010; Donoghue and Rücklin, 2016; Martin *et al.*, 2016).

However, this debate may be somewhat redundant given the extensive developmental and structural similarities observed between chondrichthyan teeth and dermal denticles. These similarities illustrate, with almost certainty, a shared common ancestry between denticles and teeth (Martin *et al.*, 2016; Rasch *et al.*, 2016). The fundamental question, therefore, is not which evolved from the other, but rather, what is the basis of their divergence? Anatomical location does not sufficiently justify the classification of these odontode types. Instead, an investigation of their developmental regulation is required in order to reveal their developmental origin and their evolutionary history.

Although the developmental regulation of teeth and denticles is almost identical, there is one definitive difference between the two structures. Research in chondrichthyans, the oldest extant gnathostome lineage to possess both odontode types, has revealed that oral teeth undergo rapid successional regeneration, with multiple dental generations developing ahead of function (Martin *et al.*, 2016). In contrast, dermal denticles do not successionally regenerate (Reif, 1978, 1980). This divergence in regenerative ability defines ‘true’ teeth from dermal denticles (Martin *et al.*, 2016). Although there is lineage divergence in dental regenerative ability, life-long successional dental regeneration (polyphyodonty) is the ancestral vertebrate condition (Martin *et al.*, 2016).

Throughout vertebrate evolution, modifications to the dentition have facilitated

vertebrate niche specialisation (Van Valkenburgh, 1989; Holliday and Stepan, 2004).

Extreme dental modification is demonstrated in the beak-like dentitions of the Tetraodontidae and the Scaridae. These teleost families develop their modified

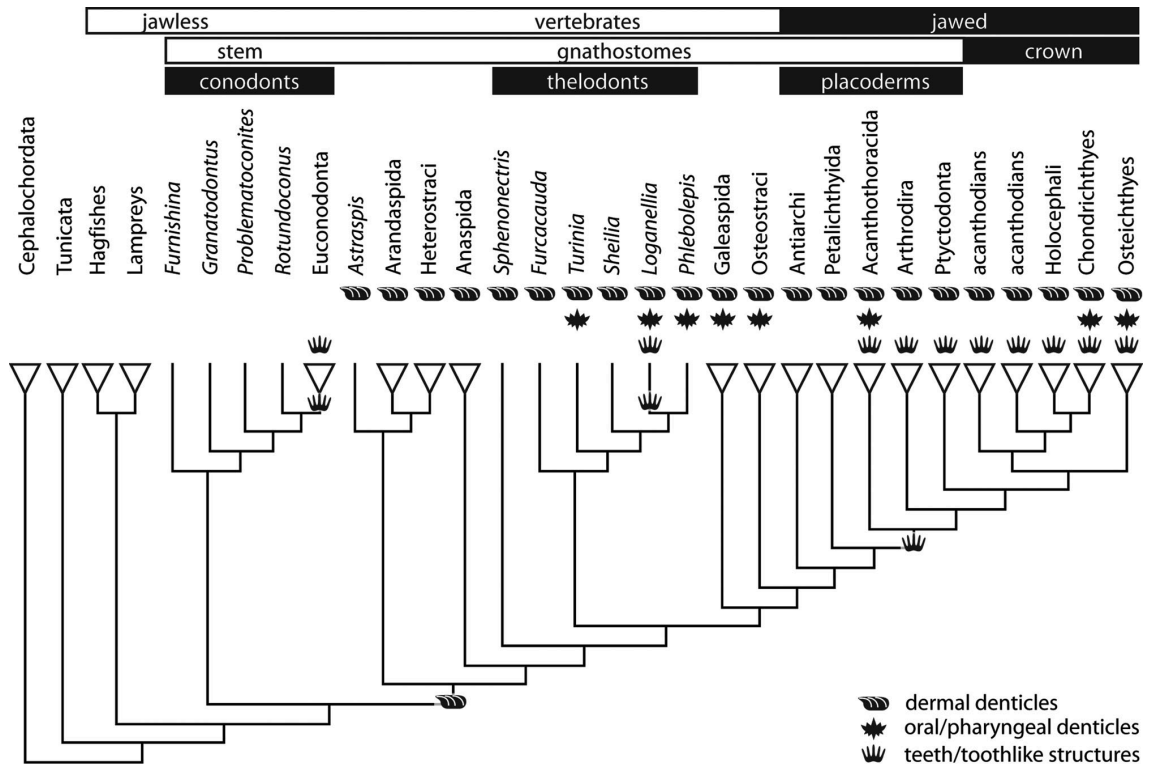


**Figure 4.** Phylogenetic tree of early diverging vertebrate lineages, revealing the presence of dermal denticles, oral/pharyngeal denticles and teeth within these groups. Figure taken from Donoghue and Rücklin (2016).

dentitions through modification of dental regeneration; they retain and fuse multiple dental generations to form hardened beak-like dentitions (Price *et al.*, 2010; Fraser *et al.*, 2012; Marcus *et al.*, 2017). Dental regenerative ability and morphological novelty appear to be intrinsically linked; the first-generation dentition of the Tetraodontidae is simplistic, with morphological specialisation appearing in the second dental generation (Fraser *et al.*, 2012). This relationship between morphological complexity and dental

regeneration is also observed in mammals, most of which have lost the ability to successively regenerate their teeth throughout life. Instead, they replace their teeth once (diphyodonty) or not at all (monophyodonty) (Juuri *et al.*, 2013). This loss of regenerative potential coincides with a change in dental shape. Mammals exhibit numerous morphologically distinct tooth families and their feeding behaviour requires the precise occlusion of the mandibular and maxillary teeth (David Polly, 2012; Jernvall and Thesleff, 2012). It is thought that this increase in morphological complexity has come at the cost of a reduction in dental regenerative potential (Fraser *et al.*, 2006).

### *Dental development*

Major developmental signalling pathways including, canonical Wnt, fibroblast growth factor (Fgf), hedgehog (Hh), bone morphogenetic protein (Bmp) and Notch, all play key roles in the regulation of odontogenesis (Thesleff and Sharpe, 1997). Researchers have dedicated significant time and resources to understanding how these pathways interact during dental initiation and morphogenesis (reviewed in: Mitsiadis *et al.*, 2005; Bei, 2009; Thesleff, 2009; Jernvall and Thesleff, 2012). The initial patterning of vertebrate teeth occurs prior to any visible changes in the oral epithelium. Early expression of Sonic Hedgehog (*shh*) and Paired-like homeodomain transcription factor 2 (*pitx2*) dictate where the teeth will form within the odontogenic band, a pattern that is highly conserved in vertebrates (Fraser *et al.*, 2004, 2008; Cobourne and Sharpe, 2010). As the epithelium thickens, a placode forms at each of the future tooth sites (Huysseune and Thesleff, 2004). The epithelium then proceeds to invaginate into the underlying mesenchyme, forming the dental lamina – an infolded region of oral epithelium from



which new dental generations develop (Buchtová *et al.*, 2008, 2012; Handrigan *et al.*, 2010; Wu *et al.*, 2013; Martin *et al.*, 2016). The degradation of this structure is thought to be responsible for the loss of dental replacement in mammals (Buchtová *et al.*, 2012).

Epithelial dental stem cells located within the vertebrate dental lamina underlie the ability for successional dental regeneration (Handrigan *et al.*, 2010; Buchtová *et al.*, 2012; Juuri *et al.*, 2013; Wu *et al.*, 2013; Martin *et al.*, 2016). Sex determining region Y-box 2 (Sox2) has been identified as the primary marker of epithelial stem cells in polyphyodonts (Gaete and Tucker, 2013; Juuri *et al.*, 2013; Martin *et al.*, 2016). Signals from within the dental epithelium and the surrounding mesenchyme regulate periodic activation of the Sox2<sup>+</sup> dental progenitors, with canonical Wnt signalling being implicated as a key regulator of this process (Gaete and Tucker, 2013; Martin *et al.*, 2016). Ectopic canonical Wnt signalling within the oral epithelium leads to the formation of supernumerary teeth and odontogenic tumours. For example, numerous supernumerary teeth develop in patients with adenomatous polyposis, a congenital disorder which results in upregulated canonical Wnt signalling via downregulation of its inhibitor APC (Wang and Fan, 2011). Furthermore, co-expression of nuclear activated  $\beta$ -catenin and Sox2 in the dental lamina has been linked to an increase in proliferation of dental progenitors in the catshark (Martin *et al.*, 2016), whilst constitutively active  $\beta$ -catenin is sufficient to upregulate dental initiation in mice (Xavier *et al.*, 2015).

Following the activation of dental progenitor cells, there is an observable increase in cell proliferation within the dental lamina (successional lamina) resulting in the formation of an epithelial placode (Handrigan *et al.*, 2010). Underlying mesenchymal

cells condense around the epithelial placode and during the subsequent ‘cap’ stage, the epithelium partly encloses the surrounding mesenchymal condensation (Fig 5) (Buchtová *et al.*, 2008; Handrigan and Richman, 2010a). This is the first sign of a ‘tooth shape’ beginning to form (Fraser *et al.*, 2013). The dental mesenchyme encapsulated within the dental epithelium is known as the dental papilla which will later give rise to the dentine secreting odontoblasts and the dental pulp of the tooth (Thesleff *et al.*, 2001).

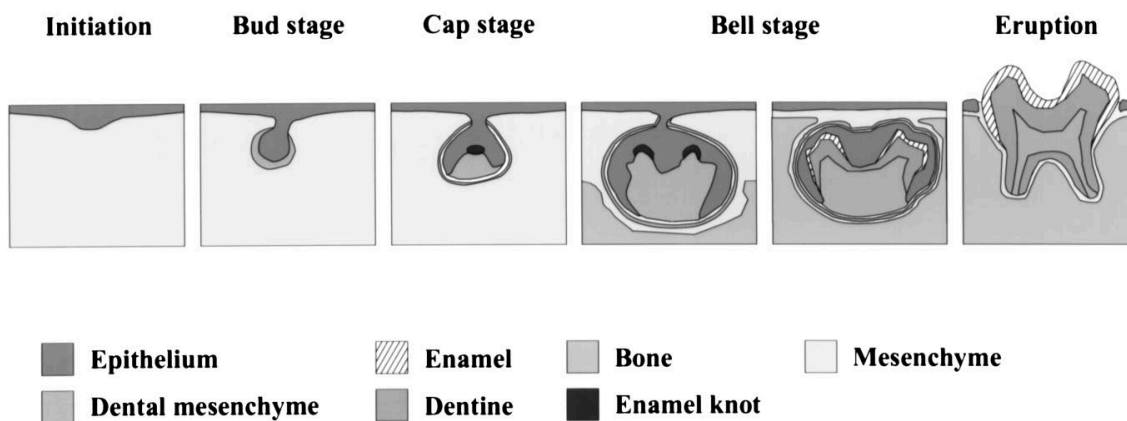


**Figure 5. Schematic representation of odontogenesis.** Dental initiation is observed as an initial epithelial thickening which then invaginated and grows during bud and cap stage. Cap and bell stages mark dental morphogenesis and matrix secretion. When the tooth has fully undergone morphogenesis it then erupts at the oral surface. Figure taken from (Thesleff and Sharpe, 1997).

The development of the dental papilla is regulated by a cluster of cells within the inner dental epithelium known as the ‘enamel knot’ (Jernvall *et al.*, 1994). This is located at the tip of the epithelial tooth bud and the future site of the primary cusp in mammals, and acts as a signalling centre during morphogenesis (Fig 5) (Jernvall *et al.*, 1994, 1998;

Vahtokari *et al.*, 1996). The enamel knot functions via regulating differential proliferation of the dental epithelium and the subsequent final tooth shape (Jernvall *et al.*, 1994; Vahtokari *et al.*, 1996). Although it is uncertain whether other vertebrates possess a defined signalling centre homologous to the enamel knot, comparable gene activation is observed within the dental epithelium in reptiles (Handrigan and Richman, 2010b; Richman and Handrigan, 2011), suggesting that this tissue plays a similar role. As development progresses through bell stage, the dental epithelium fully encloses the dental papilla, resulting in the papilla being entirely disconnected from the rest of the mesenchyme. This stage marks the terminal differentiation of the dental progenitors (Thesleff *et al.*, 2001; Tucker and Sharpe, 2004).

#### *Dental development in fishes*

Recently, we have seen an increase in the use of fish as developmental models (Schartl, 2014). Fish are highly diverse and their natural adaptations can serve as evolutionary mutant models for human disease (Albertson *et al.*, 2009; Schartl, 2014). For example, the Antarctic icefish (*Channichthyidae* sp.) which do not produce haemoglobin can be used as a model for Anaemia (Yergeau *et al.*, 2005), whilst the blind Mexican tetra (*Astyanax mexicanus*) can be used as a model for retinal degeneration (Jeffery, 2005; Albertson *et al.*, 2009). Furthermore, many fish species breed rapidly and in large numbers, whilst also exhibiting short generation times. This makes them easy and inexpensive to breed in a laboratory setting, and transgenic modification feasible on a large scale (Schartl, 2014).

Although fish constitute approximately half of all vertebrate species and possess an astonishing range of dental morphologies, relatively little dental developmental research has been conducted on fish in comparison with other vertebrate models (Fraser *et al.*, 2006, 2012). This can in part be attributed to the fact that the most widely used fish developmental model, the zebrafish (*Danio rerio*), does not develop any oral teeth (Van der heyden *et al.*, 2001).

Most fish develop a simplistic and unicuspid first generation dentition, with dental morphological complexity arising following rounds of dental regeneration (Sire *et al.*, 2002; Fraser *et al.*, 2013). As prey preference can shift throughout ontogeny, dental regeneration allows for dental shape to change accordingly (Sire *et al.*, 2002). This can be seen through the shift from a unicuspid first generation dentition, to a multicuspid replacement dentition in cichlids (Fraser *et al.*, 2013) and modified replacement beak-like dentition in pufferfish (Fraser *et al.*, 2012).

Fish also vary in their modes of dental regeneration. The cartilaginous fishes regenerate their teeth many-for-one with multiple dental generations developing ahead of function (Rasch *et al.*, 2016), whilst most teleosts replace their teeth one for one (Tucker and Fraser, 2014). Furthermore, dental regeneration takes place superficially on the oral surface in many teleost species. The cichlid and rainbow trout both exhibit a transient dental lamina which develops during the onset of dental initiation (Fraser *et al.*, 2006, 2013), whilst Sox2+ dental stem cells are found superficially on the oral surface in cichlids (Fraser *et al.*, 2013). In contrast, dental stem cells are located within a permanent deep lying dental lamina in sharks (Martin *et al.*, 2016), as is the case in

tetrapods (Tucker and Fraser, 2014).

Their dental diversity, phylogenetic position, and ease of use make fish ideal models for the study of odontogenesis in not only an evolutionary context, but also as a model for tooth loss in humans.

### **Thesis rationale**

The mouse's position as the 'go to' vertebrate developmental model has meant that our understanding of epithelial appendage regeneration has in large stemmed from research on mammalian hair and the intestinal crypt. Detailed study of the mouse has identified both the stem cells required for sustained regeneration of these structures (Cheng and Leblond, 1974; Cotsarelis *et al.*, 1990), and how these stem cells are regulated (Greco *et al.*, 2009; van der Flier *et al.*, 2009). We have also gained detailed insights into the regulation of first-generation dental initiation and morphogenesis (Jernvall *et al.*, 1998; Tucker *et al.*, 1998; Mitsiadis *et al.*, 2010), as well as the process of continuous dental growth observed in the mouse incisor (Harada *et al.*, 2002; Biehs *et al.*, 2013; Seidel *et al.*, 2017). However, the process of successional tooth regeneration is less well understood.

The next-generation sequencing revolution has opened up the possibility of using virtually any vertebrate species as a developmental model. Over the last 10 years there has been a rapid increase in the study of successional dental regeneration in non-mammalian vertebrates, including the lizard (Handrigan *et al.*, 2010), snake (Gaete and

Tucker, 2013), alligator (Wu *et al.*, 2013), teleost fish (Fraser *et al.*, 2013) and catshark (Martin *et al.*, 2016; Rasch *et al.*, 2016). Thanks to these studies, we are beginning to understand more about the processes of dental evolution, regeneration and diversification. Future whole transcriptome studies of dental progenitors in polyphyodont models will build on this research and will provide novel insight into: dental stem cell maintenance; regulation of regenerative cyclicity; and the determination of dental progenitor cell fate.

Although the fundamental process of odontogenesis is conserved throughout vertebrates, there are numerous lineage specific differences in both molecular signalling and final morphology (Fraser *et al.*, 2012). In order to make reasonable and accurate predictions through the use of comparative research, a thorough understanding of dental evolution is required. Furthermore, the choice of species included in the comparative analysis must be justified phylogenetically. The catshark (*Scyliorhinus canicula*), is phylogenetically well placed to look at the development and evolution of polyphyodonty, whilst its many-for-one conveyor belt like dentition (Reif, 1980) allows the study of how regenerative cyclicity is regulated. Detailed understanding of dental regeneration within a basal crown gnathostome lineage can be used as a reference for further study of dental regeneration in other vertebrate lineages.

This thesis aims to investigate three primary questions about the evolution of odontogenesis. 1) What is the developmental basis to dental morphological diversification? 2) How is the process of dental regeneration regulated in a basal crown gnathostome lineage? 3) How is the process of dental morphogenesis conserved?

## **Research summary**

### *Chapter 2 summary*

Given the observable diversity of vertebrate dentitions, we investigate the developmental basis of one of the most unusual dental morphologies. Tetraodontiformes are a highly derived teleost order consisting of 429 species (Yamanoue *et al.*, 2008). They are extraordinarily morphologically diverse, with species exhibiting loss of pelvic fins; reduction in the number of vertebrae; large variation in size; unusual body shapes; and highly modified dentitions (Brainerd and Patek, 1998; Tanaka *et al.*, 2005; Yamanoue *et al.*, 2008; Fraser *et al.*, 2012). The morphological novelty observed amongst the Tetraodontiformes is epitomised by the beak-like dentition of the pufferfish. Preliminary work has revealed that this dental morphology arises following a developmental shift between first and second dental generations (Fraser *et al.*, 2012). This chapter seeks to investigate how dental regeneration is regulated in pufferfish, in order to understand which key aspects of the ancestral odontogenic framework are modified during this process.

We find that the process of dental regeneration is primarily conserved during the formation of the pufferfish beak-like dentition. However, two major regulatory shifts take place. Firstly, we observe a loss of dental regeneration at all but four tooth sites. This reduction in dental regeneration occurs due to a physical barrier developing between the labial dental progenitors and the tooth forming dental cavity. We identify four insertion points through which dental progenitors can access the dental cavity and

give rise to new teeth. Secondly, a major shift in dental morphogenesis leads to the jaw-length elongation of the dental tooth bud within the dental cavity. The fusion of multiple elongated tooth generations gives rise to the final beak morphology. These modifications in dental regeneration and dental morphogenesis in a derived teleost lineage led us to question the ancestral state of dental regeneration (Chapter 3) and dental morphogenesis (Chapter 4).

### *Chapter 3 summary*

Our understanding of the developmental regulation of polyphyodonty is somewhat limited. Recent studies in a range of polyphyodont vertebrates have reaffirmed a key role for Sox2 in dental stem cells (Gaete and Tucker, 2013; Juuri *et al.*, 2013; Martin *et al.*, 2016). The conservation of Sox2 expression stems back to the early origins of true teeth (Martin *et al.*, 2016). The catshark is an emerging developmental model for several reasons: its phylogenetic position within an early diverging crown gnathostome lineage relative to tetrapods; its affordability; and its conservation status (Least Concern; IUCN (2018)). Past research has identified conservation of canonical Wnt signalling in the activation of Sox2<sup>+</sup> dental progenitors within the catshark successional lamina (Martin *et al.*, 2016). This chapter seeks to identify novel dental stem cell markers and markers expressed during the initiation of successional dental regeneration.

Following the assembly of a *de novo* transcriptome, we use predictive gene regulatory network analysis to identify novel markers of interest. This approach predicted putative interactions between novel markers differentially expressed in the successional lamina,



and genes previously known to play key roles in the dental initiation. Our results highlight the co-expression of *mycn* with Sox2 in the successional lamina. Mycn is a proto-oncogene previously implicated in the regulation of cell differentiation in neuroblastoma cells (Knoepfler *et al.*, 2002; Zhang *et al.*, 2016) but its expression pattern had not yet been described in teeth. Furthermore, GO enrichment analysis highlights canonical Wnt signalling as a gene pathway over-represented within the successional lamina, further demonstrating its role in dental initiation. This study builds on previous polyphyodont research by moving away from the candidate approach, which relies heavily on data obtained in non-polyphyodont systems.

#### *Chapter 4 summary*

The defining feature of tooth shape is the cusp. Final tooth shape is regulated by the enamel knot signalling centre, positioned at the apical tip of the primary cusp. Fgf markers are upregulated within the enamel knot, leading to rapid proliferation of the adjacent dental epithelium (Jernvall *et al.*, 1994; Vaahtokari *et al.*, 1996). Differential proliferation between the dental epithelium (within and adjacent to the enamel knot) directs downward growth, leading to the formation of a cusp (Salazar-Ciudad and Jernvall, 2010). The emergence of secondary enamel knots gives rise to further cusps (Jernvall *et al.*, 1994, 1998). Cusp number and size is variable both between and within species; mammals develop numerous tooth families, each with a distinct size and number of cusps.

The definitive presence of an enamel knot has only been described in mammals; research in other species has revealed both similarities and differences in molecular signalling relative to the mammalian enamel knot (Handrigan and Richman, 2010b; Richman and Handrigan, 2011). We investigate the expression of key markers in the catshark and reveal their expression within the non-proliferative apical tip of the dental cusp. We also describe the conservation of *fgf3* and *fgf10* expression in both primary and secondary (accessory) enamel knots. Furthermore, we manipulate canonical Wnt signalling, which has been identified as an upstream regulator of enamel knot signalling (Kratochwil *et al.*, 2002; Liu *et al.*, 2008) and observe a significant shift in tooth size, shape and cusp number. These results reveal the conservation of a non-proliferative epithelial signalling centre within an early diverging crown gnathostome lineage.

## Chapter 2

# Spatially restricted dental regeneration drives pufferfish beak development

Alexandre Thiery<sup>a1</sup>, Takanori Shono<sup>a1</sup>, Daisuke Kurokawa<sup>b</sup>, Ralf Britz<sup>c</sup>, Zerina Johanson<sup>d</sup>, and Gareth J. Fraser<sup>a2</sup>

<sup>a</sup>Department of Animal and Plant Sciences, and Bateson Centre, University of Sheffield, UK. <sup>b</sup>Misaki Marine Biological Station, University of Tokyo, Japan. <sup>c</sup>Department of Life Sciences, Natural History Museum London, UK. <sup>d</sup>Department of Earth Sciences, Natural History Museum London, UK.

1. These authors contributed equally to this work.

2. Corresponding Author: g.fraser@sheffield.ac.uk

Citation: Thiery, A. P., Shono, T., Kurokawa, D., Britz, R., Johanson, Z. and Fraser, G. J. (2017) ‘Spatially restricted dental regeneration drives pufferfish beak development’, *Proceedings of the National Academy of Sciences*, 114(22), pp. E4425–E4434.

### Abstract

Vertebrate dentitions are extraordinarily diverse both in morphology and regenerative capacity. The teleost order Tetraodontiformes exhibits an exceptional array of novel dental morphologies, epitomized by constrained ‘beak-like’ dentitions in several

families i.e. porcupinefishes, three-toothed pufferfishes, ocean sunfishes and pufferfishes. Modification of tooth replacement within these groups leads to the progressive accumulation of tooth generations, underlying the structure of their beaks. We focus on the dentition of the pufferfish (Tetraodontidae) due to its distinct dental morphology. This complex dentition develops as a result of (i) a reduction in the number of tooth positions from seven to one per quadrant during the transition from first to second tooth generations, and (ii) a dramatic shift in tooth morphogenesis following the development of the first generation teeth, leading to the elongation of dental units along the jaw. Gene expression and DiI lineage tracing reveal a putative dental epithelial progenitor niche, suggesting a highly conserved mechanism for tooth regeneration despite the development of a unique dentition. MicroCT analysis reveals restricted labial openings in the beak, through which the dental epithelium (lamina) invades the cavity of the highly mineralized beak. Reduction in the number of replacement tooth positions coincides with the development of only 4 labial openings in the pufferfish beak, restricting connection of the oral epithelium to the dental cavity. Our data suggest the spatial restriction of dental regeneration, coupled with the unique extension of the replacement dental units throughout the jaw, are primary contributors to the evolution and development of this unique beak-like dentition.

### **Significance Statement**

Teleost fishes have evolved a wonderful array of diverse dentitions. The highly derived order Tetraodontiformes exhibit the most unique dental forms among teleosts. The novel beak-like dentition of the pufferfish develops through a drastic shift in dental

morphology during ontogeny. A simple first generation tooth set is followed by the repetitive development of multiple elongated jaw-length tooth bands, which fuse together over time to form the characteristic beak. A restriction of the tooth regenerative process in all but four tooth sites, coupled with the maintenance of lifelong stem cells for perpetual tooth development is essential to the formation of this unique dentition. In pufferfish, regeneration plays a vital role in producing novel dental form, from highly conserved developmental underpinnings.

## **Introduction**

Given the known conservation of developmental signalling, morphological novelties raise important questions about their evolutionary and developmental origin (Wagner and Lynch, 2010). Vertebrate groups exhibit profound dental morphological variation, making teeth interesting models for the study of evo-devo (Jernvall and Thesleff, 2012). Dental morphology is highly specialized to diet, and prey preference can shift throughout ontogeny. The ability to regenerate and replace teeth provides the opportunity for a change in dental morphology to occur between dental generations (Sire *et al.*, 2002). This allows for niche partitioning, with different dental morphologies specialized to dietary preferences, which shift with age. Understanding the developmental basis of regeneration is therefore essential to understanding the evolution of dental morphological variation.

Our understanding of tooth development is largely based on study of the mouse, which continuously renews its incisors but is unable to produce new tooth generations

(monophyodonty) (Tucker and Fraser, 2014). In contrast, most vertebrates exhibit lifelong dental replacement (polyphyodonty) (Fraser *et al.*, 2013). Recently there has been a bid to understand such regenerative capabilities in an attempt to develop new clinical applications in humans, which lose the ability to regenerate teeth after two generations (diphyodonty) (Buchtová *et al.*, 2008; M. M. Smith *et al.*, 2009; Handrigan *et al.*, 2010; Wu *et al.*, 2013). Additionally, teeth are also useful for the evolutionary developmental study of morphological novelty; dentitions vary substantially in tooth number, shape and generation rate, yet form from a highly conserved ancestral developmental framework (Jernvall and Thesleff, 2012; Fraser *et al.*, 2013). To expand our knowledge of developmental dynamics and the evolution of novelty (evo-devo) we need to extend our research of development to new models exhibiting diverse phenotypes.

Teleosts are exceptionally diverse, reflected through the morphological variation in their dentitions (Tucker and Fraser, 2014). The extremes of dental diversity are exemplified within the teleost order Tetraodontiformes (Owen, 1840-45; Cuvier, 1805; Tyler, 1980; Andreucci *et al.*, 1982). Four families of the Tetraodontiformes (the Triodontidae (three-toothed pufferfishes), Molidae (ocean sunfishes), Diodontidae (porcupinefishes) and Tetraodontidae (four-toothed pufferfishes) have evolved a diverse set of oral phenotypes with a superficially and developmentally constrained beak-like appearance that develops through the modification of the dental regeneration mechanism (Fraser *et al.*, 2012). These diverse and unique dentitions have facilitated the occupation of a broad range of dietary niches including the acquisition of hard-shelled prey (Turingan, 1994).

The ontogenetic transition to a beaked dentition from more typical first generation teeth in pufferfishes (Fraser *et al.*, 2012) raises interesting questions regarding the regulation of tooth regeneration and the emergence of craniofacial diversity. General vertebrate dental regeneration proceeds due to the activation of epithelial dental progenitors within a dental lamina (M. M. Smith *et al.*, 2009; Juuri *et al.*, 2013; Tucker and Fraser, 2014), a region of invaginated oral epithelium where new tooth generations are initiated. In vertebrates that exhibit continuous or lifelong tooth regeneration competent dental epithelium must therefore be maintained (tissue homeostasis) in adults. Pufferfishes develop their teeth intraosseously within an encased dental cavity (Andreucci *et al.*, 1982). Given that epithelial progenitors are required for dental regeneration to take place (Tucker and Fraser, 2014) it is unclear where these cells reside in pufferfishes since the developing teeth remain separated from the oral epithelium by an osteodentine casing fused to the jaw. Here, we define tooth regeneration as the *de novo* cyclical formation of tooth units from a defined epithelial dental lamina that must be continuously maintained by a progenitor cell niche (Martin *et al.*, 2016). In this context, and for clarity, the term ‘tooth replacement’ refers to the structural formation and positional replacement of tooth units, whereas the term ‘tooth regeneration’ should refer to the developmental process by which teeth are replaced i.e. through the maintenance of a progenitor-rich epithelial dental lamina for *de novo* tooth production. Therefore, in this context, replacement is the result of regeneration.

Broadly, this study seeks to understand how novelty of form manifests in pufferfishes and the ways in which the novel dental phenotype develops over ontogenetic time. The

core questions investigated in this study are: 1) where do epithelial progenitors required for dental regeneration in the pufferfish reside; and 2) does the banded dental morphology arise from multiple sequential tooth germs coalescing early in dental regeneration, or from a single tooth germ that develops into an elongated band in each jaw quadrant, as previously hypothesized (Fraser *et al.*, 2012)? If the latter is true, this implies a loss in the number of tooth initiation sites during the transition from the first to second dental generations. Through a combination of gene/protein expression, cell lineage tracing, morphological analyses and small molecule inhibition assays, we sought to analyse the developmental basis of pufferfish tooth regeneration, and how this process might govern the ontogenetic formation of the beak-like dentition unique to pufferfishes. Here we study four species of pufferfishes due to various aspects of their husbandry and accessibility for lab-based experimentation, in addition to deciphering elements of diversity within the pufferfish clade: the freshwater Malabar or Dwarf Pufferfish (*Carinotetraodon travancoricus*); the freshwater Arrowhead pufferfish (*Pao* [previously *Monotretete*] *suvattii*); the freshwater Hairy pufferfish (*Pao baileyi*); and the marine Japanese grass pufferfish (*Takifugu niphobles*). Uncovering key developmental drivers of dental novelty within the Tetraodontidae, we shed light on how the complex novel dentition in this highly derived teleost lineage (Santini *et al.*, 2013) develops despite forming from a highly conserved odontogenic system.

## **Results**

The unusual pufferfish beak is composed of four main units, one in each jaw quadrant. Each of these is formed through the progressive accumulation of teeth, which are



continuously replaced throughout life. Instead of teeth being shed, multiple generations of teeth stack together and are embedded within a compact osteodentine mass (Britski *et al.*, 1985) (Fig 1A), together forming the highly mineralized beak (Fig 1B and C). The oldest teeth are located at the top of the dentary, whilst the newest teeth develop at its base within a continuous (jaw-length) dental cavity (Andreucci *et al.*, 1982). The dental units themselves are band-like in shape, with the teeth elongating along the length of the dental cavity from the parasymphyseal region (Fraser *et al.*, 2012). In most pufferfish species, a single tooth ‘band’ develops in each jaw quadrant, per dental generation (Fig 1A and E). These bands become connected into a single beak unit through an inter-band osteodentine mineralization (Fraser *et al.*, 2012). A further osteodentine layer encases the dentine bands in both jaws and is confluent with the beak unit of the dentary in the lower and premaxilla in the upper jaw (Andreucci *et al.*, 1982).

The generation of new teeth requires a source of epithelial progenitors (Juuri *et al.*, 2013; Martin *et al.*, 2016). In order to maintain this ability, polyphyodonts must retain a population of these cells throughout life. Epithelial dental progenitors have been localized to the dental lamina in polyphyodonts (e.g. (Handrigan and Richman, 2010a; Handrigan *et al.*, 2010; Juuri *et al.*, 2013; Wu *et al.*, 2013; Martin *et al.*, 2016), with the micro-environment maintaining these cells in an otherwise dynamic and proliferative system. Pufferfishes regenerate and replace their teeth intraosseously, within the dental cavity (Andreucci *et al.*, 1982). This region is isolated from the oral epithelium (Fig 1), yet epithelial cells within the dental cavity are a prerequisite for regeneration (Trapani, 2001). This therefore raises the question as to where dental progenitors are located in this system. There are two mechanisms that could lead to the presence of dental

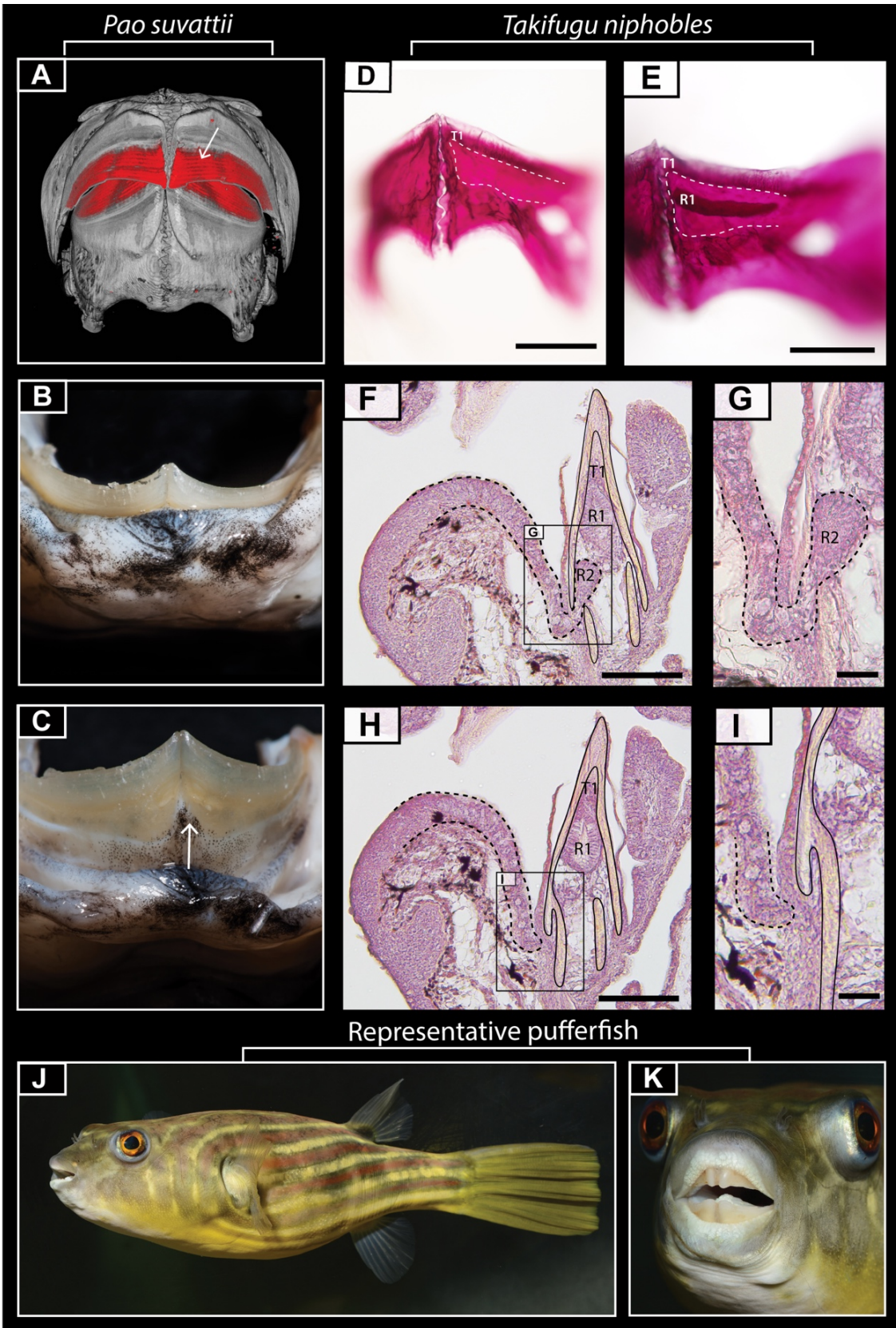


**Figure 1. Pufferfish dental morphology.** Reconstructed microCT scan of adult *P. suvattii* (A) reveals a banded dentition encased in osteodentine. Digital photos show the fleshy lip of *P. suvattii* and its attachment to the beaked dentition at the fused beak/dentary boundary (B and C). A cleft can be seen at the symphysis of the jaw, with the attachment of the labial oral epithelium to the beak following the contour of the cleft (white arrow C). Alizarin red staining of early embryonic *T. niphobles* samples reveal a single developing band in each jaw quadrant (D and E). Haematoxylin stained sagittal paraffin sections (F-H) reveal a gubernacular opening at the osteodentine/mandibular boundary in each jaw quadrant (F and G) (depicted by dotted lines in H) that is absent in serial sections of the adjacent areas (H and I). G and I are close up images of the boxed regions in F and H respectively. In the histological sections, a continuous stream of epithelium connects the oral epithelium to the regenerating teeth (R1 and 2) within the dental cavity. J and K are digital photos of *Tetraodon lineatus* showing the overall morphology of a ‘typical’ pufferfish. T1=first tooth generation; R1-2=replacement tooth generations. Scale bars: D and E 250 $\mu$ m; F and H 100 $\mu$ m; G and I 50 $\mu$ m.

epithelium in the dental cavity: 1) the preceding tooth generation provides a source of epithelial cells for newly developing teeth in a cervical loop-like fashion (as in the mouse (Harada *et al.*, 1999) although the mouse doesn’t exhibit de novo tooth generation), or 2) gaps within the beak casing enable epithelium from the externally situated dental lamina to enter the dental cavity. To understand the temporal developmental dynamics of the pufferfish replacement dentition and to determine the location of the epithelial progenitors, we investigated development of its dentition in sagittal sections.

#### *Source of epithelial dental progenitors in intraosseous pufferfish dental regeneration*

Haematoxylin staining of juvenile sagittal sections (Fig 1F-I), and reconstructed micro-CT scans of adult pufferfishes, reveal a gubernacular opening within the osteodentine

beak casing of each jaw quadrant, through which the juxtaposed labial oral epithelium connects to the dental cavity (Fig 5H-K). This suggests that a connection between the dental cavity and the oral epithelium is maintained throughout development. Proliferative cell nuclear antigen (PCNA) immunohistochemistry during second-generation tooth initiation highlights high levels of cellular proliferation within the oral epithelium (Fig 2A-C). Notably, a continuous stream of proliferative cells connects the labial oral epithelium and the developing tooth bud in the dental cavity (arrowhead in Fig 2A); this infolded labial epithelial sheet is the pufferfish dental lamina (DL in Fig 2A-C). Emerging tooth generations bud from the distal (relative to the oral surface) end of the dental lamina (Fig 2A-C). Developing teeth are then positioned orally relative to their initiation site, and continue morphogenesis inside the confines of the dental cavity (R1-R3 in Fig 2C).

The role of the dental lamina in the regeneration of teeth is well understood (Jernvall and Thesleff, 2012; Juuri *et al.*, 2013; Martin *et al.*, 2016). Sox2 (Sex determining region Y-box 2) is a transcription factor known for its role in maintaining cell pluripotency and stem cell renewal (Arnold *et al.*, 2011). It is expressed in epithelial dental progenitors in the dental lamina of all polyphyodont vertebrates (Jernvall and Thesleff, 2012; Juuri *et al.*, 2013; Tucker and Fraser, 2014; Martin *et al.*, 2016) and is thought to regulate dental progenitor cell state. Therefore, we investigated its expression during pufferfish tooth formation to determine the location of epithelial dental progenitors in pufferfishes. Sox2 immunohistochemistry assays during second-generation dental initiation in pufferfishes highlight Sox2 expression throughout the oral epithelium, and notably in the taste buds (Fig 2D). Consistent with expression

patterns described in other polyphyodonts (Fraser *et al.*, 2013; Juuri *et al.*, 2013), we note Sox2 within the pufferfish dental lamina, with strongest expression in this region proximal to the oral surface (arrowhead in Fig 2D). Double PCNA/Sox2 immunohistochemistry assays reveal expression of PCNA in the aboral dental lamina cells except where Sox2 is highly expressed (Fig 2E). These Sox2<sup>+</sup>/PCNA<sup>-</sup> cells are potentially quiescent. The continuous stream of Sox2 expression between presumptive taste bud and tooth domains (Fig 2E) suggests that teeth and taste buds in pufferfishes develop from a common early oral epithelium, as previously shown in both cichlids (Bloomquist *et al.*, 2015) and sharks (Martin *et al.*, 2016).

Sox2 alone does not confer progenitor cell identity. Therefore, we sought to identify regions of the oral epithelium containing slow cycling cells, using BrdU pulse/chase experiments in adult *C. travancoricus* (Fig 2F and G). Carrying out this experiment in adults of this species allows for the separation of rapid cellular cycling occurring during embryogenesis from that specific to lifelong cyclical dental regeneration and replacement. Following a 6-week BrdU pulse we found a high signal within the distal tip of the dental lamina (white arrowhead in Fig 2F), corresponding with the PCNA-expressing region from which we observed new teeth developing in the pufferfish embryo of *P. baileyi* (Fig 2C and E). Whilst the *C. travancoricus* samples were treated for 6 weeks, not all cells were labelled following the pulse period. This could have resulted from cells being terminally differentiated and thus non-dividing in the adult. Following an 8-week chase period, with samples left to develop in the absence of BrdU, signal was lost within the distal tip of the dental lamina (white arrowhead in Fig 2G), indicating cellular proliferation or migration out of this region. The presence of BrdU

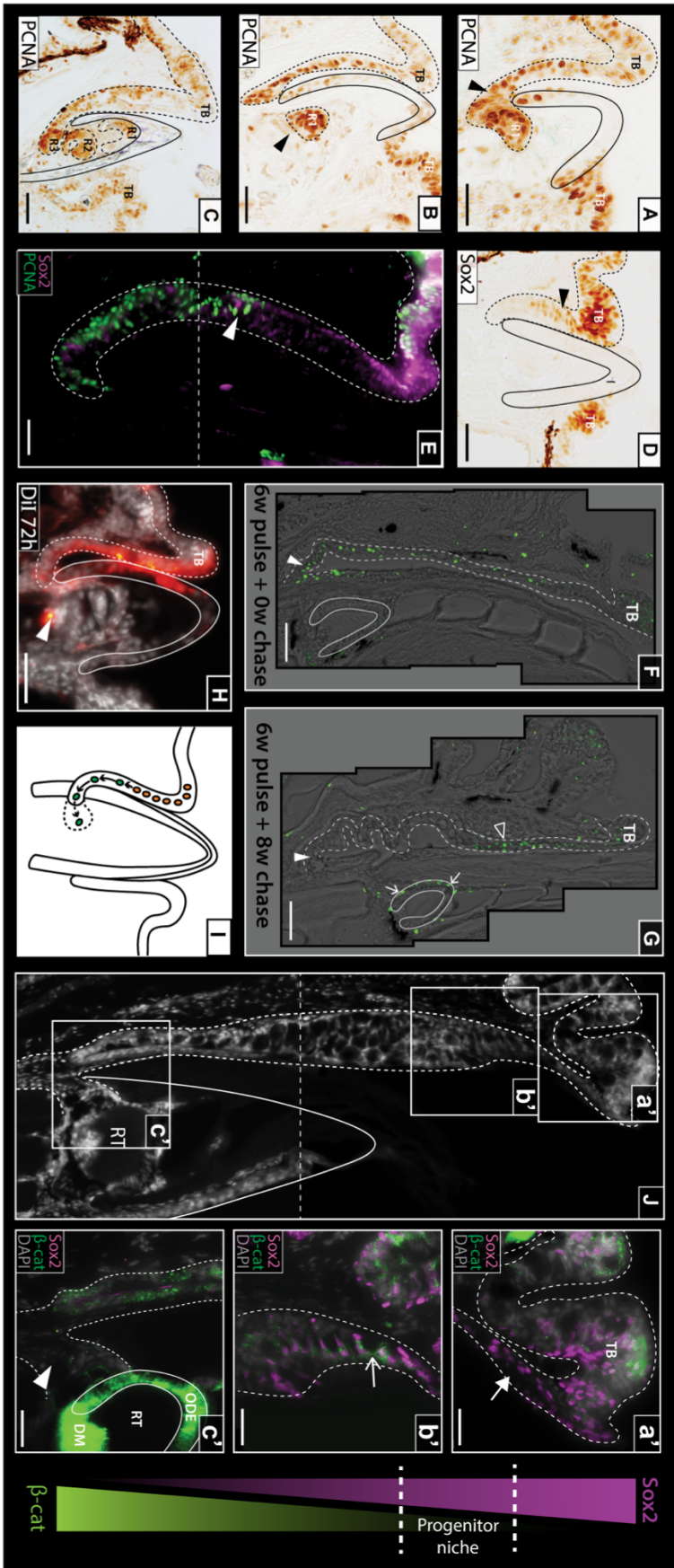


**Figure 2. Localization of a dental progenitor cell niche within the pufferfish dental lamina.**

*P. baileyi* PCNA immunohistochemistry (A-C) reveal high levels of cellular proliferation within the oral epithelium. As replacement teeth progress from late-initiation (A) to morphogenesis (C), the new tooth generation (R1) buds from the dental lamina (B). Successive rounds of replacement show the dental generations stack on one another within an enameloid outer casing (black line) (C). Sox2 immunohistochemical labelling (D) during dental replacement initiation depicts high levels of Sox2 within both the developing taste buds (TB) and the dental progenitor site located within the labial oral epithelium (dental lamina) (black arrow). Double immunofluorescence treatment for Sox2/PCNA in *T. niphobles* shows low levels of PCNA expression within the Sox2+ cells of the presumptive dental progenitor niche, cells within the aboral dental lamina exhibiting high levels of PCNA (E). Dashed line across (E) depicts image stitching of two adjacent images. BrdU pulse/chase experiments (0.2mM) show the incorporation of BrdU into dividing cells after 6-week treatment (F), with high levels of incorporation noted in the distal dental lamina next to the base of the beak (white arrowhead). After a further 8-week chase (G), label-retaining cells were found in the most superficial dental lamina cells (clear arrowhead), but not in the distal dental lamina (white arrowhead). Label retaining cells found in the dental epithelium of the developing tooth are highlighted with a white arrow. Images F and G are composites of multiple images taken at high magnification and stitched together. DiI labelling of the labial oral epithelium in *P. suvattii* highlighted this region as a presumptive source of dental progenitor cells; 72hrs post DiI treatment (H) DiI was detected within the outer dental epithelium of the tooth (white arrow). As summarized in a schematic representation (I), we observed a continuous field of Sox2+ cells between the labial taste bud and the dental progenitor site, with cells from the latter migrating and contributing to the new dental generations. Sox2/ABC double immunohistochemical labelling on adult *C. travancoricus* (J) highlights epithelial Sox2+/ABC- (a'), Sox2+/ABC+ (b') and Sox2-/ABC+ (c') regions within the dental lamina. Co-expression of these markers marks the site of activation of putative dental progenitors within the oral epithelium. Dashed line across (J) depicts image stitching of two adjacent images. Images orientated with labial to the left and oral to the top. Dotted line in all images depicts the boundary of the oral epithelium and the end of the dental lamina. TB=labial taste bud; R1-3=replacement tooth generations; RT=regenerating tooth; ODE=outer dental epithelium; DM=dental mesenchyme. Scale bars: A-E 25 $\mu$ m; F.a'-F.c' 20 $\mu$ m; G-H 50 $\mu$ m; I 15 $\mu$ m.

within the dental epithelium of the succeeding tooth generation after an 8-week chase (arrows in Fig 2G), but its absence immediately after a 6-week pulse (Fig 2F), suggests that cells from the dental lamina are contributing to the dental epithelium of the replacement dentition. Furthermore, following the chase period, there are label-retaining cells within the dental lamina region nearest the oral surface, adjacent to the first taste bud (clear arrowhead in Fig 2G). These cells are either slow-cycling or have become terminally differentiated following the incorporation of BrdU during the pulse period. Given the expression of Sox2 and lack of PCNA in the equivalent dental lamina region in the pufferfish embryo (Fig 2E), we suggest these label-retaining cells are part of a slow-cycling epithelial progenitor cell population within the dental lamina.

To establish the cellular dynamics within the dental lamina, fluorescent lipophilic dye DiI was administered to cells within the taste/dental lamina epithelium of the pufferfish prior to the initiation of dental regeneration. 72hrs following labelling, we observed DiI within the dental epithelium of the developing second-generation tooth band (Fig 2H). This result suggests that superficial taste bud/dental lamina epithelium, located labial to the beak, contribute cells for dental regeneration via migration through a gubernacular opening into the intraosseous dental cavity of the pufferfish beak (Fig 2I).

#### *Canonical Wnt signalling active in dental progenitors*

Canonical Wnt signalling is a vital and developmentally diverse set of pleiotropic molecules, performing various tissue-specific functions (Logan and Nusse, 2004). During polyphyodont odontogenesis, canonical Wnt signalling acts as a primary



activator of epithelial dental progenitors in the dental lamina (Richman and Handrigan, 2011). Sox2/activated  $\beta$ -catenin (ABC) double immunohistochemistry assays in adult *C. travancoricus* reveal their co-expression in a region of the dental lamina epithelium (Fig 2J.b'), suggesting the involvement of canonical Wnt signalling in the activation of Sox2+ putative dental progenitors. Coupled with results from the Dil assay, the absence of ABC in a subset of Sox2+ dental lamina cells provide further evidence for a discrete epithelial progenitor niche within this region (Fig 2J.a'). There is an intriguing relationship between the expression of Sox2 and ABC throughout the dental lamina; ABC expression increases whilst Sox2 immuno-localization decreases towards the site of tooth initiation (Fig 2J.a'-c'). These results uncover an opposing gradient of expression of ABC and Sox2 suggesting a genetic compartmentalization of the dental lamina. The lamina therefore is a highly dynamic and complex cell layer that requires further developmental study and functional investigation.

Concordant with Sox2/ABC immunohistochemistry, we observe expression of the Wnt effector *lef1* (Fig 3C) in the dental lamina in a pattern similar to the expression of ABC (Fig 2J) and a distal subset of Sox2/*sox2* expressing dental lamina cells (Fig 2D, E and 3A). Here, Sox2/ABC co-expression and *lef1* expression in the dental lamina suggest a conserved role for canonical Wnt signalling during pre-initiation progenitor regulation, in both embryo (Fig 3) and adult pufferfishes (Fig 2J), suggesting important genetic and cellular maintenance of dental progenitor populations from embryo to adult in a continuously regenerating dentition.

*Initiation of dental regeneration appears conserved during the development of the pufferfish beak*

Despite extensive vertebrate dental diversity, developmental regulation of dental regeneration is highly conserved (Jernvall and Thesleff, 2012) (Jernvall and Thesleff, 2012). Several members of the fibroblast growth factor (Fgf), hedgehog (Hh), bone morphogenetic protein (Bmp), canonical Wnt and Notch signalling pathways play a role in the development and regeneration of vertebrate teeth (Thesleff and Sharpe, 1997; Jernvall and Thesleff, 2012; Fraser *et al.*, 2013). We selected candidates from each of these major signalling pathways and examined expression of their pufferfish homologs in order to determine if their function was also conserved in the highly derived beaked-dentition (Fig 3). In pufferfishes, new tooth generations form from the distal, intraosseous tip of the dental lamina. Following the proliferation and migration of cells from the putative pre-initiation progenitor cell population in the dental lamina (Fig 2), we observe the expression of *lef1* (Fig 3C), *ABC/β-catenin* (Fig 2J and 3B), and expression of the Notch target *hes1* (Fig 3F) and *notch3* (G) restricted to a small pocket of cells within the dental lamina distal tip at the junction between the oral epithelium and the beak. These expression data identify both Wnt and Notch signalling as potential regulators of dental initiation at this site. As dental development progresses, cells of the dental lamina invade through gubernacular openings in the beak, into the dental cavity where tooth morphogenesis takes place. *shh* is upregulated within the dental epithelium as it extends through into the dental cavity and remains expressed in the dental epithelium throughout morphogenesis (Fig 3E).

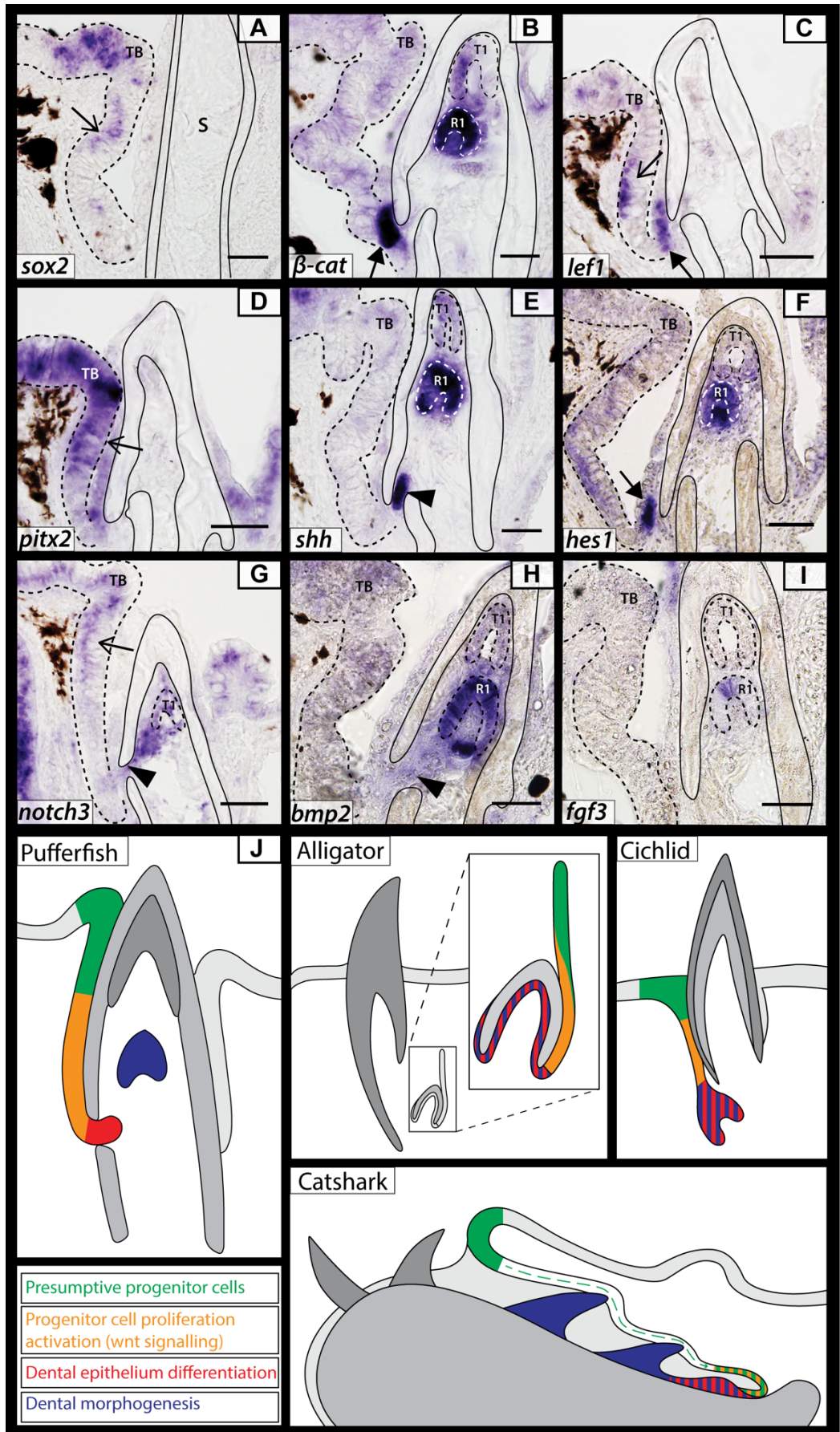


**Figure 3. Conserved odontogenic signalling regulates dental regeneration in pufferfish.**

Expression of well documented odontogenic markers belonging to Sox (*sox2* – Fig.3A), canonical Wnt signalling ( $\beta$ -*catenin* – Fig. 3B; *lef1* – Fig.3C), Pitx (*pitx2* – Fig.3D), Shh (*shh* – Fig.3E), Notch (*hes1* – Fig.3F; *notch3* – Fig.3G) Bmp (*bmp2* – Fig.3H) and Fgf (*fgf3* – Fig.3I) gene families in *T. niphobles* embryos. Open arrow marks the site of presumptive dental progenitors, with expression of *pitx2* (D), *lef1* (C) and *sox2* (A) within this region. Closed arrow marks the distal end of the dental lamina. Closed arrowhead highlights an opening within the osteodentine beak casing through which new odontogenic cells bud from the dental lamina.  $\beta$ -*cat* (B), *shh* (E), *hes1* (F), *notch3* (G), *bmp2* (H) and *fgf3* (I) all expressed within the epithelium of the latest developing teeth. J is a diagrammatic illustration of odontogenetically similar structures between various polyphyodonts (pufferfish, alligator (Wu et al., 2013, Juuri et al., 2013), cichlid (Fraser et al., 2013) and catshark (Rasch et al., 2016)). Four main developmental regions are highlighted; presumptive dental progenitors’, ‘progenitor cell activation’ marked by the co-expression of Sox and Wnt signals, ‘dental epithelium differentiation’ marked by the upregulation of various developmental genes at the distal tip of the dental lamina and the growth of a tooth bud, and ‘dental morphogenesis’. Dotted line depicts boundary of the oral epithelium and the end of the dental lamina. All images taken from 14 $\mu$ m sagittal paraffin sections. A, B, E, F, H and I from *T. niphobles* embryos 50 days post fertilization. C, D and G from embryos 32 days post fertilization. TB=labial taste bud; R1-2=replacement tooth generations; S=suture. Scale bars: B, C, D, F, G = 50 $\mu$ m; A, E, H, I = 35 $\mu$ m.

Bmp and Fgf signalling have also been extensively described during dental morphogenesis, and are involved in reciprocal interactive signalling between the dental epithelium and neural crest-derived mesenchyme (Thesleff and Sharpe, 1997; Jernvall and Thesleff, 2012; Fraser *et al.*, 2013). We found *fgf3* expression restricted to the apical tip of the dental epithelium of the developing tooth (Fig 3I, R1), with *bmp2* expressed throughout the dental epithelium and within the underlying condensed dental mesenchyme (Fig 3H, R1). These expression patterns are comparable to those observed in cichlid fishes, with *fgf3* and *bmp2* active in both the dental epithelium and dental

mesenchyme (Fraser *et al.*, 2013). These results highlight that despite the highly derived dental morphology of the pufferfish beak, Notch, Wnt, Fgf, Hh and Bmp signalling appear to maintain their roles in dental regeneration.

*Restriction in dental replacement takes place between first and second dental generations*

Pufferfishes typically develop a first generation dentition composed of multiple teeth along the jaw (Fraser *et al.*, 2012), much like the dentitions observed in other larval and juvenile teleosts. The second and subsequent tooth generations in pufferfishes undergo a major transition and do not follow the pattern set by the first generation. Four tooth bands form per dental generation, one for each jaw quadrant (Fraser *et al.*, 2012), raising the question as to whether these teeth form through the coalescence of teeth initiated at multiple sites along the jaw, or through the loss of dental replacement at all but four sites. There is interesting morphological variation in the dentition between pufferfish species. Unlike in most pufferfish species, including *P. suvattii* (Fig 1A), reconstructed *T. niphobles* micro-CT scans reveal discontinuities within the tooth band of each dental generation (Fig S1). This may indicate that potentially multiple teeth form with each round of replacement, instead of a single elongated dental unit in each quadrant of the jaw. However, given that at embryonic stages *T. niphobles* teeth develop as a single continuous banded unit (Fig 1D-E and S1), this observation may be an artefact of mineralization leading to multiple tooth units from a single initial tooth germ or of preservation resulting in the break-up of a continuous band. Investigating the early

development of the banded teeth in *T. niphobles* will help to clarify the way in which the teeth are replaced.

To understand the developmental basis of the morphological and functional shift observed in the pufferfish dentition, we examined the expression patterns of odontogenic markers during multi-generational morphogenesis using whole-mount *in situ* hybridisation. This enables a mediolateral view of gene expression patterns, providing detail during dental initiation at multiple sites across the jaw simultaneously. Dissected lower jaws of pufferfish embryos reveal the expression of *pitx2*, *shh*, *lef1* and *edar* throughout the developing tooth bands during morphogenesis (Fig 4C-G). These markers have previously been shown to play vital roles during differentiation and morphogenesis in other vertebrate dentitions (Lin *et al.*, 1999; Dassule *et al.*, 2000; Tucker *et al.*, 2004; Sasaki *et al.*, 2005). We observed the expression of these four markers in a single banded unit associated with the continuous and elongated dental epithelium for each tooth generation. This suggests that each band represents a single, highly enlarged and elongated tooth and is not formed through the coalescence of multiple teeth across the jaw.

As a result of further examination of histological serial sections in the pufferfish embryo (Fig 1F-I) and of reconstructed CT scans in the adult (Fig 5H-K), we observed four gubernacular openings, one in each jaw quadrant restricted to the parasymphyseal region. These connect the developing intraosseous dental organ to the external dental lamina (Fraser *et al.*, 2013). As development progresses and generations of teeth accumulate, the pufferfish dentition becomes increasingly mineralized. The multiple

tooth generations become entirely encapsulated by osteodentine yet these four openings remain, one in each jaw quadrant, throughout adulthood. Other members of the Tetraodontiformes, such as the Triodontidae and Diodontidae, form beaks superficially similar to those of pufferfishes. However, the triodontid and diodontid dentitions are formed through the replacement of all of the primary tooth sites. In this instance we observe gubernacular openings associated with each replacement tooth site (Fig 5C and F). These results provide evidence that the number of teeth replaced is intimately linked to the number of gubernacular openings. It is through these openings that the dental lamina is able to access the developing tooth within the dental cavity.

The oral epithelium of pufferfishes is attached to the mandible at the junction of the dentition unit and the underlying bone (Fig 1C). At the jaw symphysis, the left and right halves of both upper and lower jaw beaks are separated by a cleft (Fig 5I). The close association of the oral epithelium follows the contour of the beak, with the gubernacular openings positioned towards the top of the cleft (arrow in Fig 5I and J). Interestingly, we found *pitx2* and *shh* both expressed in the oral epithelium associated with the symphyseal cleft (Fig 4A and B), corresponding positionally to the distal dental lamina expressing *β-catenin*, *shh*, *pitx2* and *hes1* (observed in section; Fig. 3). *shh* and *pitx2* together demarcate the sites of dental initiation along the jaw (Fraser *et al.*, 2008, 2012). Their expression restricted to the symphyseal epithelium may be important in regulating the reduction in tooth site number observed between the first and second dental generations (Fraser *et al.*, 2012). Furthermore, during the early growth stages of tooth formation we observed tooth buds restricted to either side of the mandibular midline (symphysis), one initiatory unit in each jaw quadrant, identified early in development

through the expression of *pitx2*, *shh* and *lef1* within the newly developing teeth (arrowhead in Fig 4C-F). This provides further evidence that during the transition from first to second dental generations) (Fraser *et al.*, 2012), pufferfishes exhibit a loss in dental initiation at all but four parasymphyseal initiation sites.

*Inhibition of the Notch signalling pathway leads to stunted growth of the elongated banded dentition*

In order to determine how the relatively stereotypical first generation teeth of pufferfishes are replaced by the highly derived elongated bands in the adult, we sought to functionally perturb developmental pathways known to be involved in tooth morphogenesis in other vertebrates. The Notch receptor and ligand, *notch3* and *jagged1b* respectively, are both expressed within the tooth band-epithelium during early morphogenesis and subsequent differentiation (Fig 4H and I). Given observed Notch activity in the developing tooth and its importance for normal morphogenesis in developing mice teeth (Mitsiadis *et al.*, 2010), we sought to determine whether changes in Notch signalling contributes to tooth elongation in pufferfishes through pathway inhibition with the small molecule inhibitor of  $\gamma$ -secretase complex, DAPT (Fig 4K-N; e.g. (Fraser *et al.*, 2013).

Embryos at 19 days post fertilization were treated with 25 $\mu$ M DAPT for a 72h period coincident with the emergence of the second-generation dentition. During this period the dentition would normally transition from the unicuspid first-generation to the



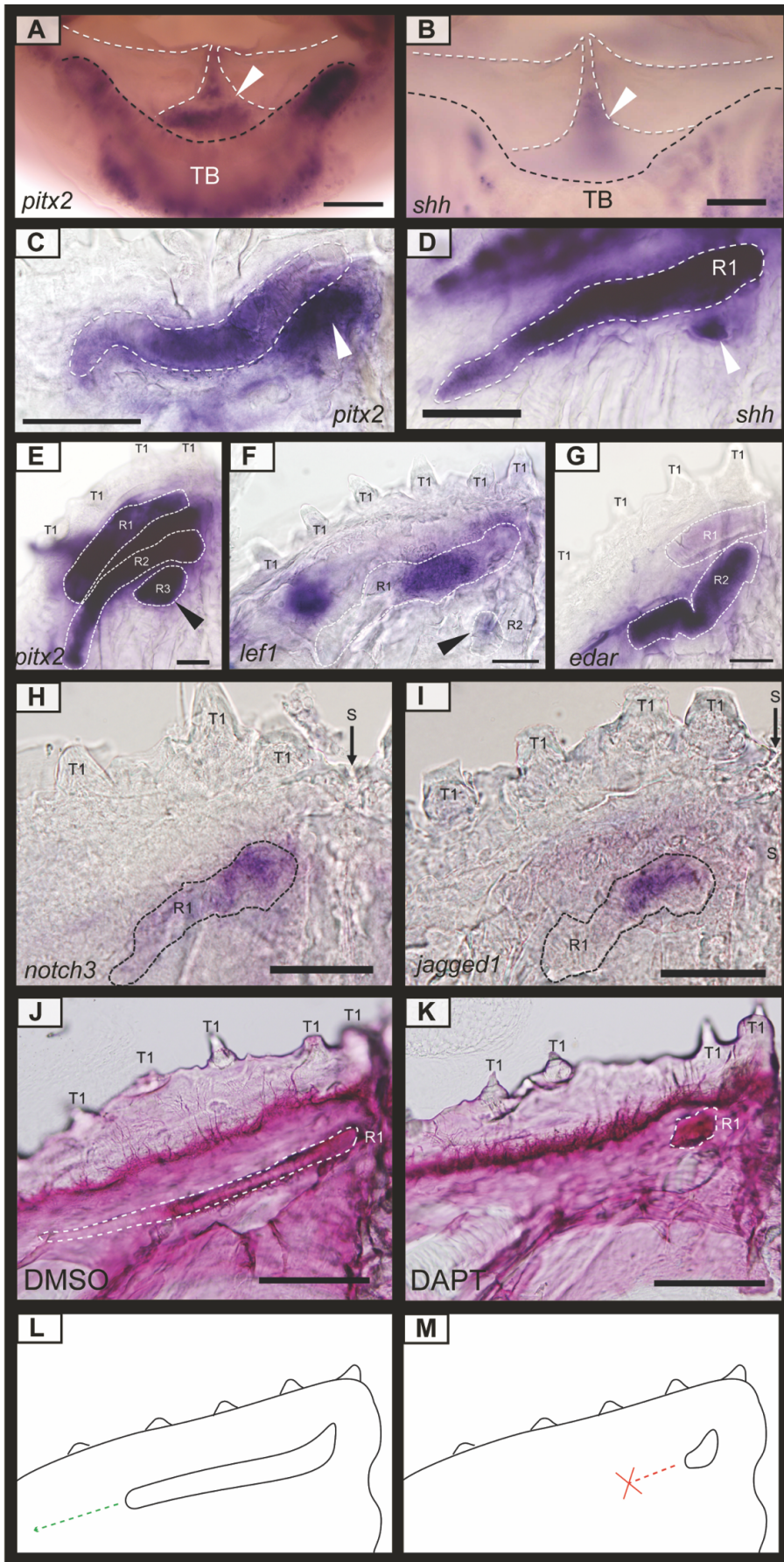
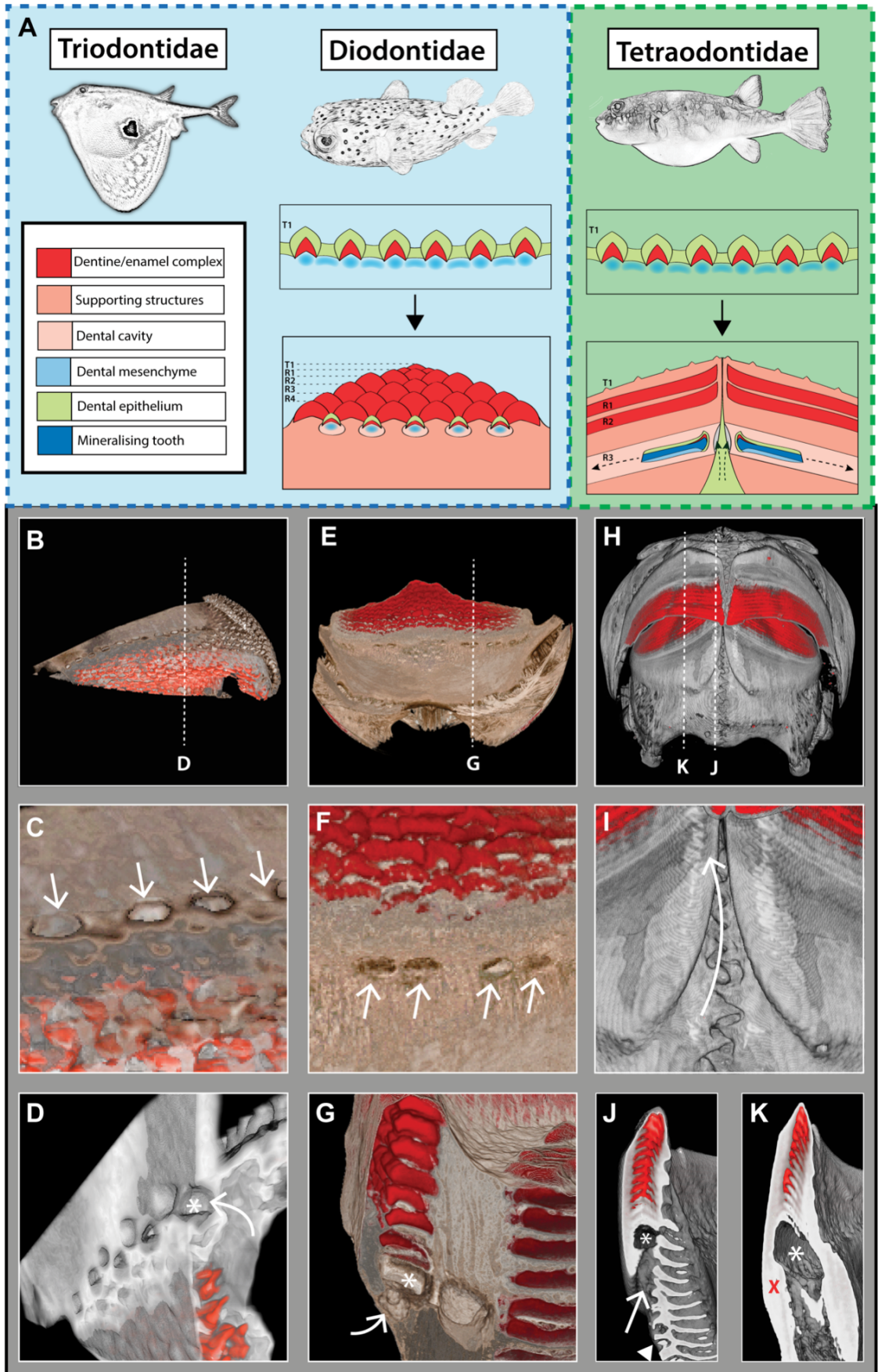


Figure. 4. Gene expression patterns during dental regeneration morphogenesis and chemical inhibition of Notch signalling through small molecule treatments. Whole-mount RNA *in situ* hybridization of the lower jaws of: *P. baileyi* at 57dpf (A-B, E-F), 53dpf (H, I), 46dpf (G); and *T. niphobles* at 50dpf(C-D); and *P. suvattii* at 26dpf (J, K). (A-B) Images taken from above the lower jaw depict expression of *pitx2* (A) and *shh* (B) in the labial epithelium at the jaw symphysis (white arrowhead). (C-L) Images of a single lower jaw quadrant, with the expression of *pitx2* (C, E), *shh* (D), *lef1* (F), *edar* (G), *notch3* (H), and *jagged1b* (I) in the developing teeth illustrated through dotted lines (C-G). New tooth units can be seen initially developing (C-F, arrowhead) at the symphysis of the beak (right of image). Alizarin red staining of *P. suvattii* embryos after treatment with 50 $\mu$ M DAPT during initiation of the second generation dentition for 72 hours, followed by a 2-week recovery period (L), and control sample treated with 1% DMSO (K). Staining reveals the mineralization of the second-generation tooth (R1, white dotted line), with the control specimens (K) elongating laterally throughout the jaw (n=5/5). 25 $\mu$ M DAPT treatment (L) resulted in the loss of dental elongation, with the mineralized tooth restricted in size at its site of initiation (n= 7/7). (M-N) Schematic representation of the phenotypes observed in the DMSO and DAPT treatments described above. T1=first tooth generation; R1-3=replacement tooth generations; S=suture. Scale bars: (A-F) 100 $\mu$ m; (G-K) 50 $\mu$ m.

banded second-generation dentition (Fraser *et al.*, 2012). Following treatment, embryos were allowed to recover for a 14-day period and then screened for morphological shifts. Control embryos (1% DMSO) underwent normal dental replacement, with a single elongated dentine band mineralizing throughout the length of the jaw quadrant (n=5/5) (Fig 4K). In contrast, following DAPT treatment, dental band elongation was inhibited (n=7/7). We observed a single truncated mineralized tooth unit, which terminated precociously near the parasymphyseal site of tooth initiation (Fig 4L), suggesting that Notch signalling is required for the normal elongation of the replacement tooth units in pufferfishes. Furthermore, these results are in line with our idea of a single initiatory site of dental replacement in each jaw quadrant in pufferfishes, with elongation of the dental unit underlying the banded tooth morphology.



**Figure. 5. Schematic representation of Tetraodontidae beak formation.** (A) Illustration of schematic highlighting the modes of dental replacement in Triodontidae, Diodontidae and Tetraodontidae. Whilst the development of the first generation teeth is conserved, the modes of dental replacement differ dramatically. Reconstructed microCT scans of Triodontidae (B-D) and Diodontidae (E-G) reveal gubernacular openings (C and F) within the labial surface of the jawbone. Virtual sagittal sections through these sites show an open connection (white arrow) between the labial surface and the dental cavity (\*) (D and G). In Triodontidae and Diodontidae (B-G), gubernacular openings can be seen associated with multiple tooth sites along the jaw. MicroCT scans of *P. suvattii* (G-H) illustrate an intraosseous, banded dentition, with virtual serial slices through the dentition at the parasymphyseal region (I) and adjacent region (J) revealing gubernacular openings restricted to the parasymphyseal region (I), with a single opening in each jaw quadrant. These openings connect the site of dental lamina attachment (white arrow, I) with the dental cavity (\*). White arrowhead in C marks the interdigitating jaw suture observable at the symphysis.

## Discussion

Our results show that the primary basis of the pufferfish beak is a loss of tooth regeneration and therefore unit replacement at all but the four most parasymphyseal tooth sites. This loss occurs during the transition between first and second dental generations (Fraser *et al.*, 2012). The developmental initiation of dental regeneration at the parasymphyseal sites in pufferfishes remains highly conserved with other polyphyodonts, despite the unique final morphology. Finally, the subsequent elongation of the dental unit leads to the banded morphology of the dentition.

The prerequisite for the formation of all vertebrate dentitions is an embryonically active dental lamina. In polyphyodont species the dental lamina must be regulated and maintained to support the production of further tooth generations (Buchtová *et al.*,

2012). Pufferfishes form their teeth intrasosseously and develop a dentition entirely confluent with the supporting jaw-bone, raising the question of where epithelial dental progenitors reside in a system in which the developing dentition has become spatially separated from the oral epithelium. Our Sox2/PCNA expression data, and DiI cell tracking data (Fig 2) show that despite the unique morphology of the Tetraodontidae beak, epithelial dental progenitors are found within the dental lamina, concordant with cichlids (Bloomquist *et al.*, 2015). The physical separation of the dental lamina from the dental cavity therefore necessitates a permanent connection between the two through the mineralized beak/jaw unit.

It is common in teleosts to confine epithelial cellular input of the dental lamina to openings for site-specific induction of new tooth generations. For example, in the oral jaws of cichlid fishes each functional tooth position has a neighbouring gubernacular opening that allows the transfer of dental epithelial cells from the surface epithelium into the bony cavity of the jaw to initiate tooth regeneration (Fraser *et al.*, 2013). Alongside pufferfishes, other members of the Tetraodontiformes i.e. the Molidae, Triodontidae and Diodontidae, have also evolved beaked dentitions. The Molidae lose the ability to regenerate their teeth throughout ontogeny, and are thought to develop a beak through mineralization of the jaws (Andreucci *et al.*, 1982). In contrast, the Triodontidae and Diodontidae develop beaked dentitions superficially similar in shape to that of the pufferfishes, however these dentitions form through replacement of all of the primary tooth sites (Fig 5). Interestingly, in these systems we identified gubernacular openings associated with each tooth site that undergoes replacement. In systems that develop teeth intrasosseously, we propose that the number of dental

initiation sites is intimately linked with the number of sites at which the dental lamina is able to access the internal dental cavity through these openings (Fig 5). Given the phylogenetic position of pufferfishes within the tetraodontiform lineage (Santini *et al.*, 2013), it is reasonable to assume that the evolution of a beak composed of multiple teeth across the jaw margin (i.e. Triodontidae and Diodontidae; Figure 5) preceded the loss of dental replacement observed in pufferfish. Several changes must have taken place during the transition to a pufferfish beak: (i) gubernacular pores are lost along the jaw margin at all but four sites; (ii) dental lamina extension into the dental cavity is restricted to these pores; (iii) establishment of an extended dental cavity that allows for the growth of a banded dentition; and (iv) an elongation of the dentition. It is likely that selective pressure on feeding has driven this morphological change, leading to a change in the feeding biomechanics in the pufferfish. Further study of the comparative biomechanics between the different beaks observed in the tetraodontiform lineage could elucidate the driving force behind this evolutionary morphological novelty.

Pufferfishes have evolved a highly derived dental morphology through the subtle modification of a conserved teleost bauplan. Whilst the final morphology is unique, the developmental regulation shares extensive features with other polyphyodont vertebrates. We identify a putative progenitor cell niche within the dental lamina with Wnt signalling notably active in a subset of Sox2+ cells. This is demonstrated through the expression of ABC and *lef1* and suggests a conserved role for Wnt signalling during initiation of dental regeneration. Wnt signalling has been identified as a key regulator of dental regeneration in polyphyodonts, with its upregulation leading to ectopic tooth germ formation in the dental lamina of snakes (Gaete and Tucker, 2013). Ectopic Wnt

signalling also leads to supernumerary teeth in mice (Wang *et al.*, 2009), with upregulation specifically in Sox2+ dental epithelial cells sufficient in generating odontomas (Xavier *et al.*, 2015). Furthermore, active Notch, Hh, Bmp, Fgf and Wnt signalling during dental differentiation and morphogenesis further highlights the conservation of developmental signalling during tooth development across gnathostome vertebrates. Our findings demonstrate the role regeneration plays in the evolution of morphological novelty, and how despite a significant morphological shift, developmental signalling during regeneration remains highly conserved.

Whilst pufferfishes have clearly utilized primarily conserved odontogenic pathways, the development of a truncated tooth bud following Notch perturbation provides insights into the development of the elongated dental morphology. Our results support the hypothesis that the multi-generational tooth bands each form from a single dental initiatory site located either side of the jaw symphysis (Fig 4K-N). The shift from a jaw length tooth band to a small restricted tooth bud when Notch signalling is inhibited in pufferfish, is remarkably similar to the mouse incisor, which develops from an elongated placode that separates into multiple smaller placodes following bmp or activin manipulation (Munne *et al.*, 2010). However, in contrast to mice, the formation of a single restricted symphyseal tooth following Notch inhibition, rather than multiple separated teeth suggests that the transition from a diodon/triodon-like beak to a pufferfish beak did not involve the coalescence of dental placodes. Notch signalling may be playing an important role in the elongation of the symphyseally restricted placode. Notch is also vital for both mouse molar and incisor morphogenesis, mediating signals between the dental epithelium and the stratum intermedium that regulates both

odontoblast and ameloblast differentiation in the mouse (Mitsiadis *et al.*, 2010). When the Notch signalling pathway is disrupted, there is a reduction in the size of mouse incisors, and defects in both enamel and dentine deposition (Mitsiadis *et al.*, 2010; Jheon *et al.*, 2016). In cichlid fishes, the inhibition of the Notch signalling pathway results in multiple phenotypes including defective mineralization of the cusps, a reduction in cusp number, and the loss of tooth replacement at multiple positions along the tooth row (Fraser *et al.*, 2013). Our intriguing result from the Notch inhibition assay could reflect either (i) the loss of an extended dental placode within the dental cavity or (ii) aborted ameloblast/odontoblast mineral-secretion. Either of these factors would be expected to result in the truncation of the tooth band after DAPT treatment.

Pufferfishes provide a rare opportunity to study a vertebrate model that offers a maturing developmental system from embryo to adult, in which the processes of development and tissue homeostasis of a regenerative dentition can be investigated. The Tetraodontiformes are an extraordinarily diverse group of teleost fishes (Tyler, 1980), ideal for the study of morphological novelty. Through the investigation of dental development, we show the existence of a highly conserved polyphyodont developmental system involved in the formation of the novel and unique pufferfish dental morphology. Whilst the regulation of tooth initiation is highly conserved, the loss of dental replacement at all but the parasymphyseal tooth sites, coupled with elongation of the dental unit, has enabled pufferfishes to develop a dentition unlike any other.

Although mammals have evolved the ability to renew their dentition through continuously growing teeth (Renvoisé and Michon, 2014), they have more generally



lost the ability to regenerate the dental unit more than once. During mammalian tooth development the dental lamina degrades, ultimately leading to a loss of polyphyodonty (Buchtová *et al.*, 2012). Whilst pufferfishes have a spatially restricted ability to regenerate their dentition, polyphyodonty is sustained, enabling this unique dental morphology to arise. This is thanks to the maintenance of a dental lamina throughout life, which houses the progenitor cells required for dental regeneration to continue. Pufferfishes represent a unique example of how the spatial restriction of dental regeneration yet continuous maintenance of polyphyodonty, has led to morphological innovation. Further developmental study of morphological novelties resulting from the process of regeneration will provide insights into how gene regulatory networks can be both conserved and altered, whilst allowing for novelty to develop in parallel.

## **Materials and methods**

### *Animals*

*P. baileyi* embryos were raised to the required stage in a recirculating aquarium system at 20–23°C at the Natural History Museum, London. Adult *P. suvattii* and *C. travancoricus* were maintained in a recirculating aquarium system at 26°C at the University of Sheffield. *P. suvattii* embryos were collected and raised to the required stage at 26°C. I obtained **fertilized *T. niphobles* eggs through induced insemination of adults collected on Arai beach, Kanagawa prefecture, Japan**. Embryos were raised to the desired stage in fresh seawater at 20°C. Adult *C. tranvicoricus*, and larval *P. suvattii*, *P. baileyi* and *T. niphobles* were anaesthetized with MS-222 and fixed in 4%

paraformaldehyde overnight at 4°C. Samples were then dehydrated through a graded MeOH series and stored at -20°C.

### *CT scanning*

Specimens of *T. niphobles* (accession number. 1905.2.4.493) and *P. suvattii* preserved in EtOH were obtained from collections at the Natural History Museum, London. Samples were scanned using the Metris X-Tek HMX ST 225 CT scanner (Imaging and Analysis Centre, Natural History Museum, London). 3D volume renderings of the microCT scans were carried out using DRISHTI (<https://github.com/nci/drishti>).

### *Histology and clearing and staining*

For histological study, samples were decalcified with 0.5M EDTA in water for 24 hours, further dehydrated in isopropanol for paraffin embedding, cleared with xylene and subsequently embedded in paraffin. 14µm sagittal paraffin sections were cut using a Leica RM2145 microtome. Slides were stained with 50% haematoxylin for 10 minutes. Stained slides were mounted with Fluoromount (SIGMA) and imaged using a BX51 Olympus compound microscope fitted with an Olympus DP71 camera. For clearing and staining, juvenile pufferfishes were stained with 0.02% alizarin red in 0.1% KOH overnight in the dark and subsequently cleared in 0.1% KOH. Once residual alizarin red had been removed, samples were transferred into glycerol through a glycerol/0.1%KOH graded series and imaged using a Nikon SMZ1500.

### *Lineage tracing (DiI)*

The labial oral epithelium of *P. suvattii* embryos 19 days post fertilization (dpf) was superficially labelled with DiI (1,1'-Dioctadecyl-3,3,3',3'-Tetramethylindocarbocyanine Perchlorate; Thermo V22885) using a microinjection capillary needle and aspirator tube assembly. Embryos were anaesthetized in MS-222 (60mg/ml) in freshwater during treatment. Embryos were then raised for a further 3 days in freshwater prior to fixation and standard paraffin embedding and sectioning.

### *cDNA and riboprobes*

*P. suvattii*, *P. baileyi*, and *T. niphobles* total RNA was extracted using phenol/chloroform phase separation and cleaned through EtOH/LiCL precipitation. RT-cDNA was made using the RETROscript 1710 kit (Ambion). Cloned cDNA sequences used to generate Digoxigenin-11-UTP (DIG)-labelled antisense riboprobes from *P. suvattii*, *P. baileyi*, and *T. niphobles* were identified through the genome database available from the International Fugu Genome Consortium (<http://www.fugu-sg.org>). cDNA clones for pufferfish *shh*, *pitx2*, *sox2*,  $\beta$ -*catenin*, *lef1*, *jagged1b*, *hes1*, *fgf3*, *bmp2*, *notch3*, and *edar* homologs were isolated through PCR, with forward and reverse primers designed from the *Takifugu rubripes* genomic sequence. Forward and reverse primers designed through Primer3. Sequences of interest were amplified from the cDNA through PCR and ligated into the pGEM-T-Easy vector (Promega). Ligation products were cloned into JM109 cells. Plasmid DNA was then extracted from chosen colonies using a Qiaprep spin Mini-prep kit (Qiagen) and sequenced (Applied

Biosystems' 3730 DNA Analyser) through the Core Genomics Facility, University of Sheffield. Verified vectors were then amplified through PCR and used as a template for probe synthesis. Sense and anti-sense probes were made using a Riboprobe Systems kit (Promega) and SP6/T7 polymerases (Promega). Probes were labelled with Digoxigenin-11-UTP (Roche) for detection during *in situ* hybridisation. A final EtOH precipitation step was carried out to purify the RNA probe.

*Forward and reverse primer sequences*

*sox2*

5'-CCAGAGGAGGAAGATGGCGCAA-3'

5'-CATGTGTAGCCTGGTCTGGGC-3'

*shh*

5'-GAAGGCAAGATCACAAGAACTC-3'

5'-ACGTTCCCCTTGATAGAGGAG-3'

*pitx2*

5'-TCTATGAGGGAACCCTTGAATATAG-3'

5'-CTGCTTGGCTTTCAGTCTCAG-3'

*β-catenin*

5'-CCCTGAGGAAGATGATGTGGACAA-3'

5'-ACAGTTCTGGACCAGTCTCTGGCTG-3'

*lef1*

5'-CAGTCCCAAATACCAGATTCATATC-3'

5'-TCTTCTTCTTCCATAGTTGTCTCG-3'

*notch3*

5'-TCTGACTACACTGGAAGCTATTGTG-3'

5'-TTGCAGTCAAAGTTGTCATAGAGAC-3'

*jagged1b*

5'-CACCTGCGTCTGTAAAGAAGGCTG-3'

5'-ACGACACCACGTACGCGGCG-3'

*hes1*

5'GACAGCCTCCGAGCACAGAAAGTC-3'

5'AGTCAAACCGCTGGGACCACT-3'

*fgf3*

5'-GTTGAATTTGTTGGATCCGGTTAG-3'

5'-TGACCTTCGTCTCTTAACTCTCTTG-3'

*bmp2*

5'-TTAGAAGCTTTCACCATGAAGAGTC-3'

5'-TTCATCCAGGTAGAGTAAGGAGATG-3'

*edar*

5'-GTA CTCCA AAGGGAAGTACGAAATC-3'

5'-AAGATCTTTCTCCTCCGACTCTG-3'

### *Immunohistochemistry*

Peroxidase-labelled section immunohistochemistry was carried out according to manufacturer's instructions using mouse anti-PCNA (1:5000) (Abcam ab29) and peroxidase-labelled anti-mouse IgG (1:250) (DAKO); or rabbit anti-Sox2 (1:500)

(Abcam ab97959) and peroxidase-labelled anti-rabbit IgG (1:250) (DAKO). The colour reaction was carried out using DAB (DAKO). Rabbit anti-Sox2/mouse anti-PCNA and rabbit anti-Sox2/mouse anti-active  $\beta$ -catenin (1:500) (Merck 05-665) double immunofluorescence was carried out in accordance with Martin *et al* (2016). Goat anti-rabbit AlexaFluor®-647 (1:250) (Thermo A-20721245) and goat anti-mouse AlexaFluor®-488 (1:250) (Thermo A-11-001) secondary antibodies were used for immunodetection. Images were taken on an Olympus BX51 upright epifluorescent microscope.

The three antibodies used for our immunohistochemistry analysis are well characterised and have been shown to react in a wide range of vertebrate species. anti-Sox2 (ab97959) and anti-PCNA (ab29) are known to react in amniotes (Lin *et al.*, 2017; Sun *et al.*, 2017), teleosts (Li *et al.*, 2010; Chen *et al.*, 2016) and cartilaginous fishes (Martin *et al.*, 2016; Cooper *et al.*, 2017). anti-Sox2 has also been shown to react in *Drosophila* (Pokholkova *et al.*, 2018), highlighting the conserved nature of this protein. Finally, anti-activated  $\beta$ -catenin (Merck 05-665) has been shown to react in mammals, including mouse (Liu *et al.*, 2012), rat (Zhou *et al.*, 2012) and human (Jansen *et al.*, 2015), and is structurally conserved in zebrafish (manufacturer information). Given the conserved nature of these antibodies and the description of their reactivity within teleosts, we deemed them suitable for immunohistochemistry analysis in the teleost pufferfish. Immunohistochemistry in the absence of a primary antibody was carried out as a control for unspecific binding of the secondary antibody.

### *Section in situ hybridisation*

Sagittal paraffin sections were obtained as previously described. Slides were deparaffinised using Xylene and rehydrated through a graded series of EtOH/PBS, before being superheated in the microwave (~95°C) with 0.01M Sodium Citrate buffer for 15 minutes. Slides were incubated in pre-heated pre-hybridisation solution pH 6 [250ml deionised-formamide, 125ml 20x saline sodium citrate (SSC), 5ml 1M sodium citrate, 500µl Tween-20 and 119.7ml DEPC-treated ddH<sub>2</sub>O] at 61°C for 2 hours. Slides were then transferred to the pre-heated pre-hybridisation solution containing DIG labelled RNA probe (1:500), 500 mg/ml yeast tRNA and 50 mg/ml heparin, and incubated overnight at 61°C. The following day, slides underwent a series of 51°C SSC stringency washes to remove unspecific probe binding [3x30m 2xSSC-T (0.05% tween-20); 3x30m 0.2xSSC-T (0.05% tween-20)]. Following the stringency washes, samples were incubated in blocking solution (2% Roche Blocking Reagent (Roche)) for 2hr at room temperature and then incubated in blocking solution containing anti-Digoxigenin-AP antibody (1:2000; Roche) overnight at 4°C. Excess antibody was washed off through 6x1hr MAB-T (0.1% tween-20) washes. Slides were then washed in NTMT and colour reacted with BM-purple (Roche) at room temperature and left until sufficient colouration had taken place. Following the colour reaction, a DAPI nuclear counterstain (1µg/ml) was carried out before mounting the slides using Fluoromount (Sigma). Images were taken using a BX51 Olympus compound microscope. Images were contrast enhanced and merged in Adobe Photoshop.

*In situ* hybridisations were performed multiple times for each probe in order to ensure the reproducibility of expression pattern. Given the qualitative nature of *in situ* hybridisations, results are discussed in the context of this uncertainty. For all genes investigated through *in situ* hybridisation, both sense and antisense riboprobes were made, with sense probes used as negative controls. Only genes which showed clear, strong expression and minimal background for the antisense probe and simultaneous negative expression for the sense probe, were used in our analysis.

#### *Whole-mount in situ hybridisation*

Whole mount *in situ* hybridisation was carried out in accordance with the section *in situ* hybridisation protocol aside from a few subtle modifications. Following rehydration, samples were treated with 0.2 $\mu$ g/ml proteinase K for 1hr at room temperature and then fixed for 20m in 4% paraformaldehyde in PBS. Samples were then placed in pre-hybridisation and probe solution as previously described. Stringency washes were carried out at 51°C [3x30m 2xSSC-T (0.05% tween-20); 3x30m 0.2xSSC-T (0.05% tween-20)]. Blocking, antibody incubation and colour reaction were carried out as previously described. Following colour reaction, samples were stored in PBS with 10% EtOH.

#### *Treatment with small molecules*

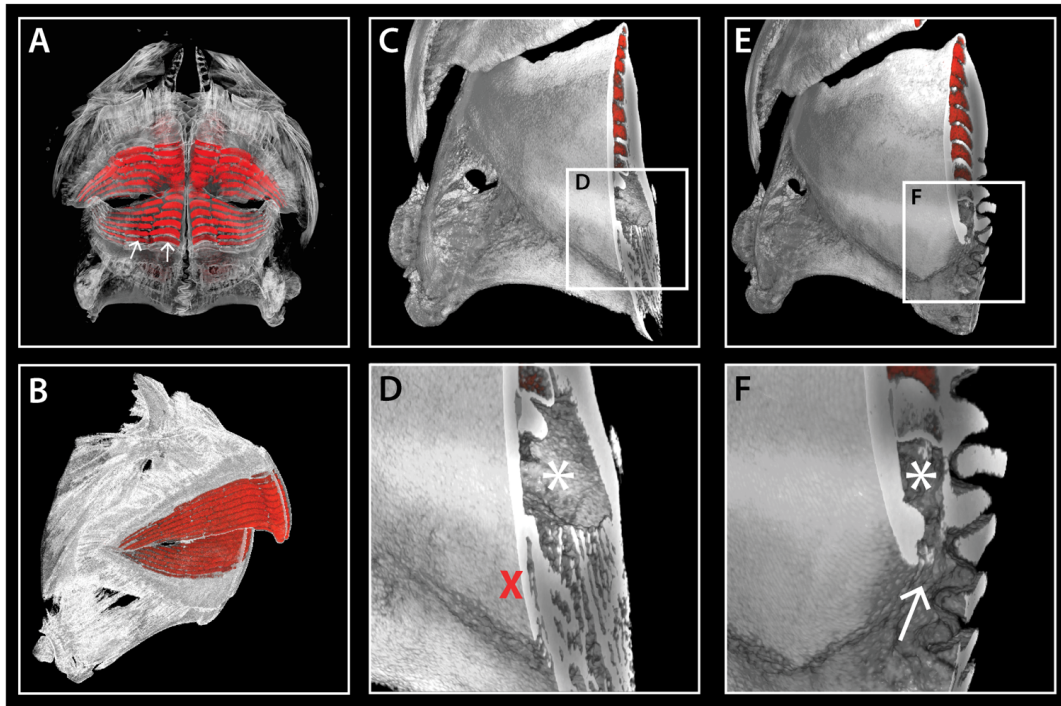


DAPT (MedChem Express) stock solution was prepared using Dimethyl Sulfoxide (DMSO) as a solvent. Treatment concentration was based on and adapted from Fraser *et al* (2013). *P. suvattii* embryos were raised to 19 dpf and treated with 25 $\mu$ M DAPT in freshwater for 3 days. 25 $\mu$ M DMSO was used as a control treatment. After treatment, embryos were washed and raised for 2 weeks in freshwater prior to fixation and clear staining.

### **Acknowledgments**

We thank Kyle Martin for comments on the manuscript; members of the Fraser lab and Nathan Jeffery for discussions; Serina Hayes for laboratory assistance; and Martin Garlovsky for digital photography. We are grateful to Hiroyuki Doi and Toshiaki Ishibashi for the donation of embryos. MicroCT imaging was carried out with assistance from Farah Ahmed and Amin Garbout of the Imaging and Analysis Centre (Natural History Museum, London). We are grateful for the support of the Light Microscopy Facility, the Bateson centre and the Molecular Ecology laboratory at the University of Sheffield. This work was generously funded by the following research support: The Leverhulme Trust Research Project Grant RPG-211 (to G.J.F), Natural Environment Research Council (NERC) Standard Grant NE/ K014595/1 (to G.J.F), The Royal Society Research Grant RG120160 (to G.J.F), The Great Britain Sasakawa Foundation (to G.J.F and T.S) and the Daiwa Anglo-Japanese Foundation (to G.J.F). This work was also funded through "Adapting to the Challenges of a Changing Environment" (ACCE), a NERC funded doctoral training partnership (to A.T) ACCE DTP (NE/L002450/1).

## Supplementary information



**Supplementary Figure 1. *Takifugu* dental morphology.** Reconstructed microCT scans of adult *T. niphobles* reveal discontinuous dentine bands encased in osteodentine (A-B). Virtual slices through the dentition at both symphyseal (C-D) and lateral (E-F) regions, reveal a single gubernacular opening (white arrow, F) in each jaw quadrant. \* = dental cavity; X = absence of gubernacular opening.

## Chapter 3

### **Small spotted catshark *de novo* transcriptome assembly reveals novel markers of successional dental regeneration**

Alexandre Thiery, Kyle Martin, Rory Cooper, Cameron Howitt and Gareth Fraser

Department of Animal and Plant Sciences, and Bateson Centre, University of Sheffield, UK.

#### **Abstract**

Sox2 has been identified as a primary marker of dental epithelial stem cells, with canonical Wnt signalling implicated in their regulation during successional dental regeneration. However, our understanding of vertebrate dental regeneration has relied heavily on research carried out in non-polyphyodont systems; a more comprehensive understanding requires the study of successional dental regeneration in polyphyodonts. Chondrichthyans regenerate their teeth cyclically throughout life and belong to a basal crown gnathostome lineage relative to tetrapods. Their phylogenetic position renders them an ideal model for the study of dental evolution and the regulation of successional dental regeneration. We performed RNAseq analyses on five distinct oral sub-regions, reflecting different stages of odontogenesis. Differential expression analysis highlighted novel markers upregulated within the successional lamina; an infolded epithelial sheet housing dental epithelial stem cells. Predictive gene regulatory network analysis

combined with prior system knowledge identified a key list of testable differentially expressed markers from a large transcriptome dataset. Candidate filtration revealed putative interactions between canonical Wnt signalling markers and *Mycn*, a proto-oncogene involved in the differentiation of neuroblastoma cells. We describe the co-expression of *mycn* with *Sox2* in the successional lamina, highlighting a potential role for this novel marker in the regulation of dental epithelial stem cells. This study reveals the power and importance of transcriptome-based approaches in the identification of novel markers regulating polyphyodont successional dental regeneration.

## **Introduction**

Vertebrate ectodermal appendages are a morphologically diverse group of epithelial organs including dermal denticles, reptilian scales, feathers and hair. Recent developmental studies have revealed ancestral homology between these structures, thought to date back 450 million years (Di-Poi and Milinkovitch, 2016; Cooper *et al.*, 2017). Despite their morphological disparity, these structures share the ability to regenerate, either via cyclical replacement (hair (Paus and Cotsarelis, 1999), feathers (Lin *et al.*, 2006) and teeth (Tucker and Fraser, 2014)) or as a result of external environmental stimuli, for example in response to wounding (denticles (Reif, 1978) and reptilian scales (Wu *et al.*, 2014)). Hair and teeth have gathered increased research attention (Huelsken *et al.*, 2001; Plikus *et al.*, 2008; Handrigan *et al.*, 2010; Juuri *et al.*, 2013) in a bid to locate epithelial stem cell niches required for their cyclical regeneration and understand the molecular pathways regulating their activation.

The evolutionary origin of teeth has long been debated, with their divergence from dermal denticles unclear (Fraser *et al.*, 2010; Donoghue and Rücklin, 2016; Martin *et al.*, 2016). Given the structural similarity between odontodes, it has recently been suggested that the differentiating feature of true teeth from other odontode types is their successional regeneration within defined tooth families (Martin *et al.*, 2016); this is as opposed to the sequential addition of dermal denticles which occurs during growth (Reif, 1978, 1980). Regenerating teeth are first found within the crown gnathostomes (Martin *et al.*, 2016), and have since diversified dramatically. From the crushing beak-like dentition of the pufferfish (Thiery *et al.*, 2017) to the venomous fangs of snakes (Zahradnicek *et al.*, 2008), modification of the dentition has facilitated vertebrate niche specialisation (Van Valkenburgh, 1989; Holliday and Stepan, 2004). Alongside morphological diversification, vertebrates have also evolved diversity in dental regeneration (Tucker and Fraser, 2014). Our understanding of dental development has been greatly enhanced by detailed developmental study of mammalian molars and the mouse incisor (Jarvinen *et al.*, 2006; Järvinen *et al.*, 2009; Juuri *et al.*, 2012). However, the developmental regulation underpinning successional dental regeneration remains understudied.

Teeth develop through continuous reciprocal signalling between the ectodermally or endodermally derived oral epithelium and the underlying neural-crest derived mesenchyme (Soukup *et al.*, 2008; Jussila and Thesleff, 2012). Prior to the development of the first teeth (in all vertebrates studied to date), a field of dental competence known as the odontogenic band (OB) is established within the oral epithelium. The joint expression of sonic hedgehog (*shh*) and paired-like homeodomain 2 (*pitx2*) demarcates

the position of the first dental generation and is followed by an epithelial thickening (Keränen *et al.*, 1999; Fraser *et al.*, 2004; Jussila *et al.*, 2014; Rasch *et al.*, 2016). The epithelium then invaginates into the underlying mesenchyme to form the dental lamina (DL) - an epithelial sheet from which future teeth develop (Tucker and Fraser, 2014). In contrast to most mammals (monophyodonty/diphyodonty), the majority of vertebrates are able to undergo multiple rounds of successional dental regeneration (polyphyodonty). There is substantial evidence that polyphyodonty depends upon the presence and maintenance of an epithelial dental stem niche found within the DL.

Numerous studies have recently implicated sex-determining region Y-related box 2 (Sox2) transcription factor as a primary marker of epithelial dental stem cells (Juuri *et al.*, 2012, 2013; Gaete and Tucker, 2013; Martin *et al.*, 2016), with Wnt/ $\beta$ -catenin signalling playing a critical role in initiating dental development from these cells (Gaete and Tucker, 2013; Martin *et al.*, 2016). Sox2 negatively regulates Wnt/ $\beta$ -catenin signalling in osteoblasts (Mansukhani *et al.*, 2005), whilst the expression of constitutively-activated  $\beta$ -catenin specifically within *sox2*<sup>+</sup> cells is sufficient to upregulate dental initiation in mice (Xavier *et al.*, 2015). Research into successional dental regeneration in diverse range of polyphyodonts is beginning to identify the mechanisms through which lifelong dental regeneration is naturally regulated (Gaete and Tucker, 2013; Wu *et al.*, 2013; Martin *et al.*, 2016; Rasch *et al.*, 2016; Thiery *et al.*, 2017).

A detailed understanding of the evolution of successional dental regeneration is required if we are to fully understand secondarily loss of polyphyodonty in derived vertebrate

lineages (i.e. mammals). The phylogenetic position of chondrichthyans within a basal crown gnathostome clade makes this group an early diverging vertebrate lineage relative to tetrapods. This renders chondrichthyans as an ideal reference point for the comparative study of successional dental regeneration. Extant chondrichthyans include sharks, rays and holocephalans (chimeras). They exhibit highly diverse dental morphologies (Smith *et al.*, 2013; Underwood *et al.*, 2015), with sharks and rays possessing a rapid rate of dental turnover best described as a dental ‘conveyor belt’ (Tucker and Fraser, 2014). Within the sharks, many teeth develop ahead of function, aligned in discrete family units. In some species, tooth families can be found separated by an enlarged inter-dental region (i.e. the frilled shark, *Chlamydoselachus anguineus*) (Smith *et al.* 2018), whereas in others the inter-dental region is all but absent, with adjacent tooth families overlapping and staggered in their initiation (i.e. small-spotted catshark, *Scyliorhinus canicula* (Rasch *et al.*, 2016)). Following numerous rounds of regeneration, this pattern is maintained as a result of seamless developmental coordination between adjacent tooth families. However how this process is regulated is unknown.

All teeth in the catshark are interconnected via a deep lying, jaw length DL (Martin *et al.*, 2016; Rasch *et al.*, 2016). Sox2+ dental progenitors initially associated with taste buds on the oral surface migrate from the oral surface and form a discrete niche within the distal tip of the DL (DL) (the successional lamina (SL)) – the site of dental initiation. Cyclical upregulation of Wnt/ $\beta$ -catenin signalling within this Sox2+ progenitor niche is associated with enhanced proliferation of the SL and the onset of dental initiation (Martin *et al.*, 2016). Although we have seen an increase in dental

regenerative research on non-mammalian models, the focus has remained centred on candidate markers initially identified in non-polyphyodont models. There is a need to move away from the candidate approach, in order to identify novel markers regulating polyphyodonty. Previous studies (Smith *et al.*, 2009; Martin *et al.*, 2016; Rasch *et al.*, 2016; Vandenplas *et al.*, 2016) of dental regeneration in the catshark laid the foundations for transcriptome analysis of the rapidly regenerating SL, providing novel insights into the mechanisms underpinning life-long dental regeneration.

We performed RNAseq analyses (Methods section: *RNAseq and differential expression analysis*) on five oral sub-regions ((i) basi-hyal taste buds (BHTB); (ii) taste-tooth junction (TTJ); (iii) SL; (iv) early developing tooth (ET); (v) late stage developing tooth (LT)) and cross-compared their expression patterns in order to identify differentially expressed markers within the SL. We carry out predictive GRN analyses using prior knowledge and our differential expression analysis data, in order to subset key markers of interest to investigate through *in situ* hybridisation. This study investigates the expression patterns of these markers specifically within the SL in order to identify novel candidates involved in the regulation of regeneration.

## **Results**

### *Histological and morphological analysis of the catshark dentition*

Computed tomography (CT) imaging of a hatchling catshark head shows the pattern of denticles on the skin surface and a clear denticle-tooth boundary at the oral surface (Fig 1A). The dentition develops in rows consisting of multiple teeth which emerge through



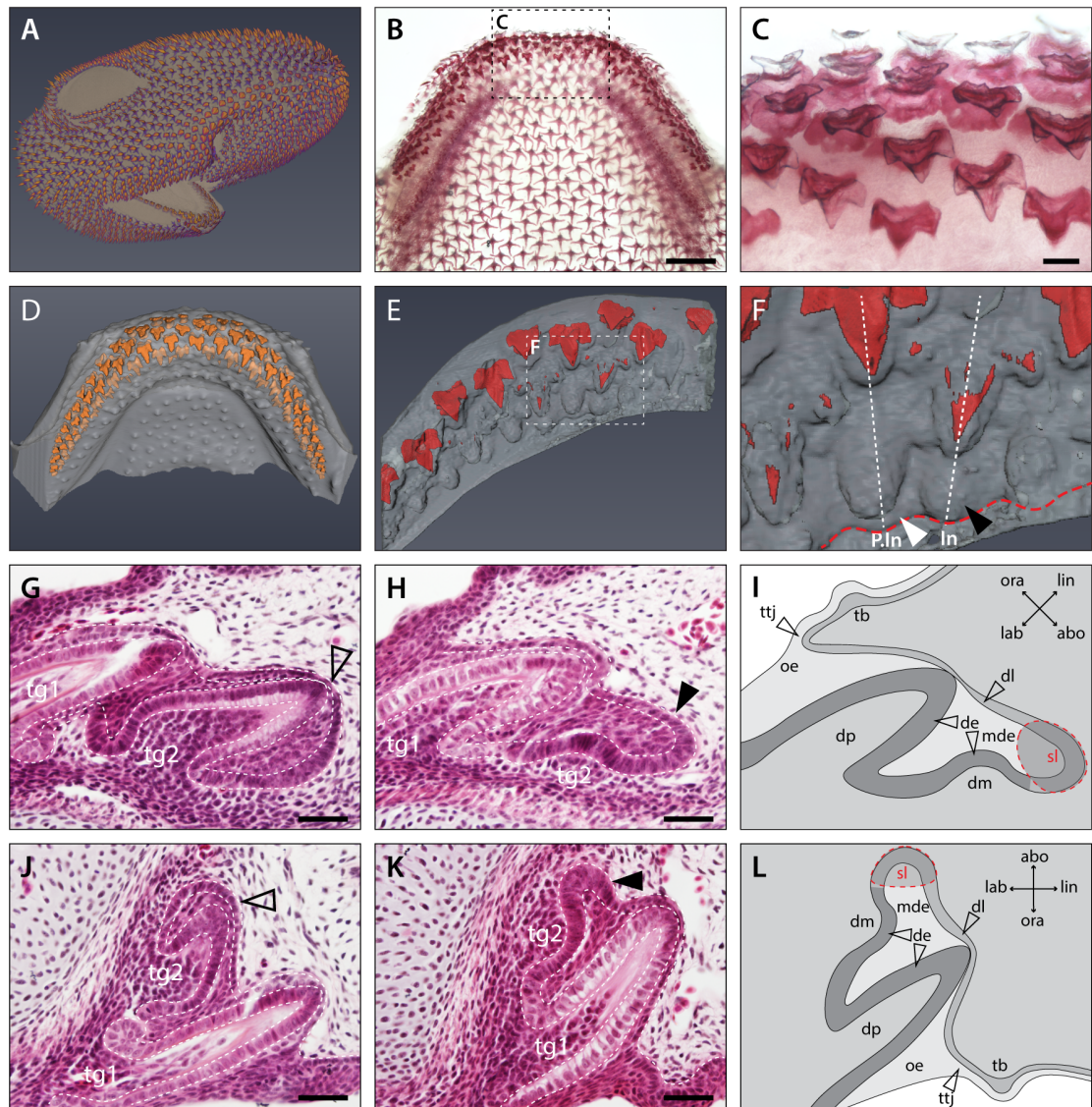


**Figure 1. Morphology and histology of the catshark dentition.** Micro computed tomography (CT) imaging of a Stage 34 catshark head depicts mineralised denticles on the skin surface and teeth in the mouth (A). Manual CT segmentation of the lower jaw (D) reveals the DL, and newly developing dental generations (E). A magnification of E (white dotted box) allows the comparison of adjacent tooth families in pre-initiation (white arrowhead), and initiation stage (black arrowhead). Histological staining with haematoxylin and eosin on sagittal cross sections of Stage 32 lower (G and H) and upper jaws (J and K), reveal the development of new tooth generations from the SL. G and J are in pre-initiation stage (shown three dimensionally in F ‘P. In’ white dotted line). H and K are in initiation stage (shown three dimensionally in F: ‘In’ white dotted line). Schematic representations of lower (I) and upper jaw (L) during dental initiation stage show the boundary between different dental tissues and axes. Scale bars are 1mm in B, 250µm in C, 50µm in G, H, J and K. ttj; taste-tooth junction, tb; taste bud, oe; oral

epithelium, dp; dental papilla, dl; dental lamina, de; dental epithelium, dme; middle dental epithelium, dm; dental mesenchyme, sl; successional lamina, ora; oral, abo; aboral, lin; lingual, lab; labial, tg1; tooth generation 1; tg2, tooth generation 2, P.in; pre-initiation stage, In; initiation stage.

successional regeneration, with the youngest teeth positioned aborally at the base of the DL and the oldest erupting from the DL at the oral surface (Fig 1G-L) (Martin *et al.*, 2016). Each row is a defined tooth family, with all teeth connected along a continuous jaw length DL (Fig 1E).

Adjacent tooth families are staggered in their development, preventing adjacent teeth from overlapping. Manually segmented CT scans reveal this asynchronous timing in dental initiation. Visible undulations associated with each tooth family can be seen at the aboral tip of the SL (Fig 1F). Histological staining of sagittal cross sections at equivalent sites along the jaw provide further insight into the relationship between tooth developmental stage and SL (Fig 1G-L). During dental morphogenesis, the SL retracts towards the developing tooth (Fig 1G and J). At this stage, the SL is in pre-initiation, marked by an absence of proliferation of Sox2+ dental progenitor cells (Martin *et al.*, 2016). Simultaneously, the adjacent tooth family is undergoing initiation. During this stage there is a visible outgrowth of the SL both in three-dimensional CT segmentation (Fig 1F: black arrowhead) and in sagittal cross section (Fig 1H and K). Initiation of dental regeneration corresponds to a significant increase in activated  $\beta$ -catenin expression and cellular proliferation throughout the SL, including Sox2+ dental progenitors, suggesting a role for canonical Wnt signalling in the regulation of this process (Martin *et al.*, 2016).

### *RNAseq analysis of dental sub-regions*

We wanted to identify novel candidate markers involved in regulating the onset of dental regeneration within the DL. In order to do this, we micro-dissected and carried out RNAseq on dental sub-regions associated with different stages of odontogenesis in hatchling catsharks (*S. canicula*). In total five sub-regions were dissected (Fig 2A): the taste-tooth junction (TTJ) which houses Sox2+ progenitors which contribute to both the teeth and taste buds (Martin *et al.*, 2016); SL which both houses dental progenitors and is the site of dental initiation (Martin *et al.*, 2016; Rasch *et al.*, 2016); early teeth (ET), including teeth in bud and cap stage; and late teeth (LT), those undergoing matrix secretion and mineralisation. The taste bud region associated with the basi-hyal (BHTB) was used as a ‘taste’ outgroup in order to identify novel candidates associated with the TTJ but absent from the BHTB. Hatchling catsharks were used for this analysis given that during embryogenesis high rates of cellular proliferation are observed within the oral tissues due to growth of the animal. It is therefore difficult to distinguish between molecular signalling associated with regeneration and that associated with general embryogenesis.

Following RNA sequencing and *de novo* transcriptome assembly, differential expression analysis (edgeR (Robinson *et al.*, 2009)) was carried out to highlight markers of interest, specifically markers that are differentially expressed within the SL. A stringent false discovery rate (FDR<0.001) was used in order to minimise false positives. We also filtered candidates which exhibited a fold expression change (FC)

greater than 2 in one tissue, relative to any of the other tissues. In total there were 3506 differentially expressed genes which met this criteria ( $FDR < 0.001$ ,  $FC > 2$ ).

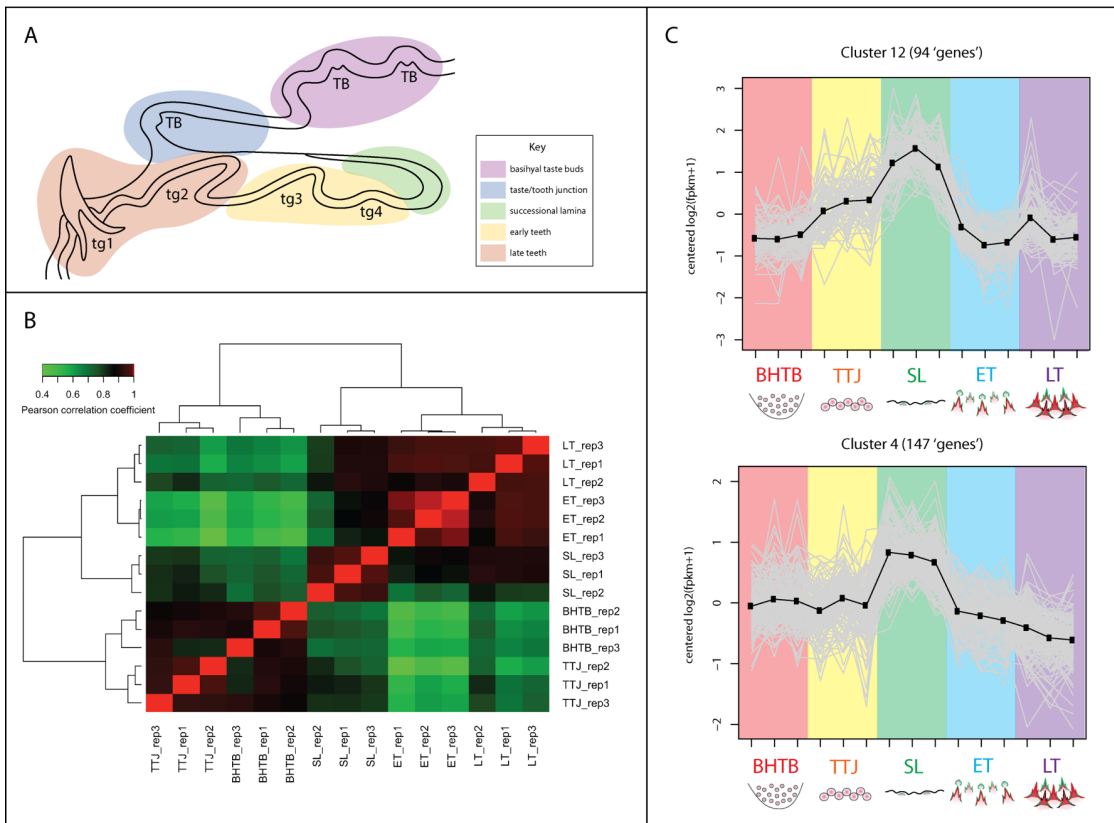


**Figure 2. RNAseq of five micro-dissected dental sub-regions reveal markers upregulated within the SL.** A) Schematic of a sagittal cross section through a catshark lower jaw depicting the sub-regions analysed by RNAseq. B) Heatmap of differentially expressed markers ( $FDR < 0.001$ ,  $FC > 2$ ) from across all RNAseq tissue replicates. Samples are grouped based on their Pearson correlation coefficient. Green represents low Pearson correlation coefficients, therefore high levels of differential expression between tissue, and vice versa for red. Dendrogram branches reveal grouping of samples based on similarity in expression levels. Replicates of each tissue type group together within distinct nodes. C) 2 of 32 K-means clusters, which are categorised into the SL super-cluster. Expression levels (fpkm+1) have been log<sub>2</sub> transformed and median centred to allow for comparison between different genes. These clusters reveal genes, which are differentially expressed ( $FDR < 0.001$ ,  $FC > 2$ ) in the SL relative to at least one other tissue type. TB, taste bud; tg, tooth generation; BHTB, basi-hyal taste buds; TTJ, taste tooth junction; SL, successional lamina; ET, early teeth; LT, late teeth.

In order to check the reliability of the RNAseq dissections, we carried out a Pearson correlation coefficient test on the transcript abundance values (TMM – edgeR (Robinson *et al.*, 2009)) of all differentially expressed genes (FDR<0.001, FC>2). This allowed for the grouping of tissue samples based on their similarity in expression (Fig 2B). For each of the tissue types, all replicates were clustered together into distinct dendrogram nodes. This shows that the tissue replicates are more closely related to each other than other tissue types. Furthermore, there is also observable sub-grouping. ET and LT samples cluster within a node, with their nearest neighbours being SL samples. In contrast TTJ and BHTB samples group within a separate node. This grouping of tissue types also reflects their position along their stages of dental development (Fig 2A), moving from taste territories (BHTB/TTJ), through to the SL, ET and LT.

Dental initiation takes place from progenitor cells at the tip of the SL (Martin *et al.*, 2016), therefore this region is the central focus of this analysis. 2609 genes are differentially expressed (FDR<0.001, FC>2) within the SL relative to other tissues. Given this large number, identifying potential candidates involved in stem cell regulation and dental initiation is problematic. As a result, we carried out various filtering steps to narrow down key targets. Firstly, k-means clustering of genes based on their change in expression between different tissue types serves as a useful tool in identifying markers with similar expression patterns between tissues of interest. For our RNAseq analysis, we clustered differentially expressed genes into 32 k-means clusters. This was to provide enough resolution as to see clear clusters, which change in expression between different tissue types, whilst not creating too many clusters that would fail to identify potential correlations between markers which subtly differ in their

expression patterns. These clusters can be attributed to specific tissues, for example clusters 4 and 12 (Fig 2C) show markers that were upregulated in the SL but downregulated in other dental tissues.

### *RNEA predicted Gene Regulatory Networks during dental initiation*

Classically, GRNs serve as a tool for describing gene interactions. These interactions require functional testing before we assume that they are real. However, predictive GRN analysis can also serve as a tool to identify novel candidates involved with a process of interest. We used a combination of predictive GRN analysis and prior system knowledge to generate informative GRNs highlighting potential novel candidates involved in the regulation of initiation of dental regeneration. Putative interactions were predicted using the Regulatory Network Enrichment Analysis tool (RNEA) (Chouvardas *et al.*, 2016). RNEA functions through projecting differentially expressed genes derived from transcriptome analyses, onto a reference map of known regulatory interactions (Chouvardas *et al.*, 2016).

Given the large number of differentially expressed genes in our analysis, we filtered our dataset by choosing biologically relevant k-means sub-clusters. These sub-clusters were organised into ‘super-clusters’, which were comprised of groups of different tissue types, e.g. TTJ/SL, TTJ/SL/ET. A total of 10 sub-clusters associated with 4 super-clusters (TTJ/SL, SL, SL/ET, TTJ/SL/ET), containing 1147 genes were included in the RNEA analysis. RNEA is able to add supplementary nodes, which are not initially included in the dataset if it deems them statistically important. The resulting GRN (Fig

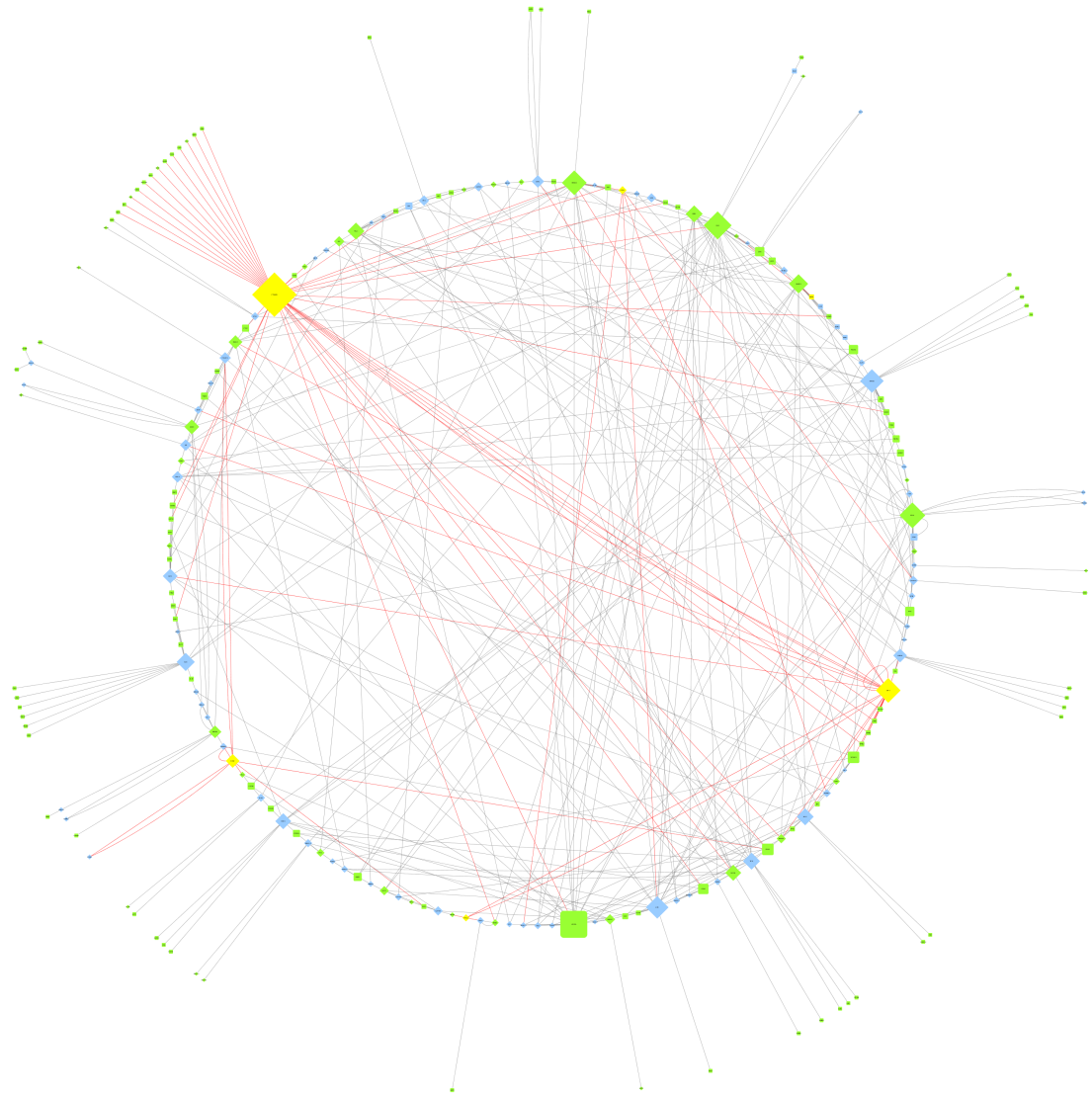


**Figure 3. SL global GRN.** GRN generated using Regulatory Network Enrichment Analysis (RNEA) (Chouvardas et al. 2016). Genes from 10 k-means clusters (4, 5, 9, 10, 12, 13, 19, 20, 22, 32) categorised into 4 super-clusters (SL, TTJ/SL, SL/ET, TTJ/SL/ET) were included in the analysis. Lines between nodes depict predicted interactions. Diamond nodes are transcription factors. Green nodes are differentially expressed markers (FDR<0.001, FC>2) belonging to the included k-means clusters. Blue nodes are nodes secondarily added by RNEA as deemed statistically important. Yellow nodes are key central nodes used to subset the network (Pitx1, Pitx2, Sox2, Lef1, Ctnnb1, and Bmp4). Red edges indicate interactions with these central nodes. Size of node reflects the number of interactions at a given node.

3) shows the predicted interactions within these sub-clusters. This GRN contains 218 genes, with 144 from the differentially expressed dataset and 74 secondarily added by RNEA. The high degree of interconnectivity and large number of nodes present within the global SL GRN make it difficult to analyse experimentally.

#### *Sub-setting GRNs based on prior knowledge of gene interactions*

Using pre-defined markers to treat as central nodes in the network can help to reduce the size of the predictive GRN. Our previous knowledge of dental development can serve as an initial reference point for establishing a concise list of primary markers. Over the past decade, Sox2 has been highlighted as a key marker of stem-potential within the DL. Simultaneously, canonical Wnt signalling (specifically  $\beta$ -catenin and *lef1*) regulates dental initiation from Sox2+ cells (Gaete and Tucker, 2013; Martin *et al.*, 2016). Markers including *bmp4*, *pitx1* and *pitx2* have also been shown to regulate the onset of odontogenesis in first generation teeth (St.amand *et al.*, 2000; Thesleff, 2003; Fraser *et al.*, 2004), whilst their importance in the regulation of regeneration is less well known.

To characterise the expression of these markers in dental regeneration in the catshark, we carried out sagittal section *in situ* hybridisation on late stage 32 embryos (St32L) (Ballard *et al.*, 1993) during which the second dental generation forms (Fig 4). *sox2* can be seen expressed in the tip of the SL (Fig 4A: black arrowhead) as well as within cells of the DL which connects with the TTJ on the oral surface. Sox2+ cells within the DL and SL mark dental progenitors from which teeth develop (Martin *et al.*, 2016). In



contrast, *β-catenin* is expressed in cells positioned more labially where new dental placodes form (Fig 4B: white arrowhead). This is in agreement with previous work in the catshark, which described the isolation of Sox2/*β-catenin*, except for during a short period in dental initiation when they are co-expressed (Martin *et al.*, 2016). Wnt readout, *lef1* is absent from the SL, but is highly expressed within the dental epithelium during placode formation (Fig 4C). *pitx1* and *pitx2* are both expressed within the middle dental epithelium (a stellate reticulum-like, group of stratified squamous epithelial cells (Martin *et al.*, 2016) (Fig 1I)), and the columnar basal epithelium of the SL (Fig 4D and E), seemingly within the same region of the SL which expresses *sox2* (Fig 4D and E: black arrowhead). However, *pitx1* and *pitx2* differ in their expression within the tooth-forming region. *pitx1* is expressed throughout the dental epithelium in both early and late teeth, whereas *pitx2* is restricted to the dental mesenchyme.

The expression of *bmp4* during dental morphogenesis is well documented. Its expression has also been found within the lingual dental epithelium in the ferret (Jussila *et al.*, 2014), where Sox2 is also expressed (Juuri *et al.*, 2013), however its role in the regulation of these dental progenitors is not known. We find *bmp4* upregulated within the dental mesenchyme and dental epithelium of developing teeth, and note its absence within the cusp forming enameloid knot. It is also expressed within the mesenchyme underlying the dental initiation site (Fig 4F: white arrowhead), with weak expression within the SL region housing dental progenitors (Fig 4F: black arrowhead). The function of these markers during dental regeneration requires further investigation, however their expression patterns render them useful targets for the identification of novel odontogenic markers in the SL.

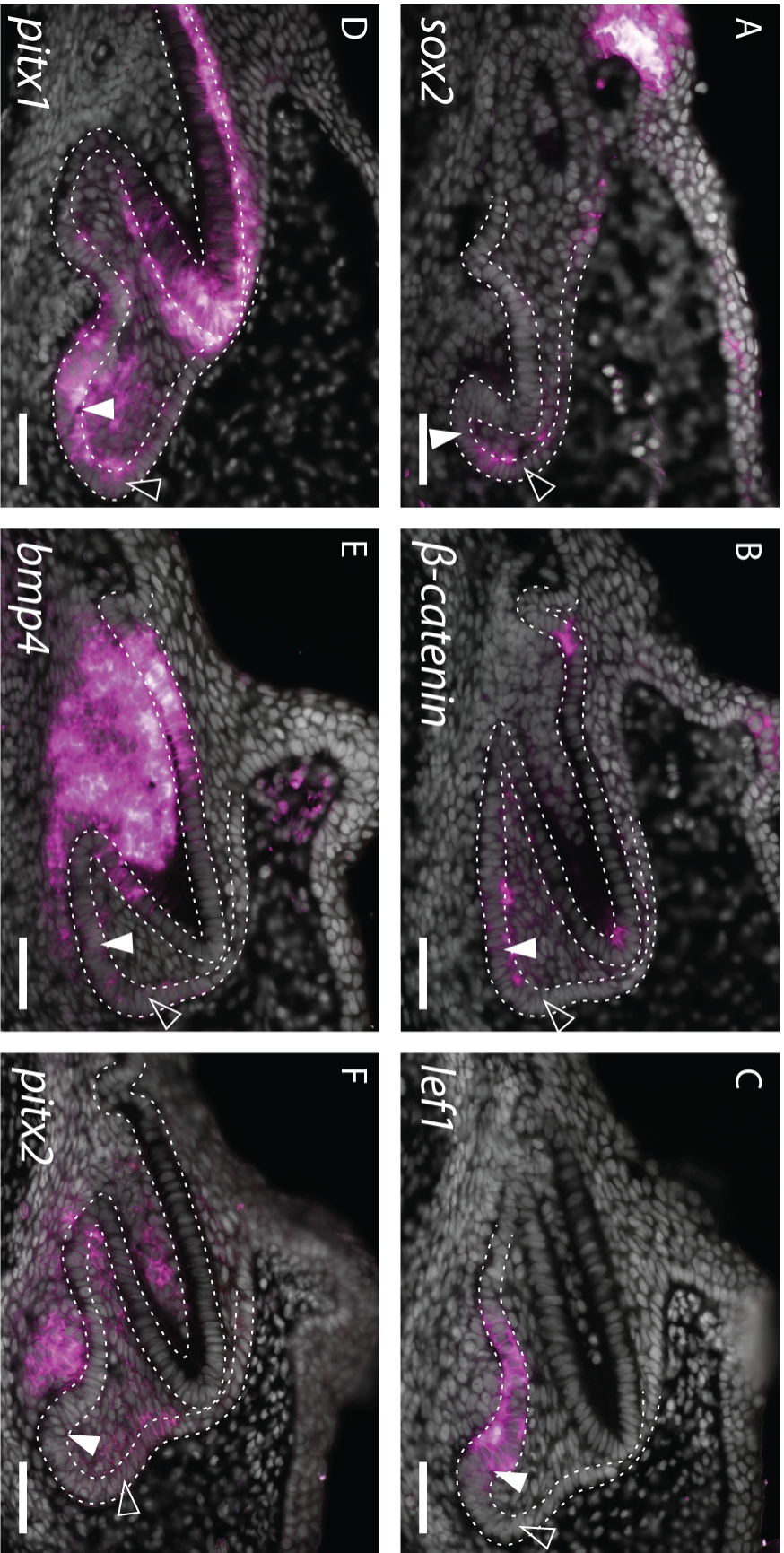


**Figure 4. Expression of known odontogenic markers.** *In situ* hybridisation of sagittal sections of late stage 32 catshark reveal expression of *sox2* (A),  $\beta$ -*catenin* (B), *lef1* (C), *pitx1* (D), *bmp4* (E) and *pitx2* (F) in the lower jaw. *sox2*, *pitx1*, *bmp4* and *pitx2* are expressed within the SL (black arrowhead).  $\beta$ -*catenin*, *lef1* and *pitx1* are expressed within the epithelium at the site of dental initiation (white arrowhead). *bmp4* and *pitx2* are expressed within the dental mesenchyme underlying the dental initiation site. White dotted lines depict the columnar basal epithelial cells of the DL and dental epithelium. Gene expression is false coloured in magenta. DAPI nuclear stain is false coloured in grey. Scale bars are 50 $\mu$ m.

By treating *lef1*, *sox2*,  $\beta$ -*catenin*, *pitx1*, *pitx2* and *bmp4* as central nodes in the global SL GRN (Fig 3), we were able to reduce the number of GRN markers from 218 to 63 (Fig S1). This process only retains markers that interact directly with at least one of the six central nodes. Whilst this is reductive, it can be used to gauge primary markers of importance, which can then become central nodes and further expand the refined network. Although this filtering process has dramatically reduced the number of nodes, the network still remains unfeasibly large to test experimentally. For example,  $\beta$ -*catenin* (*Ctnnb1*) still possesses interactions with 38 other markers.

Within the new network, markers that were not differentially expressed within the SL k-means clusters but were instead secondarily added by RNEA (Fig S1: blue markers) were not prioritised. It is important to note that these markers may still play an important role in odontogenesis and may merely be expressed throughout various dental tissues. However, these are labelled as markers of secondary importance as they are not specifically upregulated within these sub-clusters. Following this initial filtration of the new network, we prioritised the remaining markers for *in situ* hybridisation based on their associated UniProt functions and connectivity in the GRN. Markers that were

either, not cloned for *in situ* hybridisation or showed no positive expression were deleted from the final GRN (Fig 5).

#### *Gene Ontology (GO) enrichment analysis*

GO enrichment analysis of the differentially expressed super-clusters included in the GRN analysis (TTJ/SL, SL, SL/ET, TTJ/SL/ET) revealed that GO terms GO:0016055 (Wnt signalling pathway) and GO:0090090 (negative regulation of canonical Wnt signalling pathway) were significantly enriched in these clusters ( $p < 0.001$ ) relative to the whole transcriptome (Fig S2A). 11 out of 29 (GO:0090090) and 9 out of 26 (GO:0016055) of the markers associated with these GO terms remained in our GRN after subsetting the network using central nodes (Fig S1 and Fig S2B). These results further highlight the importance of Wnt signalling within SL related k-means clusters and within our GRN.

#### *Expression of predictive SL GRN markers*

Following GRN sub-setting (Fig 5A), markers were cloned for *in situ* hybridisation (Fig 5B-O). *smad1*, *smad7*, *bambi*, *fgf3*, *msx2* and *wnt11* were not found expressed within the SL, instead upregulated within the developing teeth. Of these markers, all but *wnt11* were found within either TTJ/SL/ET or SL/ET super-clusters. This could explain their high expression levels within developing early teeth. Simultaneously, the presence of these markers within a SL GRN could be a limitation of the initial micro-dissections prior to RNAseq analysis and the difficulty of working with heterogeneous cell

populations.

Two *foxl1* transcripts were initially found differentially expressed within the SL, however phylogenetic analysis identifies these markers as *foxl1* and *foxl1-like* (Fig S3). *In situ* hybridisation for both of these markers (Fig 2B-C) reveal subtle differences in their expression patterns in the teeth. Both markers are weakly expressed within the dental epithelium, however *foxl1* is also found within the dental papilla. Furthermore, they are both expressed within the epithelium at the SL dental initiation site. Foxl1 has been identified as a direct target of Hh signalling, with binding sites for the Hh signalling mediator Gli2, found within Foxl1 non-coding sequences throughout vertebrates (Madison *et al.*, 2009). Concordant with *foxl1* expression, we find *gli2* within the epithelium of the SL dental initiation site, whilst its expression also extends within the greater SL (Fig 2F). Interactions between *gli2* and *foxl1* may be regulating the proliferation of the dental epithelium, as is the case in intestinal villi (Madison *et al.*, 2009).

Runt-related transcription factor 2 (*runx2*) is expressed in the dental papilla during morphogenesis and dental mesenchyme in bell stage teeth (Fig 5G). Its expression is thought to regulate dental development prior to bell-stage, with its downregulation in later stages regulating odontoblastic differentiation (Chen *et al.*, 2009b). We also note its expression within the stratified epithelial cells of the middle dental epithelium, whilst it is absent from the distal most basal epithelial cells of the SL, corresponding with the Sox2+ progenitor cell niche (Martin *et al.*, 2016). *axin2* (Fig 5H), a readout of canonical Wnt signalling shares a similar expression pattern as *lef1* (Fig 4C) within the dental

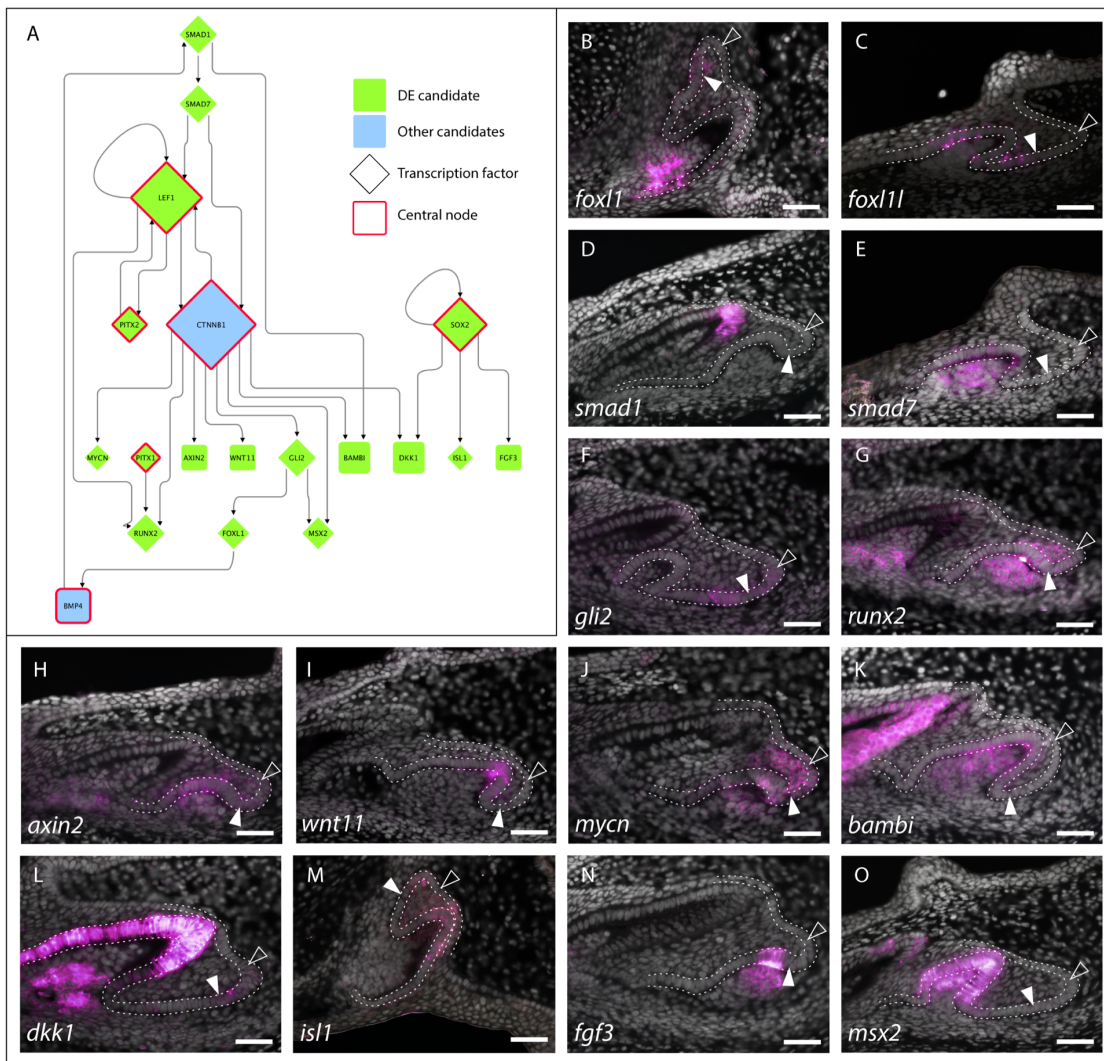


**Figure 5. Filtered SL GRN analysed through *in situ* hybridisation.** GRN filtered from SL global GRN generated by RNEA reveals potential novel candidates involved in dental initiation (A). Lines between nodes depict predicted directional interactions. Diamond nodes are transcription factors. Size of node reflects the number of interactions at a given node. Red node outline marks central nodes, with other markers interacting with at least one red node. Central nodes include Pitx1, Pitx2, Ctnnb1 ( $\beta$ -catenin), Lef1 and Bmp4. Green nodes are differentially expressed markers (FDR<0.001, FC>2) belonging to the included k-means clusters. Blue RNEA nodes have been removed from the network, except for ctnnb1 and bmp4 which are central nodes. The expression of each new candidate (candidates not outlined in red) has been examined through sagittal section *in situ* hybridisation (B-O). Images B and M are of upper catshark jaws, whereas C-L and N-O are of lower jaws. *foxl1l* (C), *smad1* (D), *smad7* (E), *wnt11* (I), *bambi* (K), *fgf3* (N) and *msx2* (O) are all absent from the SL (white arrowhead). *foxl1* (B), *gli2* (F), *runx2* (G), *axin2* (H), *mycn* (J), *dkk1* (L) and *isl1* (M) are all expressed within the

SL (white arrowhead). *runx2* (G), *axin2* (H) and *mycn* (J) are also expressed within the MDE (black arrowhead). Gene expression is false coloured in magenta. DAPI nuclear stain is false coloured in grey. Scale bars are 50µm.

epithelium of bud stage teeth, although the expression of *axin2* notably weaker. *islet1* (*isll*) shows weak expression within the teeth; its expression can be seen in both the dental epithelium and within the SL (Fig 5M).

Dickkopf is a potent antagonist of the Wnt signalling pathway, with its ectopic expression leading to a complete loss of hair, tooth and mammary gland development in mice (Andl *et al.*, 2002). During catshark tooth development, we observe *dkk1* strongly expressed throughout the dental epithelium and dental papilla, as well as weakly within the SL (Fig 5L). Given that canonical Wnt signalling is known to be critical in the regulation of epithelial appendage initiation, Dkk1 is a prime target deserving of further investigation.

Finally, the bHLH transcription factor *mycn* (N-Myc Proto-oncogene) is expressed within the dental epithelium and dental mesenchyme of early bud stage teeth. It is also expressed throughout the SL (Fig 5J). Mycn has been well described in the maintenance of neural progenitors (Knoepfler *et al.*, 2002). It is a proto-oncogene which functions to maintain cells in an undifferentiated state and has been identified as critical for maintenance of neural crest stem cells (Zhang *et al.*, 2016).

*Expression of SL markers in conjunction with Sox2*

Given the expression of *pitx1*, *lef1*, *bmp4*, *dkk1* and *mycn* within the SL, we further investigated their roles during dental regeneration. These markers were chosen as a result of: (i) previous research on their involvement in dental initiation; (ii) their expression patterns within the SL; and/or (iii) their known role in canonical Wnt signalling. Furthermore, *pitx3* was also included in this analysis, as it was more than 2-fold upregulated in the SL than any other tissue (Fig S5) and given the importance of both *pitx1* and *pitx2* during the onset of odontogenesis (St.amand *et al.*, 2000; Thesleff, 2003; Fraser *et al.*, 2004). Across the five oral tissues dissected for RNAseq, we find all of these markers upregulated within the SL and/or ET relative to other dental tissues (Fig S5). In order to characterise their expression within the catshark SL, we carried out double sagittal section *in situ* hybridisation/immunohistochemistry revealing their expression together with Sox2 (Fig 6).

Sox2 is expressed within taste buds at the TTJ on the oral surface and throughout the DL. A stream of Sox2 expression connects epithelial cells on the oral surface to the dental progenitor niche within the SL (Fig6A-F), with epithelial cell migration known to occur from the TTJ to the SL (Martin *et al.*, 2016). *lef1* can be seen expressed within the dental initiation site (Fig6A1a), but is notably absent within Sox2+ cells of the SL (Fig6A1c). There is an abrupt expression boundary between *lef1* and Sox2 (Fig6A1c), suggesting a role for canonical Wnt signalling in dental initiation outside of Sox2+ dental progenitors. Intriguingly, *dkk1* is found in a similar pattern within the dental initiation site (Fig6C1a). However, it is also see expressed within the distal most Sox2+ cells of the SL (Fig 6C1c). Given its role in antagonising canonical Wnt signalling, *dkk1*



may be working in conjunction with other Wnt signals in mediating the activation of dental progenitors during dental initiation. We also identify co-expression of a novel dental marker *mycn* in Sox2+ SL cells (Fig 6F1c and S6A1c). Unlike other markers studied (Fig 6), we also note *mycn* upregulation within the lingual DL, which connects the SL to the oral surface, and within Sox2+ taste bud cells at the TTJ (Fig S6A).

*bmp4* is expressed throughout a range of dental tissues during dental development. We observe its expression strongly upregulated within the dental papilla, and throughout the dental epithelium –although absent from the enameloid knot (Fig 6B). Its mesenchymal expression extends below and surrounding the epithelial dental initiation site. Within the SL, *bmp4* is restricted to basal epithelial cells (Fig 6B1a). As described by Jussila et al. (2014), we also note its co-expression with Sox2 within the SL, albeit within only a few cells (Fig 6B1c).

Members of the Pituitary homeobox family (Pitx) are known to be involved in multiple stages of dental development. *pitx1* and *pitx2* are both expressed in the oral epithelium prior to the invagination of the DL in the catshark (Debiais-Thibaud et al., 2015; Rasch et al., 2016). As a result of its early expression within the odontogenic band prior to dental initiation *pitx2* has been described as a odontogenic-commissioning gene (Fraser et al., 2008). Within our RNAseq dataset, we find *pitx1*, *pitx2* and *pitx3* differentially expressed within SL-related super-clusters (SL; TTJ/SL/ET; and TTJ/SL/ET respectively). *pitx1* is upregulated in the TTJ and SL, before being downregulated in the ET (Fig S5). In contrast *pitx3* is dramatically upregulated (>2fold relative to any other

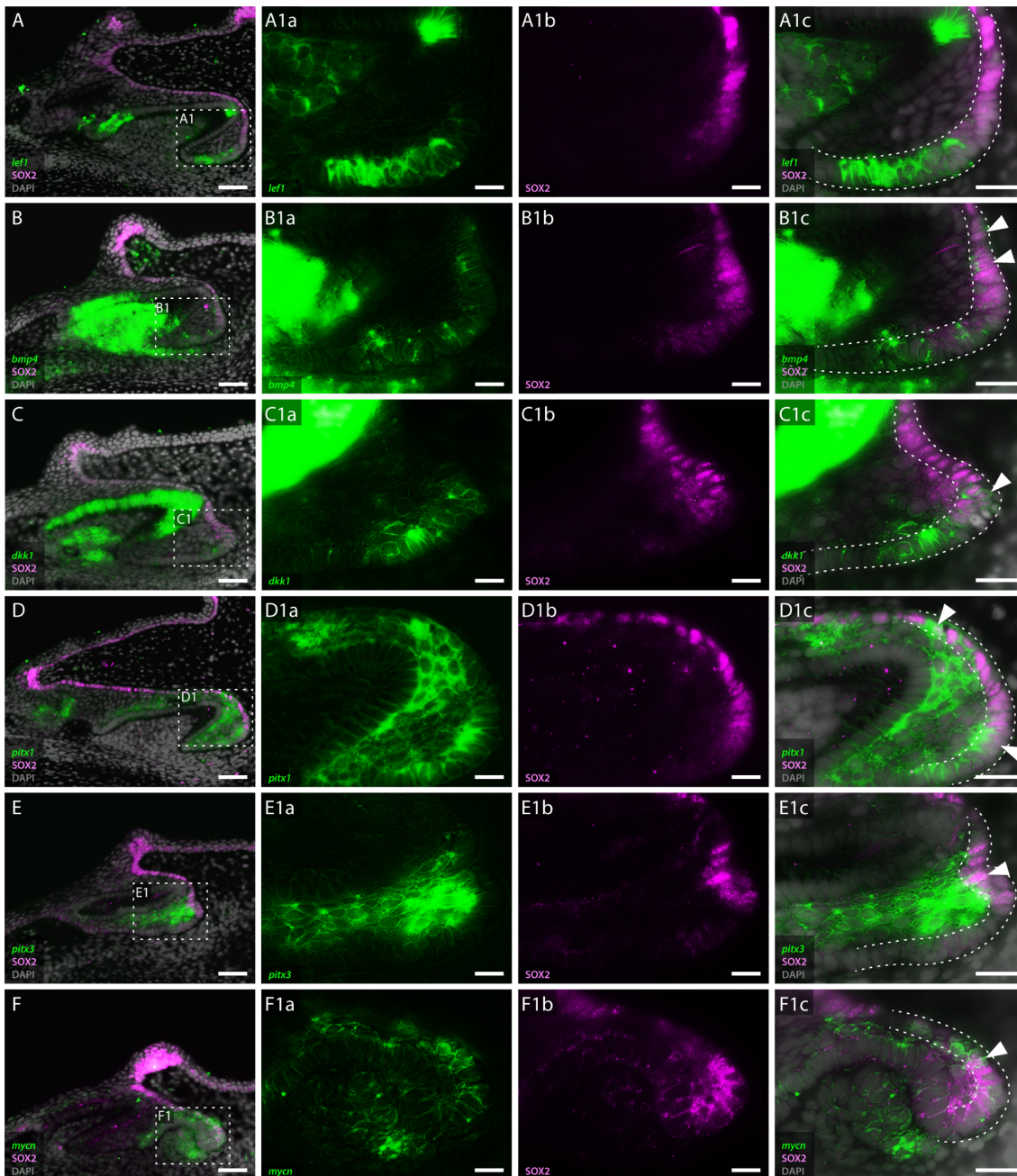


**Figure 6. Co-expression of key SL markers with SOX2.** Double section *in situ* hybridisation/immunohistochemistry on catshark lower jaws reveals co-expression of *in situ* hybridisation markers with SOX2 within the SL. Genes investigated with *in situ* hybridisation include *lef1* (A), *bmp4* (B), *dkk1* (C), *pitx1* (D), *pitx3* (E) and *mycn* (F). SOX2 is found within the taste bud on the oral surface and forms a stream of expression throughout the DL (A-F). Its expression stops abruptly at the tip of the SL (A-F1b). *lef1* (A) is expressed within the enamel knot and the new tooth forming region (A1a), but is not co-expressed with SOX2 (A1c). *bmp4* (B) is expressed within the dental mesenchyme and dental epithelium, although it is absent from

the enamel knot. It also shows weak expression within the SL (B1a), and is co-expressed with a basal epithelial cells of the SL (B1c). *dkk1* is strongly expressed in the dental epithelium and dental mesenchyme and is also expressed within the new tooth forming region (C1a). The limit of its expression sees it co-expressed with SOX2 at their boundary (C1c). *pitx1* (D) and *pitx3* (E) are both expressed within the MDE. The expression of *pitx1* extends further orally and into the basal epithelium of the SL (D1a). Both *pitx1* and *pitx3* are co-expressed with SOX2 within the SL (D1c and E1c). *mycn* (F) is found within the dental mesenchyme and the MDE (F1a). It is also extensively co-expressed with SOX2 within the basal epithelium of the SL (F1c). Gene expression is shown in green, SOX2 protein expression is in magenta and DAPI nuclear stain in grey. Dotted white boxes in A-F depict magnified region in A1-F1. White arrowheads in A1c-F1c highlight regions of co-expression between *in situ* markers and SOX2 in the SL. Scale bars are 50µm in A-F, and 25µm in A1(a-c)-F1(a-c).

tissue) in the SL before being downregulated in the ET and LT (Fig S5). Both *pitx1* and *pitx3* are expressed within the middle dental epithelium (MDE) of the SL (Fig6D, D1a, F and F1a). *pitx1* extends orally throughout the epithelium, towards the TTJ, reflecting its expression within the RNAseq analysis (Fig S5). *pitx1* is also expressed throughout the basal epithelial cells of the SL, co-expressed with Sox2<sup>+</sup> cells (Fig 6D1c). The extent of *pitx3*/Sox2 co-expression is more restricted, although there is still observable co-expression at the distal tip of the SL (Fig 6E1c). The expression of Pitx genes within the SL, and their co-expression with Sox2<sup>+</sup> cells, highlights a role for this pathway in not only dental development but also dental regeneration.

## Discussion

This study has led to a *de novo* transcriptome assembly of an emerging polyphyodont model, which can serve as a reference point for further dental regenerative research. Our

results show that predictive GRNs serve as a useful tool to identify key markers of interest from an extensive RNAseq dataset. Through utilising previous knowledge to subset a global reference GRN, we generate a sub-network, which contains multiple markers expressed within the SL. These markers include *runx2*, *gli2*, *isl1* and *foxl1*. Furthermore, this analysis led to the identification of the proto-oncogene, *mycn*, which we find expressed within Sox2+ dental progenitors for the first time.

Previous polyphyodont research has been based mainly on the candidate approach for the study of successional dental regeneration. This has inevitably relied heavily on research in mammals, which do not exhibit lifelong successional dental regeneration. Nevertheless, this approach has vastly improved our understanding of dental development and regeneration. Lineage tracing experiments revealed that Sox2+ cells in the adult originate from Sox2+ cells in the embryo (Arnold *et al.*, 2011). Although it had been previously found within taste buds (Okubo *et al.*, 2006), the first description of its expression in teeth came from the cervical loop stem cells of the continuously growing mouse incisor (Juuri *et al.*, 2012). Since then, it has been identified within dental stem cells of all polyphyodonts studied, including reptiles (Gaete and Tucker, 2013; Juuri *et al.*, 2013), teleosts (Thiery *et al.*, 2017) and sharks (Martin *et al.*, 2016). It has now become a hallmark of dental regenerative potential and has revealed an ancient link between teeth and taste buds in the evolution of polyphyodonty (Martin *et al.*, 2016).

The importance of the candidate approach cannot be understated; however, our results demonstrate the efficacy of taking a transcriptome based approach in an emerging

polyphyodont model in order to reveal novel markers expressed during successional regeneration. We describe the expression of *mycn* during dental regeneration for the first time. Its role in neural development has been extensively studied and is known to regulate proliferation and the cell cycle in neural progenitors (Knoepfler *et al.*, 2002; Zhang *et al.*, 2016). It is a target of canonical Wnt signalling, with its downregulation leading to differentiation of neuroblastoma cells (G. Brodeur, R. Seeger, M. Schwab, 1984; Szemes *et al.*, 2018). We identify its expression strongly upregulated within Sox2+ SL cells (Fig 6F1c and S6c) as well as within Sox2+ cells at the TTJ (Fig S6A). However, *mycn* expression is significantly lower within the TTJ relative to the SL (Fig S5). The extensive co-expression of *mycn* with Sox2 in the SL together with its role in neuroblastoma formation (Szemes *et al.*, 2018), implicates *mycn* in the cell cycle regulation of dental progenitors and the onset of odontogenic differentiation.

Models aimed at recreating GRNs from gene expression data have focussed on inferring networks solely using gene expression stochasticity or changes in expression under different conditions (e.g. ARACNE (Margolin *et al.*, 2006); GENIE3 (Huynh-Thu *et al.*, 2010); NARROMI (Zhang *et al.*, 2013); LBN (Liu *et al.*, 2016)). These models invariably lead to a number of false positives as they predict interactions based on co-correlated genes (Zuo *et al.*, 2017). As a result, networks derived from these models require experimental validation of predicted interactions. In this study, we identify *mycn* within our differentially expressed SL data set through predictive GRN reconstruction using RNEA and reveal its co-expression with Sox2 (Fig 6F). We use prior system knowledge to simplify our initial network to a key list of testable genes. *mycn* was not two fold upregulated within the SL, nor was it labelled a key marker of interest

following our GO enrichment analysis, revealing the importance of GRN reconstruction in this case. Although the ultimate goal is to both identify and understand interactions between genes during successional dental regeneration, we show that predictive GRNs can serve as a key tool in identifying novel candidates from transcriptome datasets, even in the absence of an annotated genome.

Aside from predictive GRN analysis, our differential expression analysis also identified the co-expression of a new marker with Sox2 in the SL. Pitx3 is a bicoid related transcription factor belonging to the paired-like homeodomain family (Semina *et al.*, 1998). The other two members of the Pitx family, Pitx1 and Pitx2, have both been implicated in the onset of odontogenesis (St.amand *et al.*, 2000; Thesleff, 2003; Fraser *et al.*, 2004). Although *pitx3* has been described during molar morphogenesis (Uchibe *et al.*, 2012), aside from negative expression (Debiais-Thibaud *et al.*, 2015), its expression during successional regeneration has not been described. We find *pitx3* more than two fold upregulated in the SL relative to any other tissue, and note its strong expression within the SL. The expression of both *pitx1* and *pitx3* within Sox2+ dental progenitors emphasises a key role for the Pitx gene family in not only the regulation of the first dental generation (St.amand *et al.*, 2000; Fraser *et al.*, 2004), but also successional regeneration.

### *Conclusion*

Despite a lack of information on gene interactions during dental regeneration, we find that predictive gene regulatory network (GRN) reconstructions, used alongside more

traditional RNAseq analysis approaches, serve as a useful tool in identifying candidate markers from initially extensive candidate lists. This work sets the groundwork for further in depth study of gene interactions, which regulate cyclical dental initiation and the overall study of dental regeneration.

## **Materials and Methods**

### *Animal husbandry*

The University of Sheffield is a licensed establishment under the Animals (Scientific Procedures) Act 1986. All animals were culled by approved methods cited under Schedule 1 to the Act. Catshark embryos (*S. canicula*) were obtained from North Wales Biologicals, Bangor, UK. Embryos were raised in recirculating artificial seawater (Instant Ocean) at 16°C. At the required stage, embryos were anaesthetised using 300mg/L MS-222 and fixed overnight in 4% paraformaldehyde at 4°C. Samples were then dehydrated through a graded series of DEPC-PBS/EtOH and kept at -20°C.

### *Paraffin sectioning and histology*

Following dehydration, samples were cleared with xylene and embedded in paraffin. 14µm sagittal sections were obtained using a Leica RM2145 microtome. For histological study, sections were stained with 50% Haematoxylin Gill no.3 and Eosin Y. Slides were mounted with Fluoromount (Sigma) and imaged using a BX51 Olympus compound microscope.

### *Micro-computed tomography (MicroCT)*

Catshark embryos were stained with 0.1% PTA (phosphotungstic acid) in 70% EtOH for 3 days to enhance contrast of soft tissues. Samples were imaged using an Xradia Micro-XCT scanner (Imaging and Analysis Centre, Natural History Museum, London). Volume rendering of the CT scans was carried out using the Avizo Lite software (Thermo Scientific). Manual segmentation of the DL in the lower jaw was carried out in order to visualise the DL three dimensionally.

### *RNAseq and differential expression analysis*

Five dental sub-regions were dissected from stage 34 (hatchling) catshark samples. The dental compartments included: the basi-hyal taste buds (BHTB); the taste-tooth junction (TTJ); the successional lamina (SL); the early developing tooth (ET); and the late stage developing tooth (LT). Tissue samples were flash frozen in liquid N<sub>2</sub> and added to TRIzol Reagent (Invitrogen) and homogenised in a tissue lyser. RNA was extracted using phenol/chloroform phase separation and further purified using the Qiagen RNeasy kit. RNA samples were sent for Illumina next-generation sequencing by the Sheffield Diagnostic Genetics Service at the Sheffield Children's Hospital. Three libraries were sequenced for each dental sub-compartment, with each library containing RNA from three pooled samples. Given the lack of a reference genome, a de-novo transcriptome was assembled using TRINITY (Grabherr *et al.*, 2011). FPKM (Fragments Per Kilobase of transcript per Million mapped reads) values were normalised to generate TMM (trimmed mean of M values) in order to compare transcript relative abundance between



tissue samples (Robinson and Oshlack, 2010). Predicted TRINITY ‘genes’ were annotated based on their closest UniProt BLAST match. Differential gene expression analysis was carried out using the *edgeR* package in R (Robinson *et al.*, 2009), in order to highlight potential markers of interest within specific dental sub-compartments. The expression levels of differentially expressed genes were compared between the different sub-compartments through calculating their Pearson correlation coefficients, and used to generate a heatmap (Fig 2).

### *RNEA analysis*

In order to highlight markers similar in their differential expression patterns, k-means clustering was used to separate differentially expressed genes into 32 clusters. k-means clusters were further grouped into ‘super-clusters’, depending on which tissue compartments a gene cluster is upregulated in. Four super-clusters associated with dental initiation (TTJ/SL, SL, SL/ET, TTJ/SL/ET) were filtered and ran through a Regulatory Network Enrichment Analysis (RNEA) (Chouvardas *et al.*, 2016). This tool predicts regulatory interactions for a given list of genes through interfacing with online databases (GO, KEGG, TarBase, TRED, TRRUST, TFactS and ORegAnno) and generates a network map revealing these interactions. Gene network maps were visualised in Cytoscape 3.5.1. In order to determine a refined gene regulatory network (GRN), we used prior knowledge of gene expression within the catshark SL in order to filter the RNEA generated predictive GRN. We treated six markers (*ctnbn1*, *pitx1*, *pitx2*, *lef1*, *sox2* and *bmp4*) as central nodes in the network, removing nodes which do not interact directly with at least one of these markers.

### *GO enrichment analysis*

Differentially expressed super-clusters (FDR<0.001, FC>2) associated with dental initiation (TTJ/SL, SL, SL/ET, TTJ/SL/ET) were submitted as a gene list to DAVID (Huang, Brad T Sherman, *et al.*, 2009; Huang, Brad T. Sherman, *et al.*, 2009), and compared relative the whole catshark transcriptome. Over-represented GO terms were filtered based on p-value < 0.001.

### *RNAseq sequence of interest identity check*

ORFs for RNAseq sequences were predicted using Geneious 10.0.5 and compared *Callorhinchus milii*, *Latimeria chalumnae* and *Lepisosteus oculatus* genome annotations. In order to verify the identity of the RNAseq sequences of interest, protein coding sequences (CDS) were extracted for the gene of interest and closest sister genes, from ensembl.org. Sequences were extracted from a range of species. Species were chosen based on their phylogenetic position and included: *Anolis carolinensis*, *Ciona intestinalis*, *Danio rerio*, *Gallus gallus*, *Gasterosteus aculeatus*, *Latimeria chalumnae*, *Lepisosteus oculatus*, *Mus musculus*, *Oreochromis niloticus*, *Oryzias latipes*, *Pan troglodytes*, *Pelodiscus sinensis*, *Petromyzon marinus*, *Rattus norvegicus*, *Taeniopygia guttata*, *Takifugu rubripes* and *Xenopus tropicalis*. RNAseq and Ensembl sequences were aligned using MUSCLE (Edgar, 2004). A maximum likelihood tree was generated from 100 bootstrap replications using PHYML (Guindon and Gascuel, 2003)

with an LG substitution model. Resulting gene trees were checked to see if the gene of interest falls within the expected node.

#### *Probe synthesis*

*S. canicula* total RNA was extracted using phenol/chloroform phase separation and cleaned through EtOH/LiCL precipitation. RT-cDNA was made using the RETROscript 1710 kit (Ambion). Probes were made using forward and reverse primers designed through Primer3. Primer sequences are available in the supplementary information (Fig S7). Sequences of interest were amplified from the cDNA through PCR and ligated into the pGEM-T-Easy vector (Promega). Ligation products were cloned into JM109 cells. Plasmid DNA was then extracted from chosen colonies using a Qiaprep spin Mini-prep kit (Qiagen) and sequenced (Applied Biosystems' 3730 DNA Analyser) through the Core Genomics Facility, University of Sheffield. Verified vectors were then amplified through PCR and used as a template for probe synthesis. Sense and anti-sense probes were made using a Riboprobe Systems kit (Promega) and SP6/T7 polymerases (Promega). Probes were labelled with Digoxigenin-11-UTP (Roche) for detection during *in situ* hybridisation. A final EtOH precipitation step was carried out to purify the RNA probe.

#### *In situ hybridisation*

Sagittal paraffin sections were obtained as previously described. Slides were deparaffinised using Xylene and rehydrated through a graded series of EtOH/PBS.

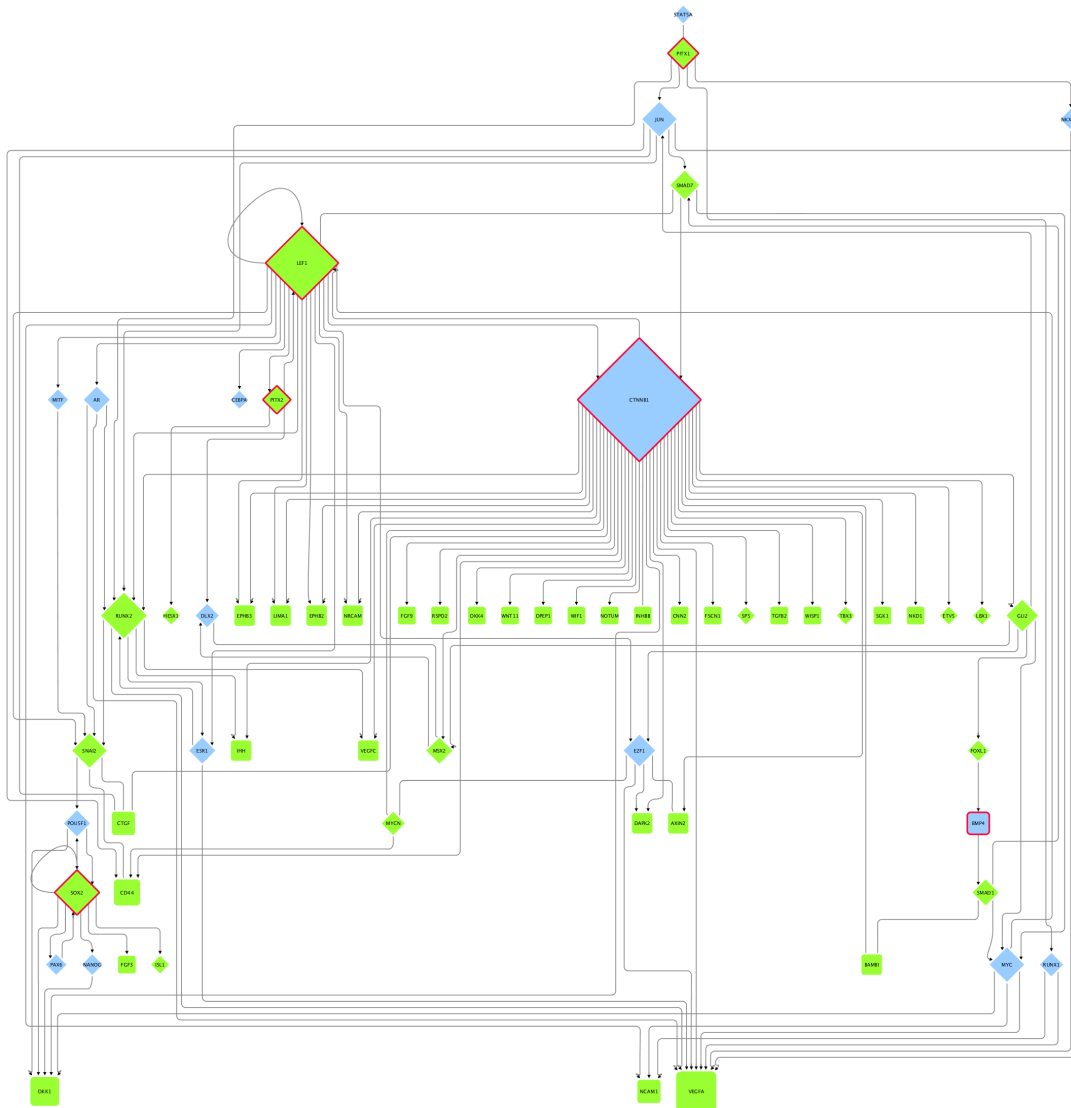
Slides were incubated in pre-heated pre-hybridisation solution pH 6 [250ml deionised-formamide, 125ml 20x saline sodium citrate (SSC), 5ml 1M sodium citrate, 500µl Tween-20 and 119.7ml DEPC-treated ddH<sub>2</sub>O] at 61°C for 2 hours. Slides were transferred to pre-heated pre-hybridisation solution containing DIG labelled RNA probe (1:500) and incubated overnight at 61°C. The following day, slides underwent a series of 61°C SSC stringency washes to remove unspecific probe binding [2x30m 50:50 pre-hybridisation solution: 2x SSC; 2x30m 2x SSC; 2x30m 0.2x SSC]. Following the stringency washes, samples were incubated in blocking solution (2% Roche Blocking Reagent (Roche)) for 2hr at room temperature and then incubated in blocking solution containing anti-Digoxigenin-AP antibody (1:2000; Roche) overnight at 4°C. Excess antibody was washed off through 6x1hr MAB-T (0.1% tween-20) washes. Slides were then washed in NTMT and colour reacted with BM-purple (Roche) at room temperature and left until sufficient colouration had taken place. Following the colour reaction, a DAPI nuclear counterstain (1µg/ml) was carried out before mounting the slides using Fluoromount (Sigma). Images were taken using a BX51 Olympus compound microscope. Images were contrast enhanced and merged in Adobe Photoshop.

#### *Double in situ hybridisation/immunohistochemistry*

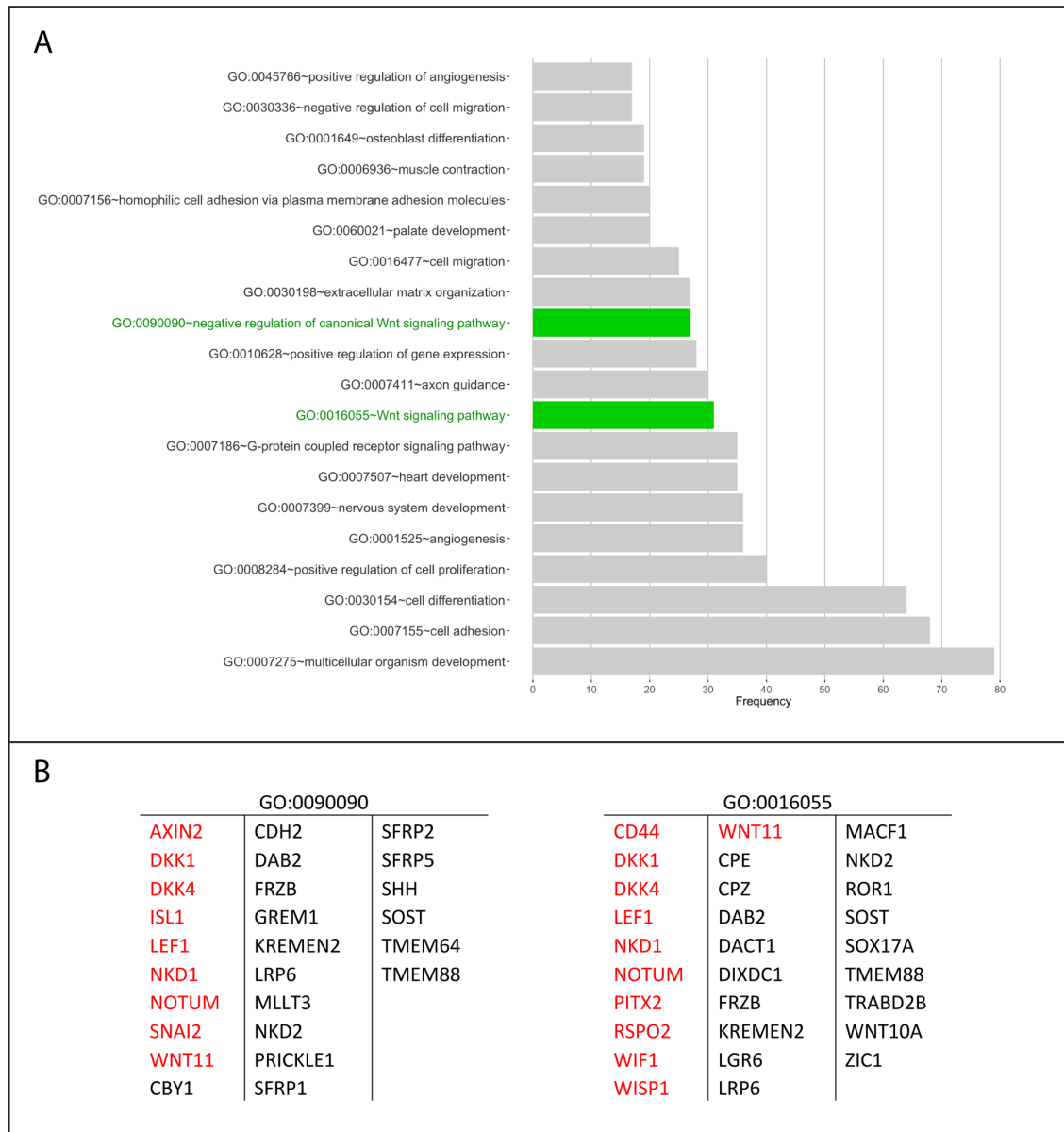
For double *in situ* hybridisation/immunohistochemistry, samples first underwent *in situ* hybridisation as previously described. Immediately after colour reaction, samples were fixed for 1 minute in 4% paraformaldehyde in PBS. Samples were then blocked with 5% goat serum and 1% bovine serum albumin in PBS-T (0.05% tween-20). Blocking solution was replaced with blocking solution containing rabbit anti-Sox2 primary

antibody (ab97959; Abcam) at a concentration of 1:500. Goat anti-rabbit Alexa-Fluor 647 (1:250) (A-20721245; Thermo) and goat anti-mouse Alexa-Fluor 488 (1:250) (A-11-001; Thermo) secondary antibodies were used for immunodetection. Samples were counterstained with DAPI (1 $\mu$ g/ml) and mounted using Fluoromount (Sigma). Images were taken using a BX51 Olympus compound microscope. Images were contrast enhanced and merged in Adobe Photoshop.

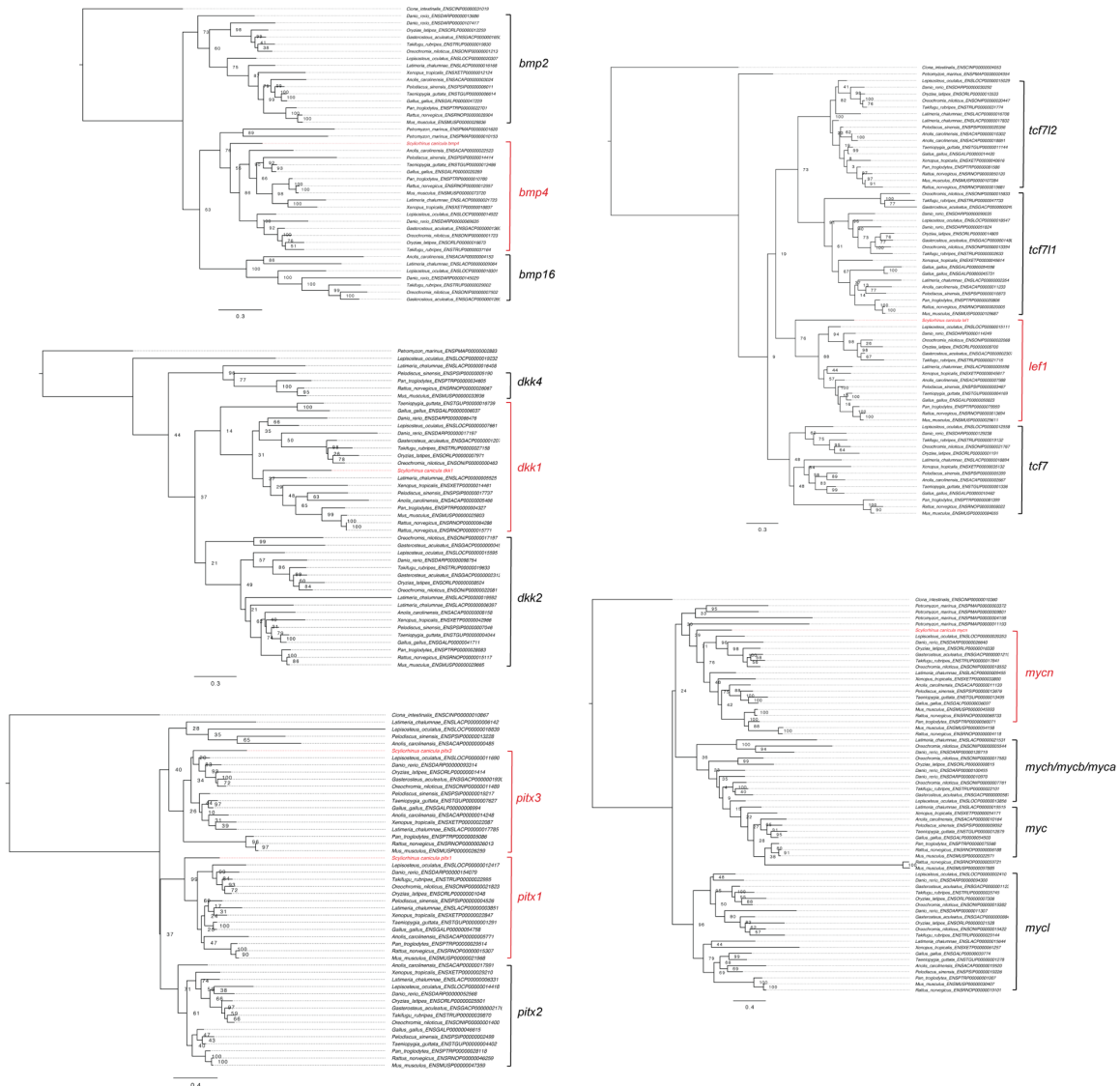
## Supplementary information



**Supplementary figure S1.** This reduced SL GRN was filtered from the RNEA generated SL global GRN (Fig 3). Key markers (*sox2*,  $\beta$ -catenin, *lef1*, *pitx1*, *bmp4* and *pitx2*) were treated as central nodes. Only markers which interact with at least one of the key nodes were retained. Lines between nodes depict predicted directional interactions. Diamond nodes are transcription factors. Size of node reflects the number of interactions at a given node. Red node outline marks central nodes. Green nodes are differentially expressed markers (FDR<0.001, FC>2) belonging to the included k-means clusters. Blue nodes are nodes secondarily added by RNEA as deemed statistically important.

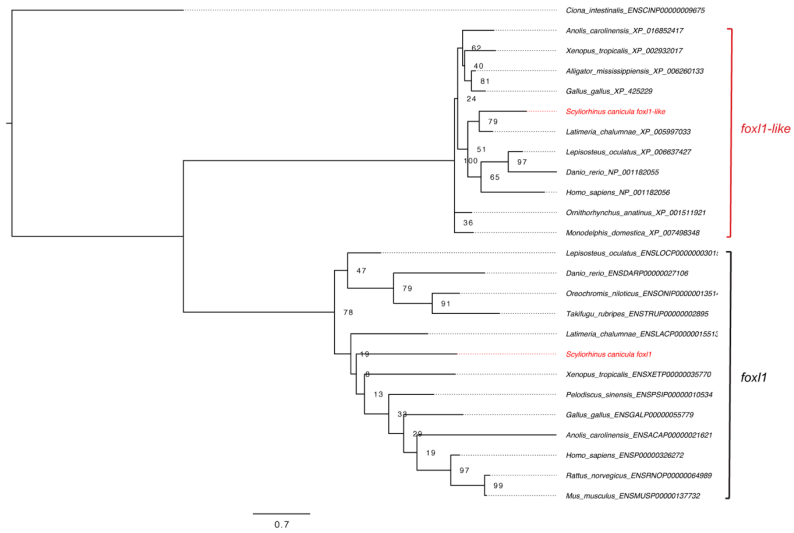


**Supplementary figure S2.** (A) GO enrichment analysis of differentially expressed super-clusters (FDR<0.001, FC>2) associated with dental initiation (TTJ/SL, SL, SL/ET, TTJ/SL/ET) revealed over-representation of GO:0016055 (Wnt signalling pathway) and GO:0090090 (negative regulation of canonical Wnt signalling pathway) within these clusters (p<0.001) relative to the whole transcriptome. (B) Candidates markers within the dental initiation super-clusters (TTJ/SL, SL, SL/ET, TTJ/SL/ET) which are also annotated with GO:0090090 and GO:0016055 are listed. Markers in red are those shared with the SL GRN refined by the use of central nodes (Fig S2).

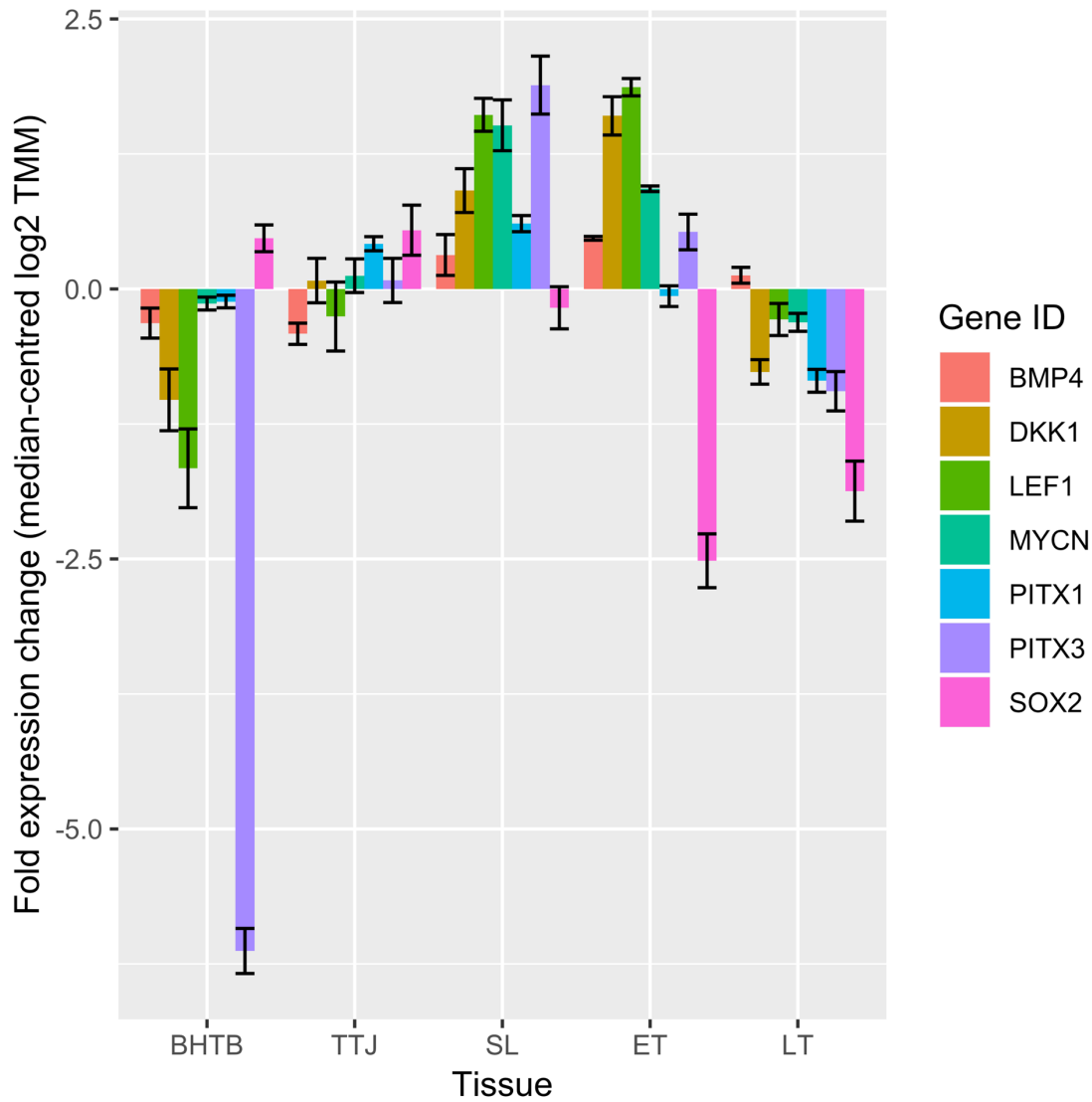


**Supplementary figure S3.** Phylogenetic gene trees for *bmp4*, *dkk1*, *pitx1*, *pitx3*, *lef1* and *mycn* reconstructed from protein coding sequences (cds) extracted from [www.ensembl.org](http://www.ensembl.org). Species included in the analysis were selected based on their phylogenetic position. Ensembl sequences were aligned to *S. canicula* sequences obtained from RNAseq. Sequences were aligned using MUSCLE (Edgar, 2004). A maximum likelihood tree was generated from 100 bootstrap replications using PHYML (Guindon and Gascuel, 2003) with a GTR substitution model (Waddell and Steel, 1997). Node labels represent bootstrap confidence values. Trees were edited in figTree v1.4.3.

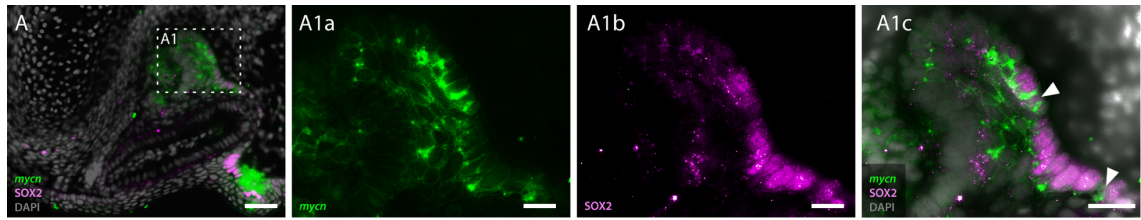




**Supplementary figure S4.** Phylogenetic gene tree for foxl1 and foxl1l reconstructed from protein coding sequences (cds) extracted from [www.ensembl.org](http://www.ensembl.org) (foxl1) and protein sequences from genbank [www.ncbi.nlm.nih.gov/genbank](http://www.ncbi.nlm.nih.gov/genbank) (foxl1-like). Species included in the analysis were selected based on their phylogenetic position. Ensembl and genbank sequences were aligned to *S. canicula* sequences obtained from RNAseq. Sequences were aligned using MUSCLE (Edgar, 2004). A maximum likelihood tree was generated from 100 bootstrap replications using PHYML (Guindon and Gascuel, 2003) with an LG substitution model. Node labels represent bootstrap confidence values. Trees were edited in figTree v1.4.3.



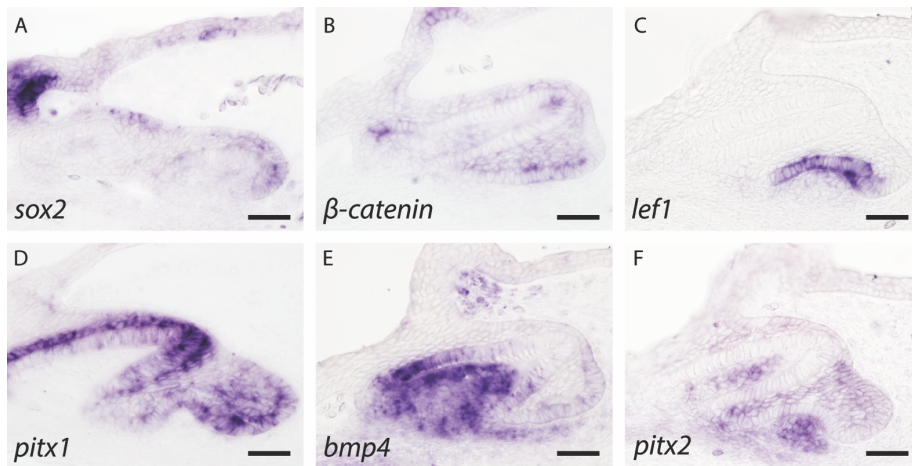
**Supplementary figure S5.** RNAseq fold expression change of key markers (*bmp4*, *lef1*, *sox1*, *pitx1*) and novel candidates (*dkk1*, *mycn*, *pitx3*) expressed within the SL (Fig 6). The mean expression value for each gene is depicted across the five dissected tissue regions for RNAseq (BHTB, TTJ, SL, ET and LT). Fold expression change (median-centred log<sub>2</sub> TMM) have been median centred and log<sub>2</sub> transformed for direct comparison between genes. Error bars represent the standard error.



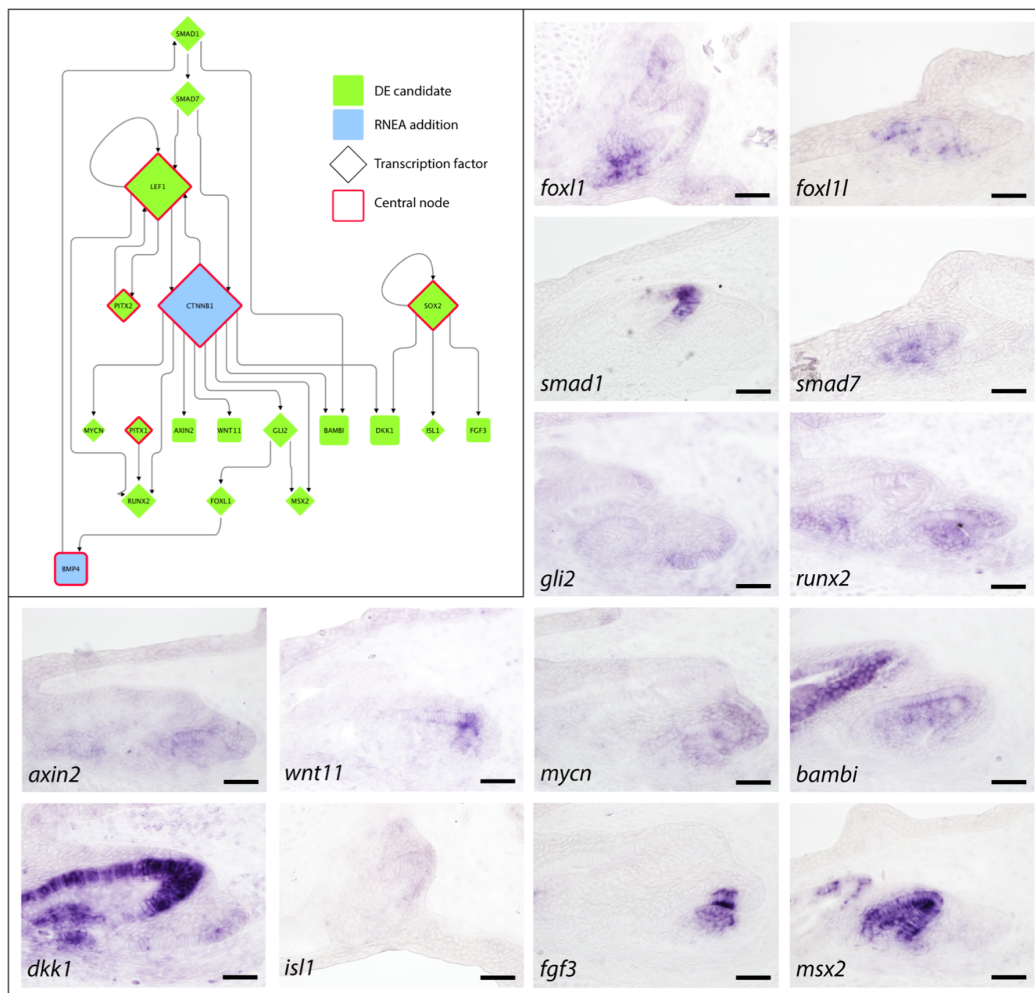
**Supplementary figure S6.** Double section *in situ* hybridisation/immunohistochemistry on catshark upper jaw depicting the expression of *mycn* (A1a) and SOX2 (A1b) within the SL. *mycn* is expressed within the taste buds at the TTJ (A), the MDE, dental mesenchyme and SL epithelium (A1a). SOX2 is co-expressed with *mycn* within the taste buds and the columnar epithelium of the SL (A1c). *mycn* expression is shown in green, SOX2 protein expression is in magenta and DAPI nuclear stain in grey. Dotted white boxes in A depict magnified region in A1. White arrowheads in A1c highlight regions of co-expression between *mycn* and SOX2 in the SL. Scale bars are 50µm in A, and 25µm in A1a-c.

Gene	Forward Primer	Reverse Primer
<i>sox2</i>	CTCGGAGATCAGCAAGAGGC	GTGCGCTCTGGTAATGTTGG
<i>β-catenin</i>	AGTGGTTAAGCTACTGCACCC	AAGCTAGCATCATCTGGACGG
<i>lef1</i>	CATGCACTCTACAGGGATCCC	TCTGGATCAGAGTCTTGCTGC
<i>pitx1</i>	TCACCGAAGTATTGTGCCTCC	TCACCGAAGTATTGTGCCTCC
<i>bmp4</i>	GGAGCACAGGTCTATGGAAAGG	GGAGCACAGGTCTATGGAAAGG
<i>pitx2</i>	ACAGCTACAAGAACTGGAGGC	ACGCTGGATTCTGAACACTGG
<i>pitx3</i>	CAAAGGACGCACCTCACAAGC	CCCGGTATGAGTAAGGGTTGG
<i>foxl1</i>	TCAGAGGGTGACATTGAACGG	CTGATGGAGAAGGGTTGGACC
<i>foxl1l</i>	GTATCTCGACCTGCCTACAGC	ATGTCAGATGCCAGTCTTGG
<i>smad1</i>	GGAATCCGAGACACTCTTGGC	TTCAACAACCAGCTCTTCGCG
<i>smad7</i>	TCCTTGCCGGTACTGATATGC	GTGTGAAATCGTGGTCGTTGG
<i>gli2</i>	TCGATATGCGACACCATGAGG	ATGCATCTGGAAGGTCACTGG
<i>runx2</i>	ATCTCTCAATCCTGCACCAGC	CCAGACAGACTCATCAATCCTCC
<i>axin2</i>	GACGGACAGTAGCGTAGATGG	TGGTGGATGTGATGATGGTGG
<i>wnt11</i>	TCTGACATGAGGTGGAAGTGC	TCTCTTGAGTTCCGTTGGAGC
<i>mycn</i>	CAAGTGGCCCCTTCTAGATCC	GCGAGTCCTTATTCCCTCCAG
<i>bambi</i>	GCATCTAACTGTGTGGCAACG	TCCAAGTCTAACTTCGCCACC
<i>dkk1</i>	TGCCTCTACAATGTCGTGAGC	GTGCAGCCTCGAATTCTTGC
<i>isl1</i>	ATTGTTCCGGGACTAAATGCGC	TGCAGCGTTTGTCTGAAACC
<i>fgf3</i>	CTTGTTGCTGAGTCTTCTGGC	AACTCTTCAGCAGGTTCTCCC
<i>msx2</i>	TCACCGAAGTATTGTGCCTCC	GGAGCACAGGTCTATGGAAAGG

**Supplementary figure S7.** List of forward and reverse primers used in the synthesis of probes for *in situ* hybridisation.



**Supplementary figure S8.** Raw *in situ* hybridisation data false coloured in Fig 4. Scale bars are 50µm.



**Supplementary figure S9.** Raw *in situ* hybridisation data false coloured in Fig 5. Scale bars are 50µm.

## Chapter 4

### **Conservation of enamel knot signalling in sharks supports homology of the dental signalling centre**

Alexandre Thiery, Rory Cooper, and Gareth Fraser

Department of Animal and Plant Sciences, and Bateson Centre, University of Sheffield,  
UK.

#### **Abstract**

The development of dental cusps is regulated by the enamel knot. This non-proliferative dental epithelial signalling centre was initially identified in mammalian molars. Fgf signalling is known to regulate differential proliferation rates between the enamel knot and the proliferative adjacent dental epithelium, leading to downward growth of the dental epithelium and the formation of the dental cusp. The presence of an enamel knot in non-mammalian vertebrates has been debated given observable differences in signalling. Here we show the conservation and restriction of *fgf10* and *fgf3* to the sites of future dental cusps in the catshark, whilst also highlighting striking differences in *bmp4* expression between the catshark and mouse. We also reveal shifts in tooth size, shape and cusp number following canonical Wnt small molecule treatment. These phenotypes mirror those observed in mammals, where canonical Wnt has also been

implicated as an upstream regulator of enamel knot signalling. *In silico* modelling of catshark dental morphogenesis demonstrates how subtle changes in signalling activators and inhibitors alter tooth shape, resembling phenotypes observed following canonical Wnt signalling perturbation. These results support the functional conservation of an enamel-knot like signalling centre throughout vertebrates and suggest that lineage specific differences in signalling are not sufficient in refuting homology of the signalling centre.

## **Introduction**

Diversification of the dentition has been instrumental in the success of vertebrates. It has become highly adapted to its respective environmental niche and as a result given rise to a plethora of unusual forms. Modification of the dentition has been achieved through variation in tooth positioning and regeneration of the tooth unit. These modifications are epitomised through the presence of pharyngeal teeth in most teleosts and the beaked dentitions of pufferfish and parrotfish which develop through the coalescence of multiple tooth generations (Britski *et al.*, 1985; Thiery *et al.*, 2017). Additionally, vertebrates exhibit observable modifications to the shape of the dental unit itself. There is an increase in dental morphological complexity throughout evolution, culminating in mammals which possess multiple regionalised tooth types (heterodonty) (Jernvall and Thesleff, 2012). There is thought to be a trade-off between tooth complexity and dental regenerative ability in the mammalian lineage, with mammals favouring precise occlusion of the dentition (Jernvall and Thesleff, 2012).

The study of dental development has focussed on transcriptional regulators, which mediate growth, morphogenesis and cellular differentiation. This process of development is regulated via interactions between the oral epithelium and underlying neural-crest derived mesenchyme (Zhang *et al.*, 2005). Major signalling pathways including, canonical Wnt, fibroblast growth factor (Fgf), hedgehog (Hh), bone morphogenetic protein (Bmp) and Notch signalling have all been implicated as important regulators of odontogenesis (Thesleff and Sharpe, 1997). Complex interactions and feedback loops between these gene pathways guide dental development. Teeth develop from an initial epithelial placode, which proceeds to proliferate and grow in size during the subsequent bud stage. Following bud stage, the tooth enters cap stage, which marks the onset of morphogenesis.

Morphogenesis of epithelial appendages coincides with a change in shape of the epithelial placode. This process can be driven via; differential proliferation rates (i.e. teeth ((Jernvall *et al.*, 1994; Salazar-Ciudad and Jernvall, 2010))), cell shape changes (i.e. intestinal crypt (Sumigray *et al.*, 2018)), or cell migration (i.e. hair (Ahtiainen *et al.*, 2014)). Signalling molecules drive reciprocal epithelial to mesenchymal signalling and regulate the morphogenesis of epithelial appendages.

During morphogenesis the tooth acquires its defining morphological feature: the dental cusp. In mammals, dental cusps are regulated by an epithelial signalling centre found at the tip of the first cusp, known as the primary enamel knot (EK). The EK is molecularly identifiable as non-proliferative and expresses Wnt, Bmp, Fgf and Hh markers (Jernvall & Thesleff 2012). Fgf signalling drives differential proliferation between the EK and

rapidly proliferating adjacent dental epithelium, leading to folding of the epithelium at the site of dental cusps and the formation of the final tooth shape (Jernvall *et al.*, 1994, 2000; Salazar-Ciudad and Jernvall, 2010). During the final stages of dental morphogenesis, the EK dramatically reduces in size as cells undergo apoptosis (Jernvall *et al.*, 1998).

In multicuspid teeth, such as mammalian molars, secondary signalling centres termed secondary enamel knots (SEK) form at the site of each extra cusp and are thought to be induced by the EK. Folding of the dental epithelium between primary and secondary EKs leads to formation of cervical loops in-between each cusp (Jernvall *et al.*, 1994; Salazar-Ciudad, 2012). Most of our understanding of tooth shape comes directly from the study of mammalian molar cusp development. Whilst it is known that EK signalling centres are found throughout mammals, their presence in other vertebrates is less clear.

In reptiles, there is no clear histologically definable EK (Buchtová *et al.*, 2008; Weeks *et al.*, 2013), although in some species there is a thickening in the inner dental epithelium which leads to the asymmetric deposition of enamel and the formation of cusps (Zahradnicek *et al.*, 2014). Furthermore, whilst in reptiles, cells of the inner dental epithelium are non-proliferative, this region is not as highly restricted to the cusp as in mammalian molars (Buchtová *et al.*, 2008; Richman and Handrigan, 2011). However, there is conservation of signalling within an EK-like signalling centre (Richman and Handrigan, 2011). Similar EK-like signalling centres have been described in teleosts, with chemical perturbation of these signalling pathways resulting in shifts in cusp number (Fraser *et al.*, 2013). Sharks, which are basal crown



gnathostomes, also possess teeth with clearly defined cusps. There is a region of non-proliferative cells within the apical dental epithelium thought to be associated with the primary cusp (Rasch *et al.*, 2016), however the presence of a definitive EK has not been clearly identified (Debiais-Thibaud *et al.*, 2015).

Lymphoid enhancer factor (Lef1) is a transcription factor, which forms part of the canonical Wnt signalling cascade. Upon activation of canonical Wnt signalling, cytoplasmic beta-catenin is stabilised, allowing for its nuclear translocation. Together with Lef1, beta-catenin and TCF proteins form a nuclear DNA binding complex which regulates the transcription of Wnt target genes (Willert and Nusse, 1998). Canonical Wnt signalling is recruited throughout dental development. Its importance has been documented in the regulation of dental initiation (Sarkar *et al.*, 2000; Jarvinen *et al.*, 2006; Järvinen *et al.*, 2018), regeneration (Gaete and Tucker, 2013; Martin *et al.*, 2016) and morphogenesis (Liu *et al.*, 2008).

Whilst over a dozen markers have been described within the mammalian EK, Wnt signalling appears to be a primary upstream regulator of EK signalling. Lef1<sup>-/-</sup> mutants exhibit an arrest of tooth development during bud stage, with the tooth cap and associated cusps failing to form and failing to express EK markers including Fgf4, Shh and Bmp4 (Kratochwil *et al.*, 2002). Fgf4 is capable of rescuing tooth development in Lef1<sup>-/-</sup> mutants (Kratochwil *et al.*, 2002). Furthermore, the inhibition of Wnt signalling during early bud stage via ectopic expression of the Wnt antagonist Dickkopf-related protein 1 (Dkk1), leads to blunted cups and a reduction in Bmp4 signalling (Liu *et al.*, 2008). These results suggest that Wnt signalling falls upstream of Fgf and Bmp

signalling in the EK. However, more complicated feedback loops are involved, as mesenchymal specific knock-down of Bmp4 (Bmp4<sup>ncko/ncko</sup>) also leads to a reduction in Lef1 expression (Jia *et al.*, 2016).

In order to determine the extent of signalling conservation between mammals and sharks during dental morphogenesis, we documented the expression of mammalian EK markers in the catshark, *Scyliorhinus canicula*. Furthermore, given the importance of Wnt signalling during dental morphogenesis and cusp formation in mammals, we sought to perturb Wnt signalling and determine its function in the catshark. Following chemical Wnt perturbation, we identify shifts in tooth shape, size and cusp number, and model the resulting phenotypes *in silico* using the ‘ToothMaker’ programme (Salazar-Ciudad and Jernvall, 2010). Our results reveal that despite differences in molecular signalling between the catshark and mammals, the fundamental components of the enamel knot signalling centre are conserved.

## **Results**

### *Histological and morphological analysis of the catshark dentition*

The first dental generation develops relatively superficially on the oral surface before the dental lamina has fully invaginated (Fig 1D). As the dental lamina grows, more generations emerge. New teeth are initiated at the tip of the dental lamina and move anteriorly in a conveyor belt-like manner. As teeth move along this trajectory, they undergo morphogenesis and matrix secretion, before erupting on the oral surface on the labial side of the dental lamina (Fig 1E). Adjacent tooth families are staggered in the

timing of their initiation (Fig 1C), resulting in differences in the stage of development of adjacent teeth. Together with the many-for-one regenerative system which catsharks

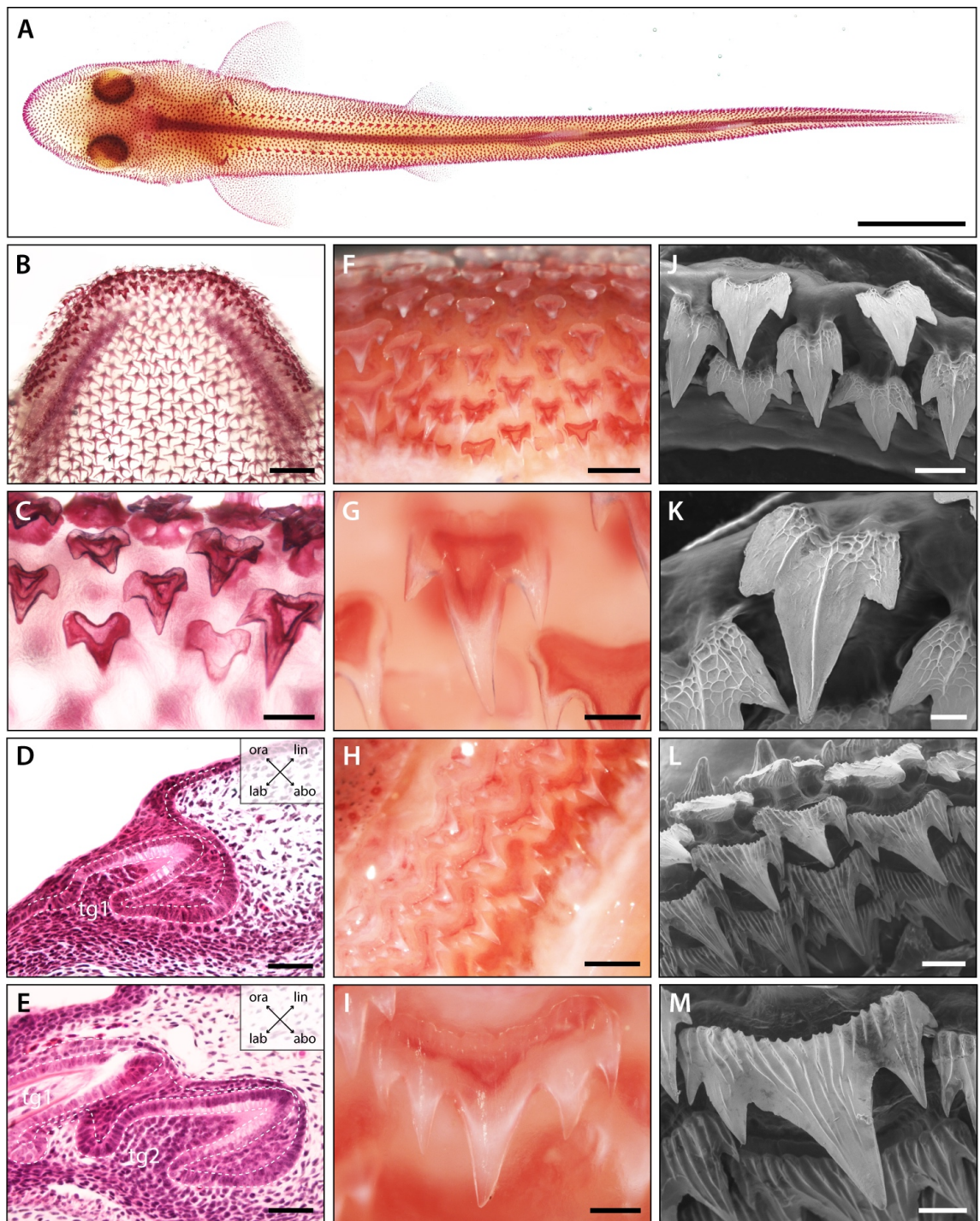


**Figure 1. Pattern and morphology of the catshark dentition.** Images of catshark samples cleared and stained with alizarin red, reveal pattern and morphology of the dentition in the

lower jaw (A-C and F-I). A) Dorsal view of hatchling stage catshark (Stage 34) revealing denticle on the body surface. B) Dorsal view of hatchling stage (Stage 34) lower jaw. C) Magnification of B, showing staggered pattern of adjacent tooth families. Histological staining with haematoxylin and eosin on sagittal cross sections through early stage 32 (D) and late stage 32 (E) lower jaws shows the growth of the DL during dental development. The first dental generation (tg1) develop relatively superficially at the oral surface, before full invagination and elongation of the DL (D). The DL then grows deep into the underlying mesenchyme, with the second (tg2) and subsequent dental generations initiated at the SL (E). The addition of numerous successional dental generations can be seen in the adult jaw (F and H). At the jaw symphysis (F), teeth often remain tricuspid (G). However, in lateral regions (H), teeth develop 5-7 cusps (I). Scanning electron microscope (SEM) images reveal tricuspid teeth in the embryo (stage 33) (J-K) and pentacuspoid teeth in the adult (L and M). Scale bars are 10mm in A; 1mm in B, F and H; 250µm in C, G, I and M; 50µm in D, E and K; 125µm in J and 500µm in L. ora; oral, abo; aboral, lin; lingual, lab; labial.

possess, this means that multiple stages of ontogenesis can be investigated within a single individual. The ability to investigate a range of dental development stages within a single individual makes the shark an ideal model for the study of odontogenesis.

There is an observable shift in cusp number between embryonic and juvenile catshark stages (Fig 1J-M). Embryonic teeth generally develop with three cusps (Fig 1C, J and K). In contrast, adult catsharks can possess anywhere between three and seven cusps depending on the position of the tooth along the jaw margin (Fig 1 F-I). Given these changes in cusp number, we wanted to investigate how the development of cusps is regulated. In order to see if there is a conserved EK signalling centre in the catshark, we documented the expression of known mammalian EK markers during odontogenesis (Fig 2). *In situ* hybridisations were carried out on sagittal paraffin sections to see the expression of EK markers in sagittal dental cross sections. We used embryonic catshark

samples at late Stage 32 (~125 days post fertilisation (dpf)) (Ballard *et al.*, 1993), as two to three dental generations had already undergone the process of dental initiation by this stage, allowing us to compare early and late stage dental morphogenesis.

#### *In situ hybridisation of key markers within the developing tooth*

Canonical Wnt signalling plays a crucial role in the formation of dental cusps in mammals (Kratochwil *et al.*, 2002; Liu *et al.*, 2008). In the catshark, transcription factors Lymphoid enhancer binding factor-1 (*lef1*) (Fig 2A) and  $\beta$ -catenin (Fig 2B) are both expressed within developing bell stage teeth. Weak expression can be seen in the dental mesenchyme (Fig 2: dm) and regions of the dental epithelium (Fig 2: de). However, there is also an observable upregulation of their expression within the apical dental epithelium (Fig 2: white arrowhead). The downstream target of canonical Wnt signalling *axin2* is also found within the dental epithelium; however, its expression is not specifically restricted to the apex (Fig 5B and C). Wnt11 has been previously identified as an activator of non-canonical Wnt signalling, although its expression has also been shown to stimulate canonical Wnt signalling in a case-specific context (Li *et al.* 2008). We note the upregulation of *wnt11* specifically within the apical dental epithelium during cap stage (Fig 2C).

Canonical Wnt antagonists Dickkopf 1 (*dkk1*) and Frizzled-related protein 3 (*sfrp3*) are also expressed within the developing tooth. *dkk1* is seen within both the dental papilla and throughout the dental epithelium in late morphogenesis (Fig 2D and 3C). Reduced proliferation is a key requirement of an EK, with differential proliferation rates within

the dental epithelium leading to the formation of dental cusps (Jernvall *et al.*, 1994). Double *in situ*/immunohistochemistry for *dkk1* and proliferative cell nuclear antigen (PCNA) revealed a small number of non-proliferative cells at the tip of the tooth during cap stage (Fig 3Ba), with a marked reduction in proliferation throughout the entire dental epithelium late morphogenesis (Fig 3Ca). Although *dkk1* is expressed throughout the entire dental epithelium during late morphogenesis (Fig 3C), during cap stage its epithelial expression is specifically restricted to the non-proliferative cells corresponding to the putative EK (Fig 3B). In the pig (Wu *et al.*, 2017), *dkk1* expression is restricted to the dental mesenchyme, with no expression observed within the dental epithelium. In contrast to *dkk1*, *sfrp3* is specifically restricted to the dental mesenchyme, with weak expression within the dental papilla (Fig 2E). In the mouse, *sfrp3* is also restricted to the mesenchyme, though its expression is much stronger than that observed in the shark (Sarkar and Sharpe, 1999). Not all canonical Wnt-related markers are expressed in equivalent tissue types during cap to early bell stage of dental development between mammals and the catshark. However, there is expression of Wnt markers within both the dental epithelium and dental mesenchyme, with an isolated yet upregulated region of expression within the putative EK. The expression of canonical Wnt antagonists *dkk1* and *sfrp3* may also be playing a role in restricting Wnt activity within the dental mesenchyme.

Aside from canonical Wnt signalling, other pathways including; Hh, Fgf and Bmp signalling, are all involved in mammalian EK signalling, although there are subtle differences in the expression of EK markers between placental and marsupial mammals. For example, *fgf3* is observed in the dental mesenchyme and EK of cap stage molars in

both mouse and the opossum (Kettunen *et al.*, 2000; Moustakas *et al.*, 2011). However, *fgf10* is expressed in both EK epithelium and dental mesenchyme in the opossum (Moustakas *et al.*, 2011), whereas it is absent from the EK epithelium in the mouse (Jernvall *et al.*, 1994; Kettunen *et al.*, 2000). Interestingly, the expression of *fgf3* and *fgf10* is almost identical between the shark and opossum. We find *fgf3* expressed in the tip of the dental epithelium, whilst its mesenchymal expression is confined just below the epithelium (Fig 2F). The expression of *fgf10* is highly restricted to only a few epithelial cells at the tip of the developing tooth during cap stage (Fig 2G). This expression is located precisely within a small cluster of non-proliferative dental epithelial cells, marked by a lack of PCNA expression (Fig 3Ab). The importance of Fgf signals in regulating the differential proliferation of the EK relative to surrounding dental epithelium (Jernvall *et al.*, 1994; Kettunen *et al.*, 2000), together with the highly specific expression of *fgf10* within this non-proliferative region provides strong support of an EK in the catshark. The similarity in expression between marsupial mammals and sharks raises the possibility that loss of *fgf10* in the EK in placental mammals is a lineage-specific modification in EK signalling.

During the induction of mammalian molars, *bmp4* is involved in reciprocal epithelial to mesenchymal signalling, during which the odontogenic potential shifts from the dental epithelium to the dental mesenchyme. Concordant with this shift in odontogenic potential, *bmp4* shifts from epithelial and mesenchymal expression, to mesenchymal only (Vainio *et al.*, 1993). As with *fgf3* (Fig 2F), *lef1* and  $\beta$ -*catenin* (Rasch *et al.*, 2016), *bmp4* is also expressed in the dental epithelium and condensing mesenchyme during bud stage in the catshark (Fig S1A). The increase in mesenchymal *bmp4* expression

between bud (Fig S1A) and cap stages (Fig S1B), reflects the epithelial to mesenchymal shift in odontogenic potential observed in mammals (Vainio *et al.*, 1993). However,

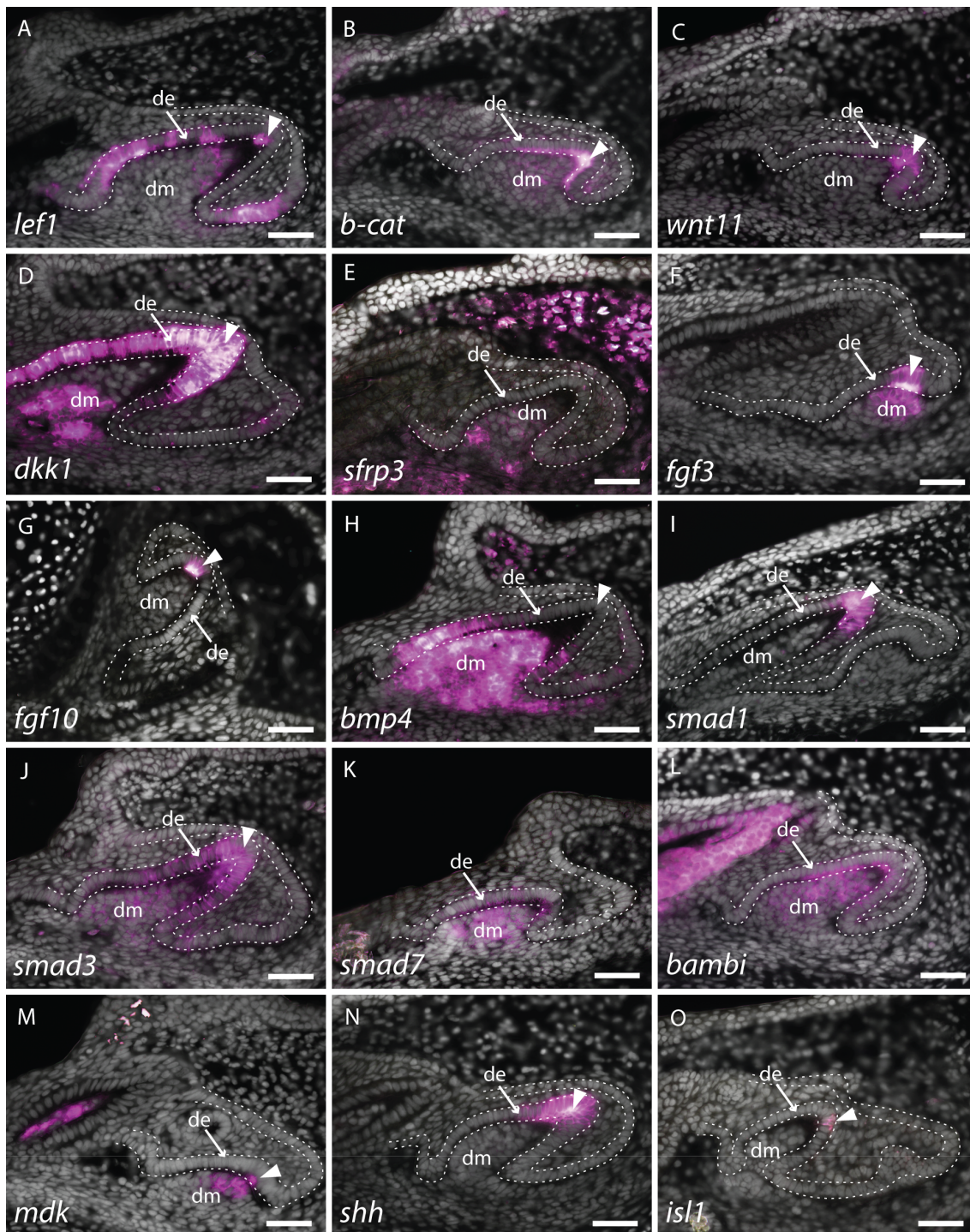


**Figure 2. Expression of enamel knot markers during catshark dental morphogenesis.** In situ hybridisations on sagittal paraffin sections of late stage 32 catshark jaws, reveal the expression of markers involved in major developmental pathways, including canonical Wnt



signalling (A-F), Fgf signalling (G and H) and Bmp signalling (H-L). Wnt markers, *lef1* (A),  $\beta$ -*catenin* (B) and *wnt11* (C) are all expressed within the apical tip of the developing tooth during cap stage. Weak expression can also be seen within the dental mesenchyme and surrounding dental epithelium in *lef1* (A) and  $\beta$ -*catenin* (B). Weak expression of the Wnt inhibitor, *sfrp3* is found within the dental mesenchyme during cap stage, whereas *dkk1* is also found within the dental epithelium later in morphogenesis (D). The expression of Fgf markers *fgf3* (F) and *fgf10* (G) is highly specific to the EK during late bud to early cap stage, with *fgf3* weakly expressed in the dental mesenchyme below the EK. *bmp4* (H) expression is absent from the EK during late morphogenesis, but is strongly expressed within both the rest of the dental epithelium and dental papilla. *smad1* (I) is found within the apical tip of the dental epithelium, whilst *smad3* (J) is also expressed in the dental mesenchyme during late cap stage. Bmp inhibitors *smad7* (K) and *bambi* (L) are both expressed throughout both epithelium and mesenchyme of developing teeth. *mdk* (M) and *isll* (O) expression is restricted to a few cells of the EK, with *mdk* also expressed within the underlying dental mesenchyme. In contrast, *shh* (N) expression is extensive broad, but is still restricted to the apical tip of the dental epithelium. Gene expression is false coloured in magenta. White arrowhead points to expression within the apical tip of developing teeth and putative EK. White dotted lines depict the columnar basal epithelial cells of the dental lamina and dental epithelium. DAPI nuclear stain is false coloured in grey. All images are of lower jaws, except G, which is of the upper jaw. Scale bars are 50 $\mu$ m. de, dental epithelium; dm, dental mesenchyme.

unlike in mammals, *bmp4* remains expressed within sub regions of the dental epithelium throughout the duration of morphogenesis (Fig S1).

Given the epithelial expression of *bmp4* during bud stage, it had previously been suggested that it may play a role in putative EK signalling in the catshark (Rasch *et al.*, 2016). Following the epithelial to mesenchymal shift in *bmp4* in the mouse, it is then secondarily upregulated within the EK during late cap stage (Jernvall *et al.*, 1998). However, we do not observe any secondary upregulation within the putative EK in the catshark. Instead, its expression is rapidly downregulated within the apical tip of the tooth (Fig 3D). This region of *bmp4* downregulation corresponds specifically to a

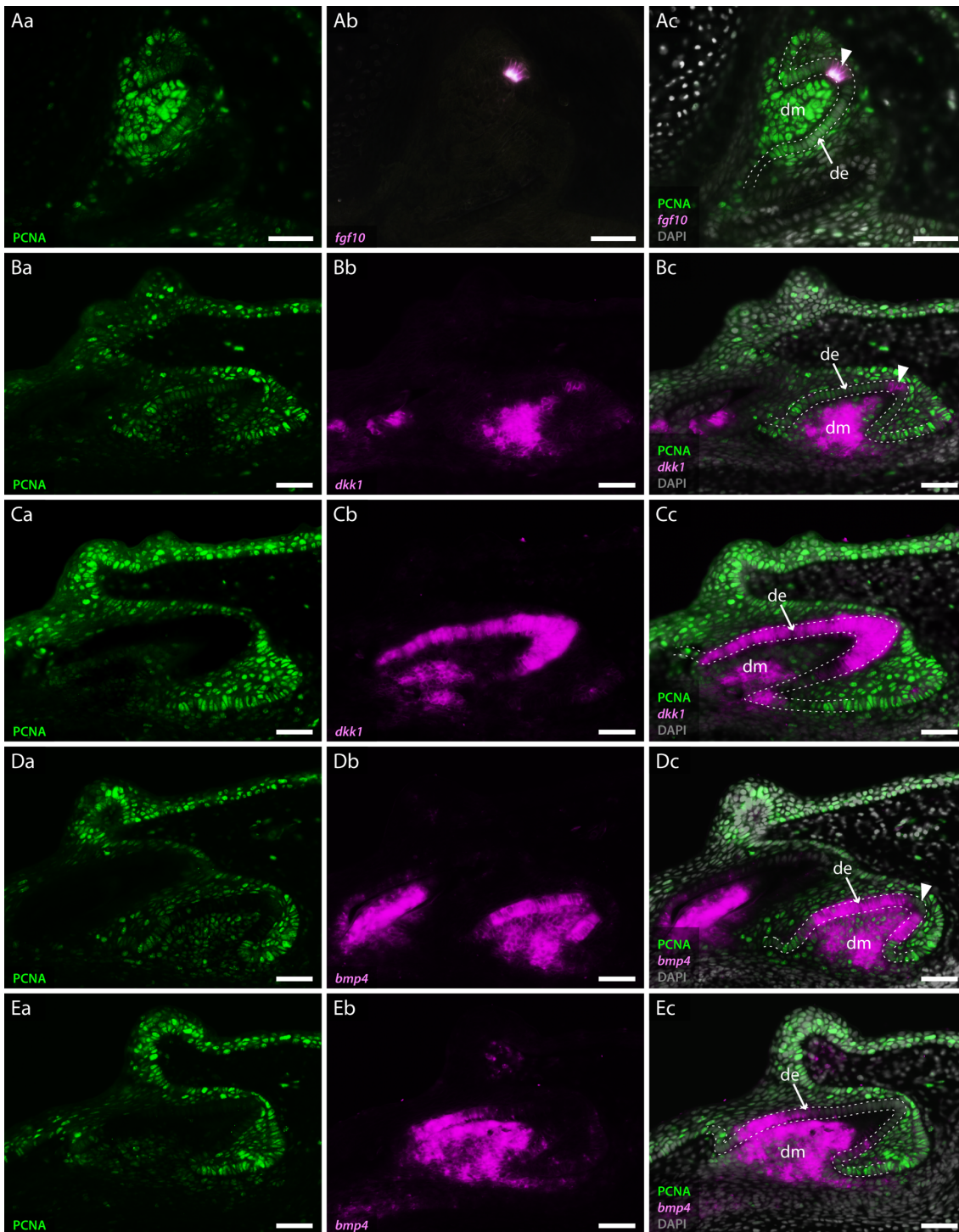


**Figure 3. Co-expression of odontogenic markers regulating dental morphogenesis with PCNA.** Double section *in situ* hybridisation/immunohistochemistry on catshark jaws reveals co-expression of markers involved in EK signalling and proliferative cell nuclear antigen (PCNA), within teeth undergoing cap stage (A, B and D) and late morphogenesis (C and E). Images Aa-

Ea reveal expression of PCNA. Images Ab-Eb reveal expression of *in situ* hybridisation markers. Images Ac-Ec reveal co-expression of PCNA and *in situ* hybridisation markers. PCNA expression is absent from the tip of the dental epithelium, corresponding to the EK in cap stage teeth (Aa, Ba and Da). The extent of PCNA expression within developing teeth decreases as teeth undergo morphogenesis (Ca and Ea). *fgf10* is expressed within a small subset of dental epithelial cells corresponding to the EK (Ab). Its expression is inversely complementary to the expression of PCNA (Ac). *dkk1* expression is initially upregulated in the dental mesenchyme during cap stage (Bb), with restricted epithelial expression present only within non-proliferative cells of the EK (Bc). During late morphogenesis *dkk1* expression weakens within the dental mesenchyme, with observable upregulation of its expression throughout the entire dental epithelium (Cb and Cc). Unlike *dkk1* and *fgf10*, *bmp4* is absent from the apical tip of the dental epithelium throughout dental morphogenesis (Db and Eb). *fgf10* (A) is shown in the upper jaw; *dkk1* (B and C) and *bmp4* (D and E) are shown in the lower jaw. Gene expression is shown in magenta, PCNA protein expression is in green and DAPI nuclear stain in grey. White dotted lines depict the outer dental epithelium of the developing tooth. Scale bars are 50µm. de, dental epithelium; dm, dental mesenchyme.

restricted group of non-proliferative epithelial cells (Fig 3Dc). Throughout later stages of morphogenesis, *bmp4* becomes further restricted to only the lateral epithelial cells of the developing tooth (Fig 3E). The precise exclusion of *bmp4* from the non-proliferative tooth apex (Fig 3D and E) raises the possibility that instead of regulating putative EK signalling, it is involved in the restriction of other EK markers.

The Smad protein family play a crucial role in TGFβ signal transduction, including Bmp signalling (Massagué, 2012). Here, we show the expression of *smad1*, *smad3* and *smad7* during dental morphogenesis. Smad1 and Smad3 are phosphorylated following Bmp signalling and enable its signal transduction, whilst Smad7 is a negative feedback regulator of TGFβ signalling (Xu *et al.*, 2003; Massagué, 2012). *smad1* (Fig 2I) is expressed within the putative EK at the tip of the developing tooth, whilst *smad3* (Fig

2J) and *smad7* (Fig 2K) are both expressed throughout the dental epithelium and dental mesenchyme. Furthermore, as with *smad7*, BMP and activin membrane-bound inhibitor (*bambi*) is expressed in both dental epithelium and dental papilla (Fig 2L). Although interactions between these signalling molecules are complex, the expression of Bmp markers within and around the putative EK indicates a role for Bmp in EK signalling.

*fgf3*, *fgf10*, Sonic Hedgehog (*shh*) and *midkine* (*mdk*) have previously been found expressed within the apical tip of developing teeth in the catshark, corresponding to the putative EK (Rasch *et al.*, 2016). Here, we also find these markers expressed within the same tissues. *mdk* is expressed within both the tooth apex and underlying dental mesenchyme (Fig 2M) whilst *shh* is found exclusively within the apical tip of the dental epithelium (Fig 2N). EKs comprise a small number of cells at the very apical tip of a developing tooth and can be hard to morphologically distinguish from surrounding dental epithelium in sagittal cross-sections. Therefore, we also used whole mount *in situ* hybridisation to examine the expression of markers throughout the entire tooth unit.

#### *Whole mount in situ hybridisation in first generation teeth*

As the first dental generation develops superficially, prior to full invagination of the dental lamina, teeth can be seen developing directly on the oral surface. We carried out whole mount *in situ* hybridisations for *fgf3*, *fgf10*, *bmp4* and *shh* on early Stage 32 (~90dpf) catshark embryos, during which the first dental generation undergoes morphogenesis (Fig 4). This allowed us to identify whether markers expressed within the apical tip of developing teeth in sagittal sections were specifically restricted within

cuspid forming regions in whole mount.

As with our section *in situ* hybridisation data (Fig 3), *bmp4* is excluded from the epithelium at the leading edge of the tooth in whole mount. Instead, its expression appears to be primarily restricted to the dental papilla in both upper (Fig 4A) and lower jaws (Fig 4B). In contrast, *shh* can be seen expressed within the dental epithelium and specifically upregulated within the leading edge of the tooth (Fig 4E and F). *shh* is confined to the EK in mammalian molars (Vaahtokari *et al.*, 1996; Hardcastle *et al.*, 1998), and although we do see strong expression within both the primary cusp (Fig 4E and F: black arrowhead) and secondary cusps (Fig 4E and F: white arrowhead), its expression is not strictly restricted at these sites. Depending on the stage of morphogenesis, the extent of *shh* expression within the inter-cuspid dental epithelium is variable. Alongside playing a role in EK signalling, the expression of *shh* within the epithelium at the leading edge of the tooth suggests that it may also be involved in establishing an anterior to posterior growth gradient.

Unlike with *shh*, *fgf3* and *fgf10* expression is clearly associated with both the primary cusp (Fig 4C, D and G: black arrowhead) and secondary cusps (Fig 4C, D and G: white arrowhead). Whilst there is expression of *fgf3* within the dental mesenchyme, its epithelial expression is restricted solely to the site of future cusps. *fgf10* is exclusively expressed within the cuspid forming dental epithelium, in agreement with the expression pattern observed in section (Fig 3Ab). The expression patterns of *shh*, *bmp4* and *dkk1*, in or around the dental cusps, and more importantly the precise restriction of *fgf3* and *fgf10*

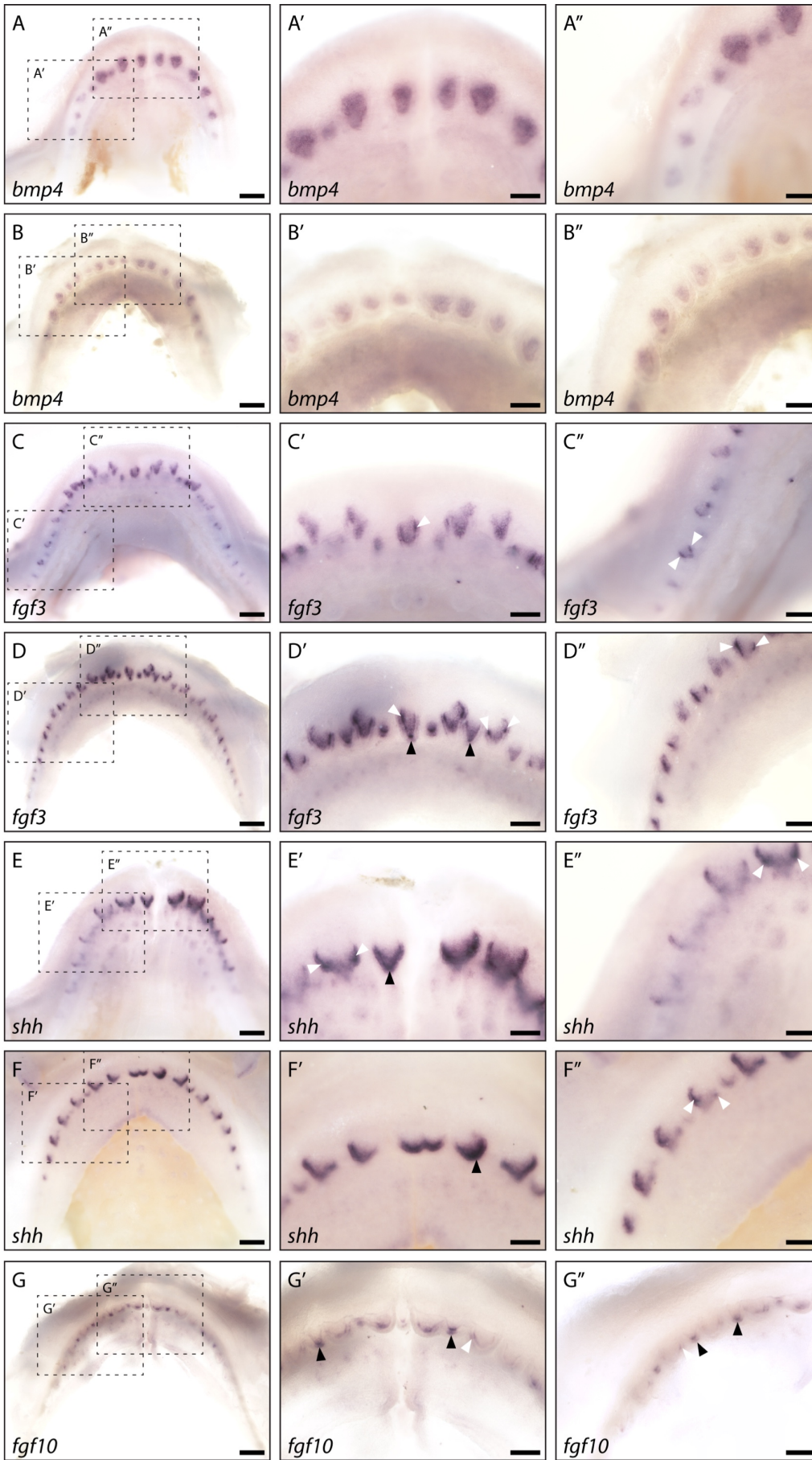


**Figure 4. Whole mount *in situ* hybridisation reveals enamel knot-specific gene expression.**

Whole mount *in situ* hybridisation on catshark lower (A, C and E) and upper (B, D, F and G) jaws highlights the expression of *bmp4* (A and B), *fgf3* (C and D), *shh* (E and F) and *fgf10* (G) across the jaw. Images are of early stage 32 (~90dpf) samples, with developing first generation teeth visible on the jaw margin. Images A-G are low magnification images. Images A'-G' are magnified images of the central teeth along the jaw. Images A''-G'' are magnified images of the left lateral side of the jaw. *bmp4* expression is visible throughout the dental papilla, but appears absent from the dental epithelium (A', A'', B' and B''). *fgf3* expression is strongly upregulated within both primary EKs (D': black arrowheads) and secondary EKs (C', C'', D' and D'': white arrowheads). Weaker *fgf3* expression is also noted within the dental mesenchyme (C', C'', D' and D''). *shh* expression is absent from the dental mesenchyme. However, its expression is can be seen throughout the dental epithelium at the leading edge of the developing tooth (E', E'', F' and F''). Although its expression is not restricted to the EK throughout morphogenesis, clear *shh* expression within both the primary EKs (E' and F': black arrowheads) and secondary EKs (E', E'' and F'': white arrowheads). As with *fgf3*, *fgf10* expression is also restricted to the future cusp forming primary (G' and G'': black arrowheads) and secondary EKs (G' and G'': white arrowhead), however its expression does not extend into the dental mesenchyme. Dotted black boxes in A – G depict magnified region in A' – G' and A'' – G''. Scale bars are 250µm in A-G and 125µm in A' – G' and A'' – G''.

to these sites (Fig 4), demonstrate the conservation of an EK signalling centre at the dental cusp sites in the shark. Wnt/ $\beta$ -catenin signalling has been implicated upstream of key pathways (Bmp, Fgf and Msx) regulating dental morphogenesis (Kratowil *et al.*, 2002; Liu *et al.*, 2008). Having identified the presence of a putative EK during dental development in the catshark, we wanted to test the role of canonical Wnt signalling in the regulation of dental shape. IWR-1-endo is a canonical Wnt antagonist. It functions through stabilising cytoplasmic Axin2 in turn increasing proteasome-mediated degradation of cytoplasmic  $\beta$ -catenin, leading to a decrease in canonical Wnt signalling, whilst simultaneously not promoting *de novo axin2* mRNA synthesis (Fig S8) (Chen *et*

*al.*, 2009a). In contrast, CHIR99021 selectively inhibits the kinase activity of GSK3 (Ring *et al.*, 2003). This prevents the formation of the  $\beta$ -catenin destruction complex and in turn leads to a stabilisation of cytoplasmic  $\beta$ -catenin and a subsequent increase in canonical Wnt signalling (Fig S8) (Wagman *et al.*, 2004). Wnt signalling was both upregulated and downregulated using 2 $\mu$ M CHIR99021 and 1 $\mu$ M IWR-1-endo, respectively. We treated samples for 14 days, allowing for the initiation of on average one tooth generation. Samples were treated at approximately 100dpf (mid-stage 32), by which point one to two generations are undergoing morphogenesis.

#### *RT-qPCR following canonical Wnt manipulation*

Firstly, in order to test the effect of small molecule treatment on canonical Wnt activation, we quantified the expression of the downstream Wnt target *axin2* through RT-qPCR. *axin2* was chosen as a chemical treatment readout given that it is a direct target of canonical Wnt signalling (Jho *et al.*, 2002; Aulehla *et al.*, 2003) and is routinely used as a readout for canonical Wnt activity (e.g. Suomalainen and Thesleff, 2010; Gaete and Tucker, 2013; Chen *et al.*, 2014). Furthermore, although IWR1-endo activates canonical Wnt signalling through the stabilisation of Axin2 protein levels, IWR1-endo has been shown to not induce *de novo axin2* mRNA synthesis. Therefore, increased levels of *axin2* expression following chemical treatment are due to increased canonical Wnt signalling mediated *axin2* transcription (Chen *et al.*, 2009a). In wild-type samples, *axin2* is expressed in both the successional lamina and dental epithelium of the developing tooth (Fig 5B and C). Directly after 14 days treatment, the dental lamina and developing tooth generations were dissected from the lower jaw and total RNA was extracted (Fig S2). Two-step RT-qPCR was carried out on the extracted RNA. The



concentration of IWR1-endo (1 $\mu$ M) and CHIR99021 (2 $\mu$ M) used was relatively low in order to prevent mortality during the long treatment times. Long treatments (14 day treatment + 28 day recovery) were necessary to ensure that developing teeth had undergone morphogenesis before phenotypic screening. In order to measure the full extent of chemical treatment on the expression of *axin2*, we also carried out RT-qPCR after the full initial 14 day treatment. Following 1 $\mu$ M IWR-1-endo treatment, we observed an average of 51% decrease in the expression of *axin2* relative to 0.1% DMSO control samples (Fig 5A). In contrast, following 2 $\mu$ M CHIR99021 treatment we see a 180% increase in the expression of *axin2*. Across treatments there is not a statistically significant effect ( $p = 0.05$ ) of treatment on the expression of *axin2* (ANOVA:  $F_{2,6} = 3.63$ ,  $p = 0.09$ ), however given a  $p$ -value of 0.09 and a low number of biological replicates (3), we cannot rule out that there is a biologically significant effect present. In order to compare between treatments, we carried out post hoc Tukey multiple comparisons of means test. Neither IWR-1-endo (Tukey:  $p = 0.55$ ) or CHIR99021 (Tukey:  $p = 0.32$ ) treatments differed significantly from control (DMSO) samples in their expression of *axin2*. When compared to each other, the difference in the effect of IWR-1-endo and CHIR99021 treatment on *axin2* is greater than when compared to control treatments, although there is not a significant effect (Tukey:  $p = 0.08$ ). The effect of CHIR99021 (Wagman *et al.*, 2004) and IWR-1-endo (Chen *et al.*, 2009a) on canonical Wnt signalling is well documented. Although we do not find a significant effect of treatment on the expression of *axin2* (ANOVA:  $F_{2,6} = 3.63$ ,  $p = 0.09$ ), the effect of CHIR99021 (Wagman *et al.*, 2004) and IWR-1-endo (Chen *et al.*, 2009a) on canonical Wnt signalling is well documented. Our low number of biological replicates is possibly leading to this experiment being statistically underpowered. This prior knowledge should be taken into account when drawing conclusions from this

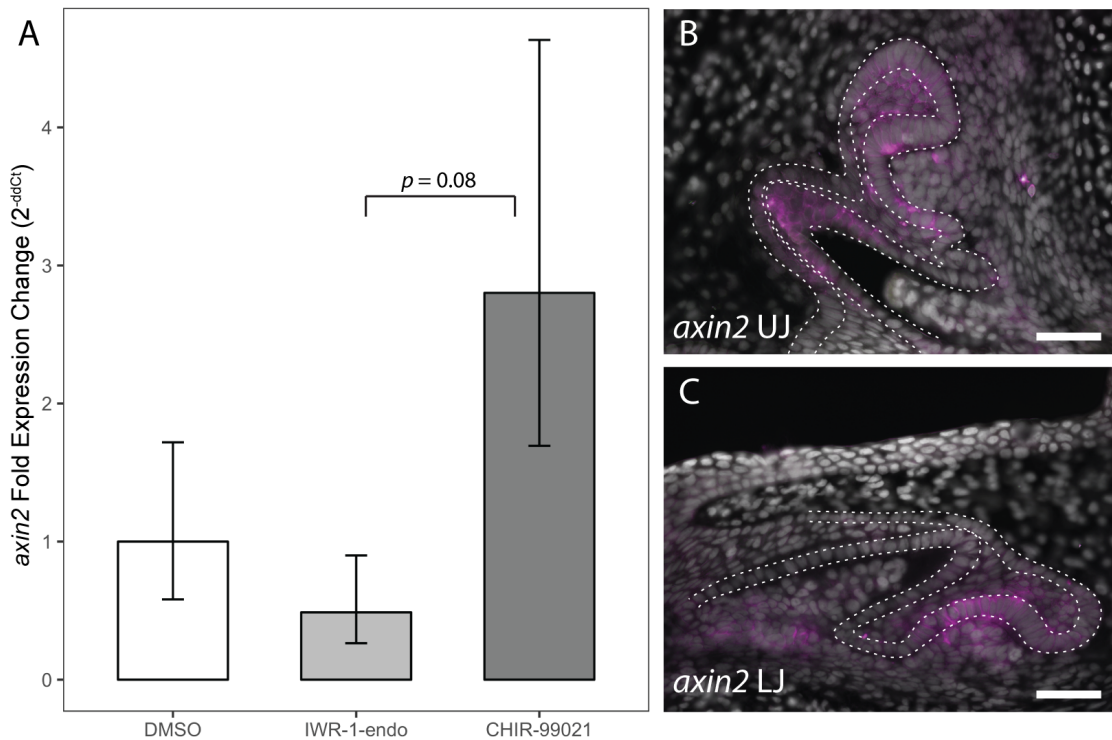


**Figure 5. RT-qPCR following small molecule manipulation of canonical Wnt signalling.**

A) RT-qPCR reveals *axin2* fold expression change following small molecule treatment with 0.1% DMSO (control), 1 μM IWR-1-endo and 2 μM CHIR99021. The dental lamina from the lower jaw was dissected immediately following two-week treatment. Three biological replicates were taken for each treatment. Expression levels were calculated using the ddCt method (Livak and Schmittgen, 2001). Normalised expression levels (2<sup>-ddCt</sup>) were calculated relative to 0.1% DMSO control samples in order to compare fold expression change. Error bars represent standard error. We assessed the effect of treatment on the expression level of *axin2* using a one-way ANOVA. Pairwise comparisons between treatments were made using a post hoc Tukey test. There is no significant difference in the expression of either treatment relative to DMSO. However, when compared to each other, the effect of IWR-1-endo and CHIR99021 treatment on *axin2* expression was marginally significant (Tukey:  $p = 0.08$ ). Wild type sagittal section *in situ* hybridisation for *axin2* in both upper jaw (B) and lower jaw (C) reveals expression throughout the dental epithelium of newly developing teeth and successional lamina. Weak expression is observable in the condensing dental mesenchyme. White dotted lines depict the columnar basal epithelial cells of the dental lamina and dental epithelium. Gene expression is false coloured in magenta. DAPI nuclear stain is false coloured in grey. Scale bars are 50 μm.

experiment. Furthermore, given the difference in *axin2* expression observed between the two treatments (Tukey:  $p = 0.08$ ), our results suggest that treatment may be having an effect on canonical Wnt signalling.

#### *Geometric morphometric analysis of tooth shape and size following Wnt treatment*

Following treatment, samples were left to recover for a further 28 days before we examined the treatment effect upon final tooth shape. Drastic shifts in the shape of teeth were observed following treatment (Fig 7). Abnormalities in cusp development were seen across both IWR-1-endo and CHIR99021 treated samples, however, given the presence of reduced cusps and uneven tooth edges (serrated in appearance), quantifying the number of cusps was not feasible. In order to accurately compare changes in tooth shape following treatment, we carried out two-dimensional (2-D) geometric morphometric measurements of mineralised teeth following treatment (Fig 6). Furthermore, dental differentiation and mineralisation takes place unidirectionally, from the apex towards the base of the tooth. This wave of mineralisation could lead to further variability in measurements of final tooth shape. In order to mitigate for this dynamic mineralisation process, only teeth which were fully mineralised and for which the base of the tooth could be clearly seen, were included in our measurements.

Landmark based geometric morphometrics uses Cartesian co-ordinates instead of traditional linear measurements in order to accurately measure biological shape (Seetah *et al.*, 2014). A measure of size known as the Centroid size can then be obtained from these co-ordinates. This is calculated as the square root of the sum of squared distances

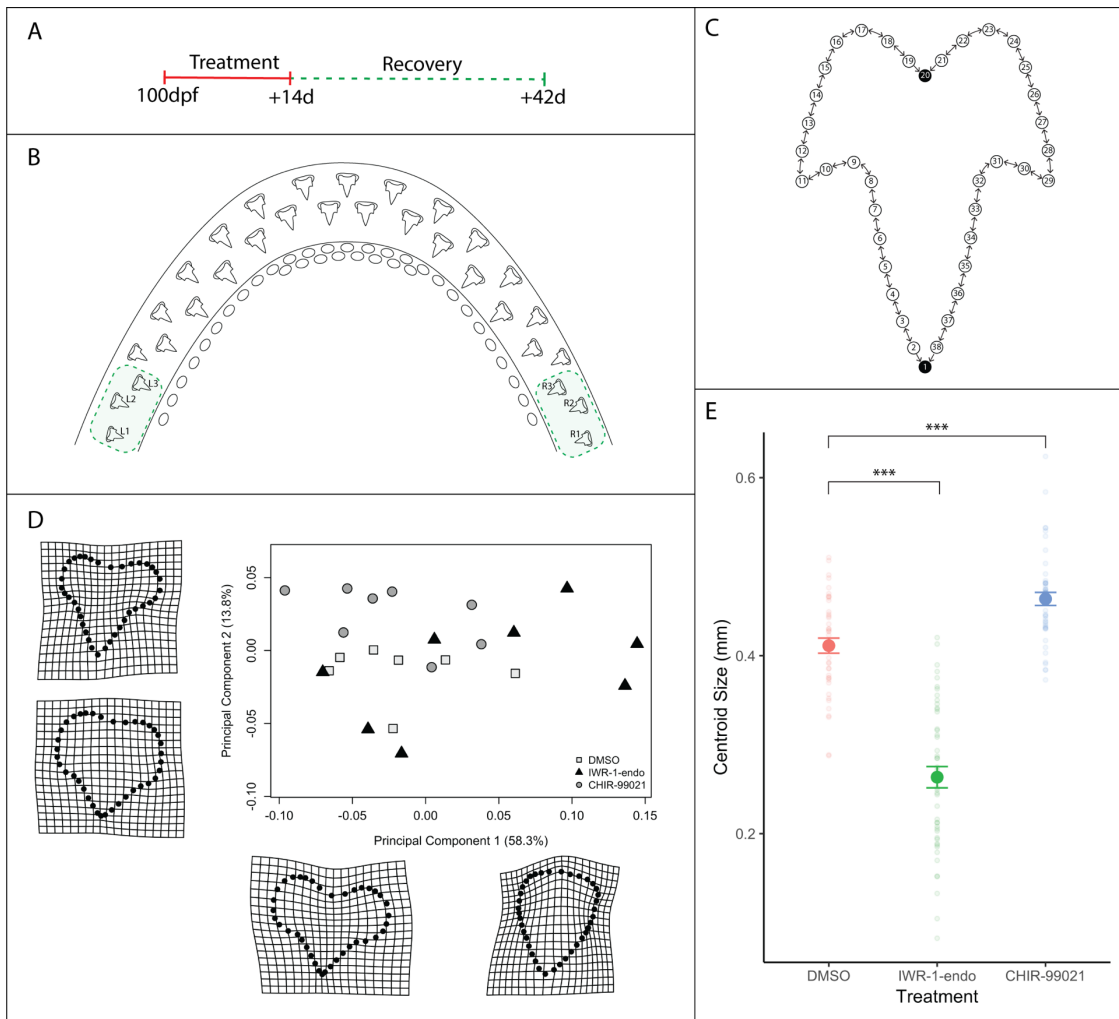


**Figure 6. Geometric morphometric analysis reveals change in shape and size following canonical Wnt manipulation.** Small molecule treatments consisted of a two-week treatment with 0.1% DMSO (control), 1 $\mu$ M IWR-1-endo and 2 $\mu$ M CHIR99021 and a subsequent four-week recovery (A). The three most lateral teeth at both left and right lower jaw margins (B) were included in the geometric morphometric analysis. A total of 38 landmarks were used to label tooth shape (C). Two fixed landmarks were placed at the tip of the primary cusp and at the base of the tooth, represented by black circles. 18 sliding semi-landmarks were placed on either side of the tooth (white circles), which were allowed to move relative to adjacent landmarks. The direction of movement is depicted by directional arrows in the schematic (C). Following Procrustes alignment of landmark co-ordinates and principle component analysis of the resulting shapes, the average PC1 and PC2 scores for each sample were plotted in order to depict the position of treated samples within a given shape space (D). PC1 accounted for 58.3% of the variation observed between samples, whereas PC2 accounted for 13.8%. Warpgrids shown in D reveal representative shapes at maximum and minimum PC1 and PC2 values. There

is a significant effect of treatment on overall tooth shape (Procrustes ANOVA:  $R^2 = 0.09174$ ,  $F_{2,115} = 8.2771$ ,  $p < 0.001$ ), whilst controlling for variation within samples. There is also a significant effect of sample on shape (Procrustes ANOVA:  $R^2 = 0.27092$ ,  $F_{20,115} = 2.4442$ ,  $p < 0.001$ ). Aside from shape, Centroid size was also measured following treatment (E). There is a significant effect of treatment on Centroid size (ANOVA:  $F_{2,115} = 235.5886$ ,  $p < 0.001$ ), whilst controlling for variation within samples. There is also a significant effect of sample on Centroid size (ANOVA:  $F_{20,115} = 7.2957$ ,  $p < 0.001$ ). Faint circular points are plots of each individual data point, revealing the distribution of the data. Error bars represent standard error.

from each landmark to the centroid (Klingenberg, 2016). The co-ordinates obtained from the landmarks are then transposed, scaled (relative to the centroid size) and rotated, giving a final measurement of shape which can be compared across different treatments (Klingenberg, 2016). For our analysis, we used a 2-D landmark based geometric morphometric approach. We placed two fixed homologous landmarks on each tooth, one at the tip of the primary cusp and one at the base of the tooth. 18 sliding-semilandmarks were then distributed evenly between these two points on either side of the tooth, given that there were no other homologous features shared by all samples (Fig 6C). Sliding semi-landmarks are allowed to move between one another so that they best match corresponding points between other samples. The underlying assumption is that the curves along which the landmarks slide are homologous, even if the landmarks themselves are not (Perez *et al.*, 2006).

We chose to compare the shape of the three most lateral teeth of both the left and right lower jaw margins (Fig 6B) to mitigate variation observed between dental generations elsewhere in the jaw. Furthermore, there is substantial variation in tooth number during this stage of development and therefore a direct comparison of tooth positions elsewhere in the jaw is problematic. Dental differentiation and mineralisation also takes

place unidirectionally, from the apex towards the base of the tooth. This wave of mineralisation could lead to further variability in measurements of final tooth shape. In order to mitigate for this dynamic mineralisation process, only teeth which were fully mineralised and for which the base of the tooth could be clearly seen, were included in our measurements. After carrying out a general Procrustes analysis (GPA), we found a significant effect of treatment on overall tooth shape (Procrustes ANOVA:  $R^2 = 0.09174$ ,  $F_{2,115} = 8.2771$ ,  $p < 0.001$ ), whilst controlling for variation within samples. We also found a significant effect of sample on shape (Procrustes ANOVA:  $R^2 = 0.27092$ ,  $F_{20,115} = 2.4442$ ,  $p < 0.001$ ), highlighting variation found within sample measurements.

Principle component analysis of the GPA reveals that 58.3% of the variation in tooth shape observed between samples can be explained by a single axis of variation (PC1), with a further 13.8% explained by a second axis of variation (PC2) (Fig 6D). As a result of high variation in dental shape, secondary cusps are not fully represented in the morphometric analysis. However, their presence can somewhat be revealed through a bulging of the tooth at sites adjacent to the primary cusp (Fig 6D: warpgrids). The shift in dental shape observed across PC1 attributes to a change in width of the tooth and an apparent change in cusp number. 4 out of 8 IWR-1-endo treated samples can be seen exhibiting extreme unicuspid dental morphologies (PC1 = 0.05 ~ 0.15), whilst 5 out of 8 CHIR99021 treated samples exhibit wide teeth with more distinctive cusps (PC1 = -0.1 ~ 0). We also observe an increase in the variation of dental shapes across the PC1 axis following Wnt downregulation with IWR-1-endo (pairwise F-test:  $F_{41,47} = 0.277$ ,  $p < 0.001$ ) (Fig S3). These results show that dental shape is being dramatically affected as a result of canonical Wnt manipulation, although it is difficult to discern directional

changes in morphology.

It is not only shifts in shape we observe as a result of treatment, but also dramatic changes in the size of teeth. Centroid size derived from GPA is a measure of an objects scale. This provides more detail than directional measurements such as length or area which are affected by an objects shape (Seetah *et al.*, 2014; Klingenberg, 2016). Following treatment, we found a significant effect of treatment on Centroid size (ANOVA:  $F_{2,115} = 235.5886$ ,  $p < 0.001$ ), whilst controlling for variation within samples (Fig 6E). However, there was also a significant effect of sample on Centroid size (ANOVA:  $F_{20,115} = 7.2957$ ,  $p < 0.001$ ).

In order to compare the mean Centroid size between treatments, we carried out post hoc Tukey multiple comparisons of means test. There is a significant decrease in Centroid size (-35.9%) following IWR-1-endo treatment (Tukey:  $p < 0.001$ ), whilst conversely there is a significant increase in Centroid size (+12.8%) as a result of CHIR99021 treatment relative to control samples (Tukey:  $p < 0.001$ ) (Fig 6E). These findings reveal a directional change in tooth shape as a result of canonical Wnt signalling manipulation, given that IWR-1-endo and CHIR99021 downregulate and upregulate Wnt signalling respectively.

#### *Canonical Wnt signalling development of dental cusps*

Representative images of lateral teeth included in the geometric morphometric analysis reveal clear changes in tooth size (Fig 7). IWR-1-endo treatment resulted in stunted

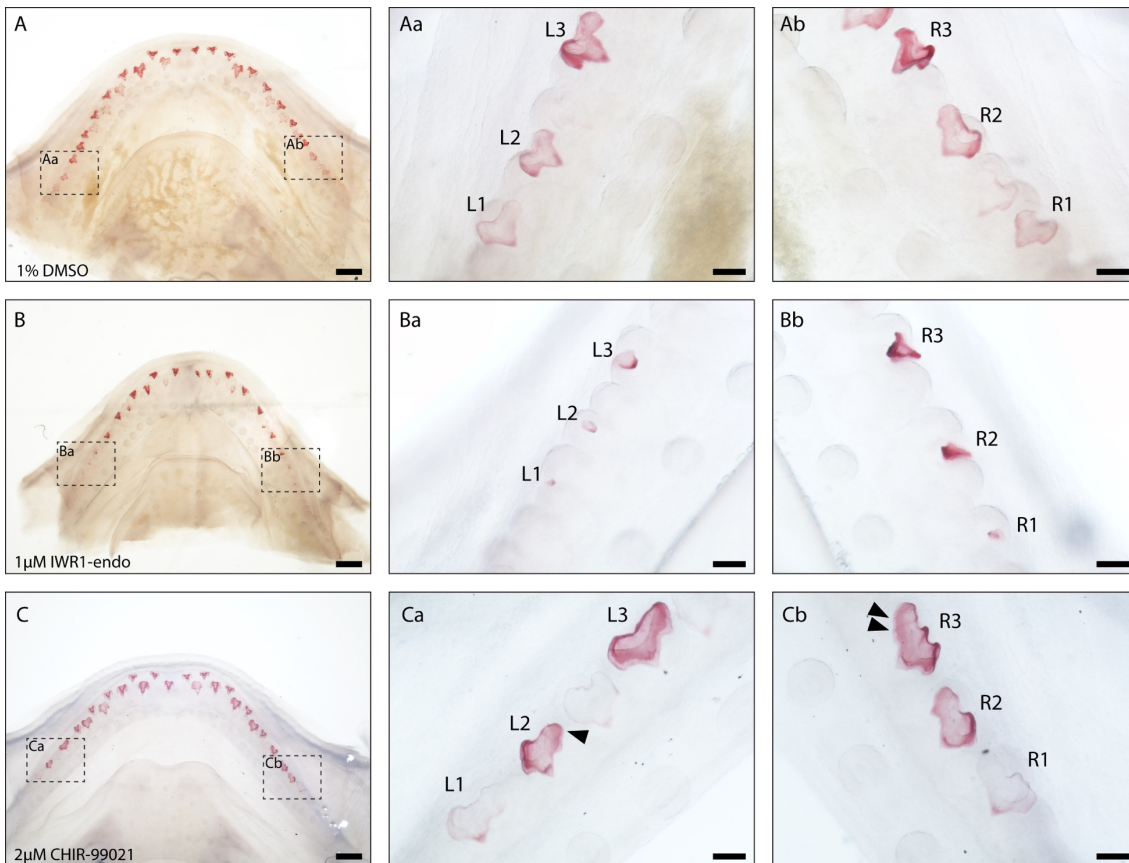


**Figure 7. Clear and stained samples reveal observable shift in tooth shape in lateral teeth following canonical Wnt manipulation.** Representative images of 0.1% DMSO (control) (A), 1µM IWR-1-endo (B) and 2µM CHIR9902 (C) treated lower jaws following two-week treatment and four-week recovery. Samples have been cleared and stained. Aa-Ca and Ab-Cb are magnified images of left and right lateral jaw regions respectively. A tricuspid dentition is visible in 0.1% DMSO treated teeth (Aa and Ab). A shift to a unicuspid morphology takes place following treatment with 1µM IWR-1-endo (Ba and Bb). In contrast, a widening of the teeth is observed following 2µM CHIR9902 (Ca and Cc). Black arrowheads represent the addition of putative supernumerary cusps. Dotted black boxes in A-C depict magnified region in Aa – Ca and Ab – Cb. Scale bars are 500µm in A-C and 100µm in Aa – Ca and Ab – Cb.

teeth, with the developed teeth failing to undergo normal morphogenesis yet successfully undergoing mineralisation (Fig 7B). Most lateral teeth exhibit a reduction in secondary cusp size, with some teeth exhibiting a unicuspid morphology with a complete loss of secondary cusps (Fig 7B). Observations of dental morphology at other



sites along the jaw reveal a range of dental defects following treatment (Fig 8). There is a consistent loss/reduction in secondary cusps along the jaw (Fig 8B1 and 8B2), which is concurrent with the morphologies observed in the lateral teeth included in the geometric morphometric analysis, although not all teeth exhibit this phenotype (Fig 8B3). We also observed the development of duplicated teeth (Fig 8B3). This may arise from fusion of tooth buds belonging to adjacent tooth families, as a result of a loss in the zone of inhibition between tooth sites. However, given that adjacent teeth are staggered in the timing of their development, it is more likely that shifts in signalling during early morphogenesis has resulted in defects in the folding of the dental epithelium resulting in the formation of two primary cusps.

In contrast, upregulation of canonical Wnt signalling via CHIR99021 treatment resulted in teeth more similar in appearance to the standard catshark dentition. Lateral CHIR99021 teeth are clearly larger and wider than controls (Fig 7A and B), with regions of the teeth appearing to initiate the formation of ectopic cusps, although these do not always fully form (Fig 7B: white arrowheads). Interestingly, within other regions of the jaw we do see the development of fully formed 4<sup>th</sup> cusps (Fig 8C2 and C3). This is similar to the phenotypes we see in juvenile catsharks, which develop teeth with up to 7 cusps. The development of 4<sup>th</sup> cusps can also be seen within some of the control teeth (Fig 8A3). However, the proportion of teeth exhibiting 4<sup>th</sup> cusps is significantly lower in control samples (1%), than CHIR99021 treated samples (12%) (chi-square:  $X^2 = 16.887$ ,  $df = 1$ ,  $p\text{-value} < 0.001$ ). Furthermore, the position and size of cusps in DMSO treated samples is very consistent. There is a clear single primary cusp, with two secondary cusps equal in size. Extra cusps develop laterally and are smaller in size than

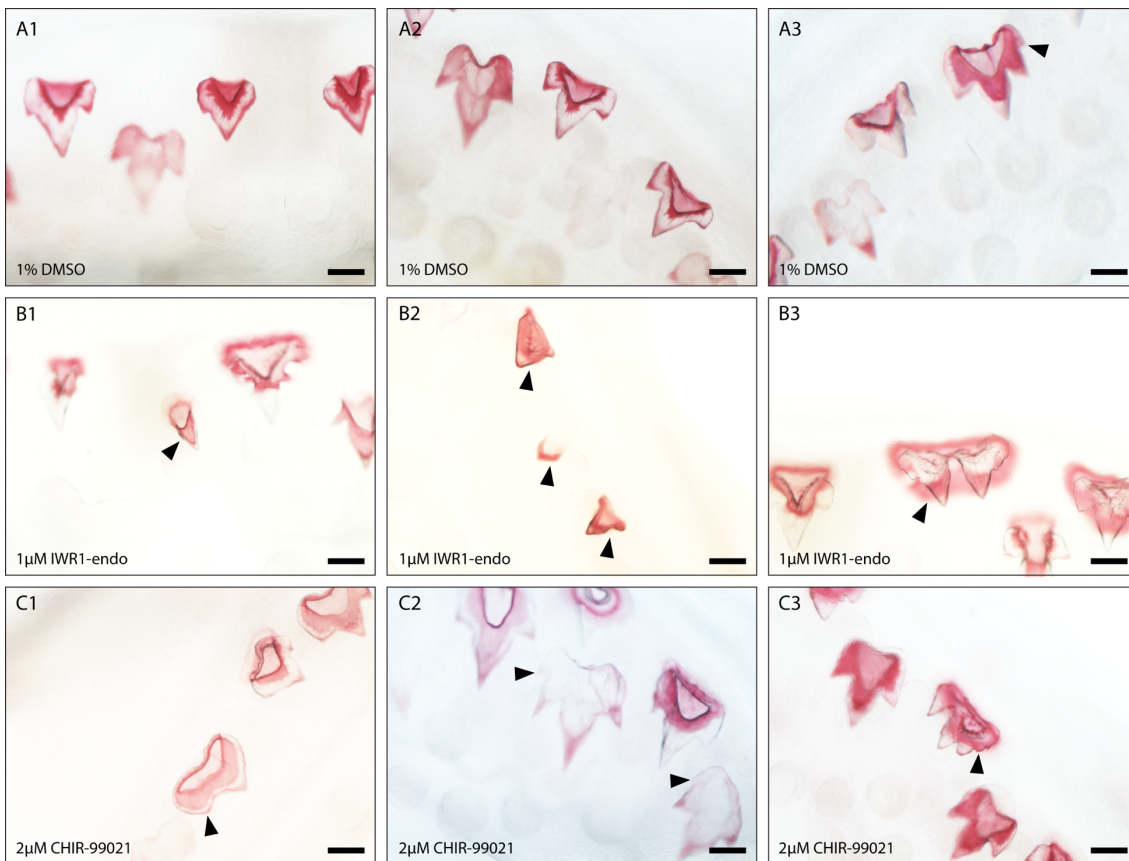


**Figure 8. Dental diversity following canonical Wnt manipulation.** Selected images depicting dental diversity following 0.1% DMSO (control) (A1-A3), 1µM IWR-1-endo (B1-B3) and 2µM CHIR9902 (C1-C3) treated lower jaws following two-week treatment and four-week recovery. 0.1% DMSO are relatively similar in shape, although the presence of four cusps is observed in a small subset of teeth (A3). Following 1µM IWR-1-endo treatment, there are numerous mineralised unicuspid and stunted teeth (B1 and B2). There are also teeth which appear duplicated in nature, but which are connected to a single root (B3). In contrast, 2µM CHIR9902 treatment leads to a widening of the teeth and defects in the position of cusps (C1) and the development of supernumerary cusps (C2 and C3). Black arrowheads point to cusp defects and/or shifts from the typical tricuspid dental morphology. Scale bars are 100µm.

the initial secondary cusps. This is not the case in CHIR99021 treated specimens. We note cases whereby secondary cusps are enlarged and can be difficult to distinguish apart from the primary cusp. We also observe teeth bearing multiple small cusps which

resemble serrated teeth. The defects observed in final tooth shape highlight an important role for Wnt during dental morphogenesis. The specific directional shifts in the number of cusps associated with down and up regulation through IWR-1-endo and CHIR99021 treatment respectively, implicate canonical Wnt in the regulation of cusp development and therefore possibly in EK signalling.

#### *In silico modelling of tooth shape following Wnt manipulation*

Salazar-Ciudad & Jernvall (2010) developed a computational model (ToothMaker) capable of modelling vertebrate dentitions based on 12 cellular and 14 genetic parameters with predetermined values. In order to establish the baseline parameters capable of generating a wild-type catshark tooth, we started with parameters established in modelling the seal dentition (Salazar-Ciudad and Jernvall, 2010). We iterated through each parameter at 10% intervals; using a process of elimination to refine the final tooth parameters (Fig S4). Following shifts in dental morphology as a result of canonical Wnt manipulation, we sought to determine which parameters were capable of generating comparable shifts *in silico*.

We identified two genetic parameters, which were individually capable of generating comparable phenotypes to the chemically treated samples. Both decreasing the activator auto-activation ( $Act = 0.1$ ) (Fig 9J) and increasing the inhibition of the activator ( $Inh = 8$ ) (Fig 9M), resulted in unicuspid phenotypes strikingly similar to IWR-1-endo treated samples (Fig 9G). These results are biologically relevant. IWR-1-endo increases the production of the canonical Wnt inhibitor Axin2 (Chen *et al.*, 2009a). The resulting

function of increasing *Axin2 in vivo*, can be equally compared to increasing the inhibitor (Inh) or decreasing the effect of an activator (Act) as a result of increased inhibition, *in silico*. The converse is true for CHIR99021, which stabilises cytoplasmic  $\beta$ -catenin leading to upregulated canonical Wnt signalling (Wagman *et al.*, 2004). This can be compared to decreasing the effect of an inhibitor, which would lead to higher cytoplasmic  $\beta$ -catenin (Inh = 1.2) (Fig 9O), or increasing the activator itself (Act = 0.22) (Fig 9L).

The resulting phenotype generated by the model results in both wider teeth, and an increase in cusp number (Fig 9L and O). This is directly comparable to the phenotypes observed following treatment with CHIR99021 (Fig 9I). In the model, the regulation of the inhibitor and activator stems from the EK signalling centre (Salazar-Ciudad and Jernvall, 2010). The recreation of comparable phenotypes through the alteration of biologically relevant genetic parameters supports our findings, which demonstrate a critical role of canonical Wnt signalling in the regulation of cusp number from the catshark EK.

A shift in cusp number is also observed throughout ontogeny, with an increase from 3 cusps in the embryo, to 5 or 6 cusps in juveniles (Fig 9A-C). Simultaneously changing the width of the initial tooth site (Bwi) together with Act is capable of recreating 5 and 6 cusped teeth (Fig 9D-F). As sharks grow, the size of new teeth increases (Fig 9A-B: scale). It is likely that an increase in the size of the initial tooth site generates larger teeth with more numerous cusps. Our findings show that increasing canonical Wnt activation results in teeth more similar to the adult phenotype, seen through an increase in cusp number following CHIR99021 treatment.

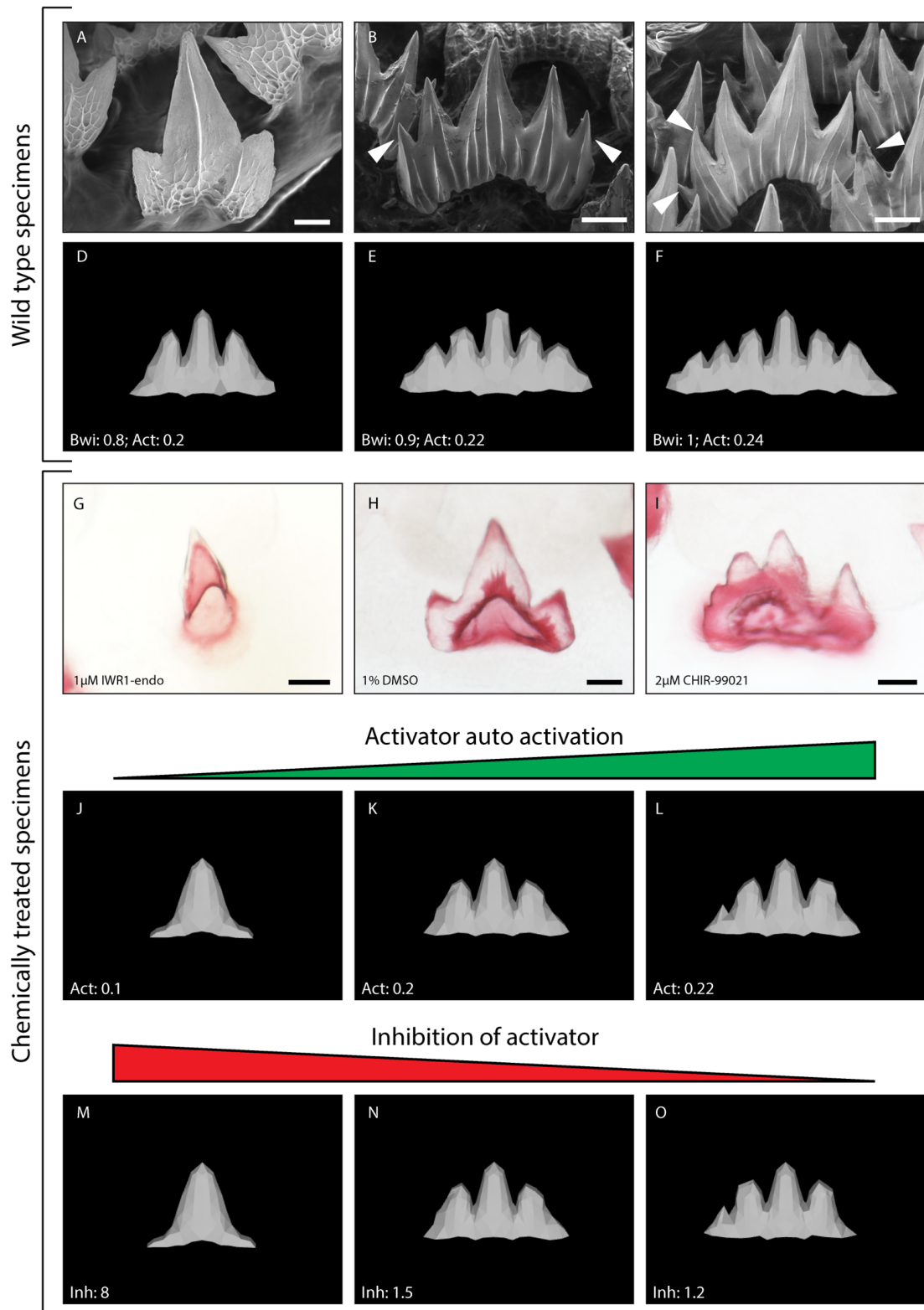


**Figure 9.** *in silico* modelling of the catshark dentition recreates phenotypes comparable to canonical Wnt manipulation. Wild type SEM images of embryonic (A) and juvenile (B and C) catshark samples shows a shift in cusp number from 3 to 6/7 cusps during ontogeny. The

computational model ‘ToothMaker’ (Salazar-Ciudad and Jernvall, 2010) was used to generate *in silico* models of the dentition (D-F; J-O). Baseline catshark parameters for the model are available in the supplementary information (Fig S4). Increasing the boundary width (Bwi) of the initial tooth site and activator auto-activation (Act) is sufficient to shift teeth from a tricuspid (D) to a 5 (E) or 6 (F) cusped dentition. 12000 iterations of the model were ran when modelling shifts in the dentition, which take place during ontogeny (D-F). *in silico* modelling is also capable of reproducing dental morphologies observed following chemical treatment (G-O). 1 $\mu$ M IWR-1-endo resulted in unicuspid teeth (G), whereas 2 $\mu$ M CHIR9902 resulted in the development of supernumerary cusps (I). Either an increase in activator auto activation (Act) (J-L) or decrease in inhibition of activator (Inh) (M-O), is sufficient to shift teeth from a unicuspid (J and M) to tricuspid (K and N) and quadricuspid (L and O) morphology. 10000 iterations of the model were run when modelling the effect of small molecule treatment. White arrowheads represent the addition of extra cusps during ontogeny. Scale bars are 50 $\mu$ m in A and G-I, and 200 $\mu$ m in B and C.

## Discussion

Overall, our results demonstrate that an EK-like signalling centre regulates the formation of dental cusps in the catshark, with canonical Wnt signalling playing an important role in this process. We identify restricted expression of Fgf markers within the non-proliferative apical dental epithelium corresponding to the EK in mammals, and highlight shifts in cusp number and tooth shape following canonical Wnt manipulation.

### *Catsharks possess an enamel knot-like signalling centre*

Low levels of proliferation at the apical tip of the developing tooth has hinted at the presence of an EK in sharks (Rasch *et al.*, 2016), although three-dimensional restriction of signalling molecules within a distinct signalling centre is yet to be described. We note the expression of *fgf10* and the canonical Wnt inhibitor *dkk1* within the non-

proliferative dental epithelium (Fig 3). Furthermore, our whole mount *in situ* hybridisation data reveals restricted upregulation of *fgf3* and *fgf10* within both primary and secondary cusp regions (Fig 4) and therefore the presence of a spatially restricted dental epithelial signalling centre. In mammals, the expression of EK markers precedes dental shape change (Vaahtokari *et al.*, 1996). Similarly, we observe the restricted expression of *fgf3* (Fig 2F) and *fgf10* (Fig 3A) very early during dental morphogenesis, prior to the establishment of the overall tooth shape. This suggests that signalling precedes dental shape change and suggests that Fgf signalling may be driving this process as in mammals (Jernvall *et al.*, 1994; Kettunen *et al.*, 2000). Further investigation of EK markers prior to dental morphogenesis is key in discerning the role and regulation of EK driven dental morphogenesis in the shark.

Importantly, the mammalian EK itself, is unable to respond to the Fgf signals which it emits as it lacks Fgf receptors (Kettunen *et al.*, 1998). Instead, these receptors are found within adjacent dental epithelial cells, and are important for the induction of differential proliferation between the EK and surrounding epithelial tissue (Kettunen *et al.*, 2000). Further research is needed to identify whether this lack of receptors predates the evolution of the mammalian dentition, and whether it is fundamentally required for the formation of cusped teeth. Given the conservation of localised Fgf signalling within in the shark EK, we hypothesise that a similar lack of receptors drives differential proliferation between the EK and surrounding dental epithelium in the basal gnathostome lineage.

Various developmental characteristics have been used to define the presence of an EK, including spatial restriction of the signalling centre, a lack of cell proliferation, and apoptosis of the epithelial cells within the EK. Apoptosis has been implicated as an important developmental process in regulating the silencing of embryonic signalling centres (Vaahtokari *et al.*, 1996). Apoptosis has been described in both primary and secondary mammalian EK through TUNEL assays and the expression of the pre-apoptotic marker, p21 (Vaahtokari *et al.*, 1996; Jernvall *et al.*, 1998). Apoptotic assays have so far revealed a lack of apoptosis within the inner dental epithelium of reptiles (Buchtová *et al.*, 2008; Handrigan and Richman, 2010b) and the catshark (Debiais-Thibaud *et al.*, 2015) - this has been used to refute the presence of an EK altogether (Debiais-Thibaud *et al.*, 2015). However, it has also been shown that mice develop cusps following the loss of apoptosis in caspase-3 deficient mice (Matalova *et al.*, 2006). Although morphological defects are identified in non-apoptotic mouse molars (Matalova *et al.*, 2006), these results suggest that apoptosis is not fundamentally required in the formation of dental cusps (Richman and Handrigan, 2011).

Whilst there are observable differences in signalling between the mammalian and chondrichthyan EKs (Debiais-Thibaud *et al.*, 2015), this does not refute the presence of an EK in sharks. Instead, these differences highlight potential lineage specific modifications which have led to the diversification of the vertebrate dental morphology. Given the presence of enameloid, as opposed to 'true' enamel within the Chondrichthyes (Gillis and Donoghue, 2007), it has been proposed to term this signalling centre in sharks the enameloid knot (Rasch *et al.*, 2016).



Our results reveal a complete lack of *bmp4* expression within the non-proliferative apical dental epithelium. Its expression in surrounding tissues suggests that unlike in mammals, where *bmp4* is secondarily upregulated within the EK, *bmp4* may play a role in restricting the expression of other signalling molecules to the EK in the shark. Furthermore, *shh* is a key marker of the EK in mammals. Although we note its expression within the apical dental epithelium, there is little downregulation of its expression within the inter-cusp dental epithelium. Asymmetric *shh* expression is thought to regulate polarised growth of the developing feather bud (Ting-Berreth and Chuong, 1996) as it does in the zone of polarising activity (ZPA) within the vertebrate limb bud (Riddle *et al.*, 1993). It is possible that *shh* is playing a similar role in teeth in sharks; *shh* may be regulating polarised growth of the tooth along the oral/aboral axis, but not the medial/lateral axis along which the cusps form. Despite differences in the gene specific expression patterns of the mammalian and chondrichthyan EKs, representative markers of canonical Wnt, Bmp and Hh signalling are all found expressed within the apical dental epithelium.

#### *Canonical Wnt signalling as a regulator of natural shark dental variation*

Chondrichthyan dental morphology is highly variable between species (Corn *et al.*, 2016). This variability allows for fossil samples to be commonly identified on their dentition alone (Whitenack and Gottfried, 2010). Variation in chondrichthyan tooth shape is typically observable as a modification of the cusp. Examples include: the multicuspid saw-like teeth of the sixgill shark (*Hexanchus griseus*); the elongated

primary cusp of mako shark teeth (*Isurus oxyrinchus*); serrated teeth of the tiger shark (*Galeocerdo cuvier*); and the tricuspid teeth of the small-spotted catshark (*S. canicula*) (Corn *et al.*, 2016). Our chemical manipulations of the canonical Wnt signalling pathway result in a shift in cusp number and an increase in the variability of tooth shape. Furthermore, the diversity of phenotypes observed following treatment include unicuspid, multicuspid and serrated teeth.

Canonical Wnt signalling is known to lie upstream of EK signalling during mammalian molar morphogenesis, with its upregulation and downregulation leading to supernumerary EKs and the formation of blunted cusps respectively (Jarvinen *et al.*, 2006; Liu *et al.*, 2008). In the shark, our findings indicate a similar role for Wnt signalling during dental morphogenesis. Here, its manipulation dramatically disrupts cusp development. As a result, we speculate that alterations to the canonical Wnt pathway may also underlie the natural diversity of tooth shape found between chondrichthyan species. However, although our chemical manipulation phenotypes match what would be expected as a result of disrupted EK signalling, we cannot exclude the possibility that the observed shifts in shape arise as a result of changes in size of the teeth or developmental arrest of tooth morphogenesis. Analysis of canonical Wnt signalling targets within the EK following chemical manipulation, could provide further clarity as to which of these developmental processes is driving shape change.

Canonical Wnt signalling is involved at multiple stages of dental development and also lies upstream in the EK signalling cascade (Jarvinen *et al.*, 2006). There is therefore likely to be an intimate link between the stage of development of a tooth and the

molecular downstream effect following treatment. Given that the timing of dental initiation is variable across the jaw margin in the shark, there is likely to be significant variation in the response to chemical treatment depending on tooth position. Furthermore, there is a substantive delay between our measurements of the molecular response (axin2 expression) and the phenotypic response (alizarin red staining). This was unavoidable due to the slow process of dental mineralisation, leading to a time gap between the onset of dental morphogenesis and full dental mineralisation. A transcriptomic screen at multiple time points following treatment would reveal the downstream molecular response and could help explain the variability in observed phenotypes.

An *in silico* model of dental morphogenesis developed by Salazar-Ciudad and Jernvall (2010) demonstrates how dental shape can be regulated by a variety of cellular and genetic parameters in the EK. Subtle changes to these parameters lead to a drastic change in dental shape and cusp number. We show that small changes to two genetic parameters regulating activation (Act) or inhibition (Inh) of the activator in the EK, is sufficient in generating teeth representative of upregulation and downregulation of canonical Wnt signalling respectively. The similarities observed following Wnt treatments and *in silico* EK signalling manipulations, provide both an element of validation for the *in silico* model and further evidence of a role for canonical Wnt signalling in the chondrichthyan EK.

*EK-like signalling centre present prior to the evolution of teeth*

Odontodes are thought to have initially evolved outside of the oral cavity, with teeth arising through co-option of the underlying odontode gene regulatory network (Fraser *et al.*, 2010; Donoghue and Rücklin, 2016; Martin *et al.*, 2016). Dermal denticles (non-regenerative odontodes present on the skin surface of chondrichthyans) and teeth are deeply homologous, sharing a high degree of structural and developmental conservation (Martin *et al.*, 2016). We observe identical expression patterns for *fgf3*, *bmp4* and *shh*, within and around the apical tip of developing teeth (Fig 2) and dermal denticles in the catshark (Cooper *et al.*, 2017). As a result, we believe it is likely that the origin of an apical epithelial signalling centre regulating differential epithelial proliferation in epithelial appendages, evolved early within the vertebrate lineage and predates the evolution of teeth.

### *Conclusion*

Although there are differences in the expression of key mammalian EK markers in the shark, there is also conservation of key Wnt, Fgf and Shh markers. Contrary to prior assertions, these results provide evidence of an EK signalling centre in an early vertebrate lineage. EKs are non-proliferative signalling centres within the enamel organ of developing teeth (Jernvall *et al.*, 1994). We therefore suggest that mammalian specific gene expression patterns within the EK are merely lineage specific modifications of an ancestral signalling centre, and cannot be used alone in determining the presence of EKs in other vertebrate groups.

### **Methods**

### *Animal husbandry*

The University of Sheffield is a licensed establishment under the Animals (Scientific Procedures) Act 1986. All animals were culled by approved methods cited under Schedule 1 to the Act. Catshark embryos (*S. canicula*) were obtained from North Wales Biologicals, Bangor, UK. Embryos were raised in recirculating artificial seawater (Instant Ocean) at 16°C. At the required stage, embryos were anaesthetised using 300mg/L MS-222 and fixed overnight in 4% paraformaldehyde at 4°C. Samples were then dehydrated through a graded series of DEPC-PBS/EtOH and kept at -20°C.

### *Sectioning and Histology*

Following dehydration, samples were cleared with xylene and embedded in paraffin. 14µm sagittal sections were obtained using a Leica RM2145 microtome. For histological study, sections were stained with 50% Haematoxylin Gill no.3 and Eosin Y. Slides were mounted with Fluoromount (Sigma) and imaged using a BX51 Olympus compound microscope.

### *Scanning Electron Microscopy (SEM)*

SEM images were obtained using a Hitachi TM3030Plus Benchtop SEM at 15000 Volts.

### *Probe synthesis*

Protein coding sequences for *S. canicula* were obtained from a *de-novo* transcriptome assembly (Martin et al. unpublished). Sequences were compared with a range of other vertebrate sequences taken from ensembl.org in order to verify sequence identity. *S. canicula* total RNA was extracted using phenol/chloroform phase separation and cleaned through EtOH/LiCL precipitation. RT-cDNA was made using the RETROscript 1710 kit (Ambion). Probes were made using forward and reverse primers designed through Primer3. Primer sequences are available in the supplementary information (Fig S5). Probes were chosen to be ~400-800bp in length. Sequences of interest were amplified from the cDNA through PCR and ligated into the pGEM-T-Easy vector (Promega). Ligation products were cloned into JM109 cells. Plasmid DNA was then extracted from chosen colonies using a Qiaprep spin Mini-prep kit (Qiagen) and sequenced (Applied Biosystems' 3730 DNA Analyser) through the Core Genomics Facility, University of Sheffield. Verified vectors were then amplified through PCR and used as a template for probe synthesis. Sense and anti-sense probes were made using a Riboprobe Systems kit (Promega) and SP6/T7 polymerases (Promega). Probes were labelled with Digoxigenin-11-UTP (Roche) for detection during *in situ* hybridisation. A final EtOH precipitation step was carried out to purify the RNA probe.

### *Section in situ hybridisation*

Sagittal paraffin sections were obtained as previously described. Slides were deparaffinised using Xylene and rehydrated through a graded series of EtOH/PBS. Slides were incubated in pre-heated pre-hybridisation solution pH 6 [250ml deionised-

formamide, 125ml 20x saline sodium citrate (SSC), 5ml 1M sodium citrate, 500µl Tween-20 and 119.7ml DEPC-treated ddH<sub>2</sub>O] at 61°C for 2 hours. Slides were transferred to pre-heated pre-hybridisation solution containing DIG labelled RNA probe (1:500) and incubated overnight at 61°C. The following day, slides underwent a series of 61°C SSC stringency washes to remove unspecific probe binding [2x30m 50:50 pre-hybridisation solution:2x SSC; 2x30m 2x SSC; 2x30m 0.2x SSC]. Following the stringency washes, samples were incubated in blocking solution (2% Roche Blocking Reagent (Roche)) for 2hr at room temperature and then incubated in blocking solution containing anti-Digoxigenin-AP antibody (1:2000; Roche) overnight at 4°C. Excess antibody was washed off through 6x1hr MAB-T (0.1% tween-20) washes. Slides were then washed in NTMT and colour reacted with BM-purple (Roche) at room temperature and left until sufficient colouration had taken place. Following the colour reaction, a DAPI nuclear counterstain (1µg/ml) was carried out before mounting the slides using Fluoromount (Sigma). Images were taken using a BX51 Olympus compound microscope. Images were contrast enhanced and merged in Adobe Photoshop.

#### *Double in situ hybridisation/immunohistochemistry*

For double *in situ* hybridisation/immunohistochemistry, samples first underwent *in situ* hybridisation as previously described. Immediately after colour reaction, samples were fixed for 1 minute in 4% paraformaldehyde in PBS. Samples were then blocked with 5% goat serum and 1% bovine serum albumin in PBS-T (0.05% tween-20). Blocking solution was replaced with blocking solution containing mouse anti-PCNA primary antibody (ab29; Abcam) at a concentration of 1:2000. Goat anti-rabbit Alexa-Fluor 647

(1:250) (A-20721245; Thermo) and goat anti-mouse Alexa-Fluor 488 (1:250) (A-11-001; Thermo) secondary antibodies were used for immunodetection. Samples were counterstained with DAPI ( $1\mu\text{g}/\text{ml}$ ) and mounted using Fluoromount (Sigma). Images were taken using a BX51 Olympus compound microscope. Images were contrast enhanced and merged in Adobe Photoshop.

#### *Whole mount in situ hybridisation*

Whole mount *in situ* hybridisation was carried out in accordance with the section *in situ* hybridisation protocol aside from a few subtle modifications. Following rehydration, samples were treated with  $0.2\mu\text{g}/\text{ml}$  proteinase K for 1hr at room temperature and then fixed for 20m in 4% paraformaldehyde in PBS. Samples were then placed in pre-hybridisation and probe solution as previously described. Stringency washes were carried out at  $61^\circ\text{C}$  [3x30m 2xSSC-T (0.05% tween-20); 3x30m 0.2xSSC-T (0.05% tween-20)]. Blocking, antibody incubation and colour reaction were carried out as previously described. Following colour reaction, samples were stored in PBS with 10% EtOH.

#### *Small molecule treatment*

10mM IWR-1-endo (product no) and 5mM CHIR99021 (product no) stock solutions were made using dimethyl sulfoxide (DMSO) as a solvent. At ~100dpf (mid stage 32), catshark samples were extracted from their egg cases and incubated in 70ml polypropylene containers. Samples were treated with  $1\mu\text{M}$  (1:10000 stock dilution) IWR-1-endo (N = 8),  $2\mu\text{M}$  (1:2500 stock dilution) CHIR99021 (N = 8). 0.1% DMSO



was used as a control (N = 7). Chemical stock solutions were diluted in artificial seawater with 1% Penicillin/Streptomycin. Samples were treated with 20ml of solution, which was replaced every two days for a total treatment period of two weeks. Following treatment, samples were raised in artificial seawater for a further 4 weeks. After recovery, samples were sacrificed using 300mg/L MS-222 and fixed overnight in 4% paraformaldehyde at 4°C. Samples were then stained with 0.02% alizarin red in 0.1% KOH overnight in the dark and subsequently cleared in 0.1% KOH. Once residual alizarin red had been removed, samples were transferred into glycerol through a glycerol/0.1%KOH graded series and imaged using a Nikon SMZ1500.

#### *RT-qPCR*

Immediately following two-week small molecule treatment and prior to the four-week recovery stage, samples were taken for two step RT-qPCR analysis. Three biological replicates were taken for each treatment (3x 1 $\mu$ M IWR-1-endo; 3x 2 $\mu$ M CHIR99021 and 3x 0.1% DMSO). Samples were anaesthetised in 300mg/L MS-222 and decapitated. The dental lamina from the lower jaw was dissected and removed from the sub lying Meckel's cartilage in ice cold DEPC-treated PBS. Tissue samples were placed in TRIzol Reagent (Invitrogen) and homogenised in a tissue lyser. RNA was extracted using phenol/chloroform phase separation and purified through EtOH precipitation. RNA concentration and quality was checked using the Qubit RNA HS Assay Kit (Invitrogen) and NanoDrop 8000 (Thermo Scientific) respectively (Fig S2). For the RNA reverse transcription, we used 200ng of template RNA and assumed a 1:1 RNA:cDNA synthesis. cDNA was transcribed using the Maxima First Strand cDNA Synthesis Kit

(Thermo Scientific). 50ng of cDNA was used in the final qPCR reactions (SensiMix SYBR No-ROX Kit; Biorline). We quantified the expression of two genes through qPCR; *axin2* as a downstream target of canonical Wnt signalling and GAPDH as a reference gene using the QuantStudio 12k Flex (Life Technologies). Three separate qPCR reactions (technical replicates) were carried out for each biological replicate to check for pipetting errors. Given that all technical replicates were within 0.5 cycle threshold (Ct) from one another, the mean was taken for each biological sample. Expression changes were calculated using the ddCt (Delta Delta Ct) method (Livak and Schmittgen, 2001). This method compares the raw amplification levels of a gene of interest relative to a housekeeping gene (GAPDH), giving a single standardised expression measurement (dCT) for each treatment whilst controlling for pipetting error. Treatment expression levels (ddCt) are then compared relative to the control treatment. Expression levels are on the log scale given the exponential increase in PCR product following each PCR cycle. Normalised expression levels (fold expression change;  $2^{-\Delta\Delta Ct}$ ) were calculated relative to 0.1% DMSO control samples (Fig 5). We assessed the effect of treatment on the expression level of *axin2* using a one-way ANOVA. Pairwise comparisons between treatments were made using a post hoc Tukey test.

### *Geometric morphometric analysis*

Images taken from the small molecule treated clear and stained specimens were analysed using 2-D geometric morphometrics. Images of the three most lateral teeth on both the left and right side of the lower jaw were included in the analysis. TPS files containing the treatment images were generated in tpsUtil (Rohlf, 2009b). Landmark

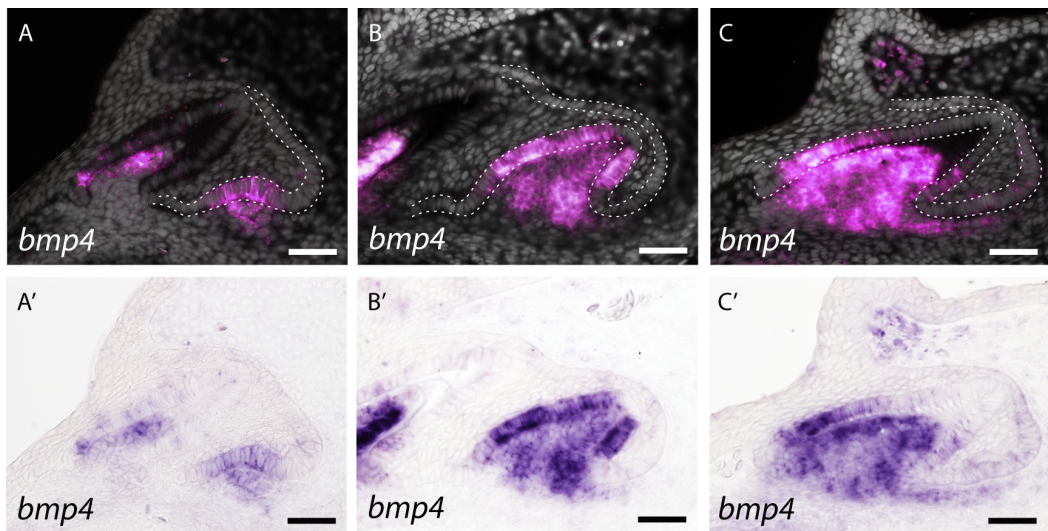
coordinates were assigned using tpsDig2 (Rohlf, 2009a). Two fixed landmarks were placed on each tooth, one at the tip of the primary cusp and one at the base of the tooth. 18 sliding-semilandmarks were then distributed evenly between these two points on either side of the tooth. TPS files were analysed using the R package *geomorph* (Adams *et al.*, 2018). A generalised Procrustes analysis (GPA) was carried out in order to rotate, centre and rescale image co-ordinates. Following GPA, we measured the effect of treatment and sample on Centroid size using a linear model, with both factors included as fixed effects. Comparisons between treatments were made using a post hoc Tukey test. Next, we assessed the contribution of treatment and sample to shape (Procrustes aligned coordinates) using a linear model (*procD.lm* function in the *geomorph* R package (Adams *et al.*, 2018)) with both factors included as fixed effects. In order to plot the shape data, a principle component analysis was conducted on the Procrustes aligned co-ordinates and plotted based on the principle components which explain the most variation in the data (Fig 6). We measured the variance for principle component 1 within treatments and carried out a pairwise F-test to test for changes in variance as a result of treatment.

#### *ToothMaker modelling of catshark dentition*

In silico models of the catshark dentition were generated using the computational model ToothMaker (Salazar-Ciudad & Jernvall 2010). Initial baseline parameters were taken from the seal dentition (Salazar-Ciudad & Jernvall 2010). We iterated through each parameter at 10% intervals; using a process of elimination to refine the final wild type tooth parameters for the catshark (Fig S4). Trial and error was then used to determine

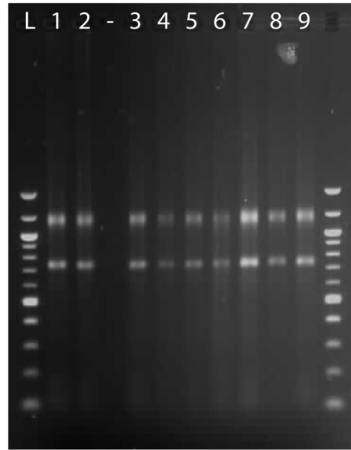
which parameters were capable of generating teeth resembling those produced following small molecule treatment. 10000 iterations of the model were run when modelling the effect of small molecule treatment. 12000 iterations of the model were ran when modelling shifts in the dentition, which take place during ontogeny.

## Supplementary information

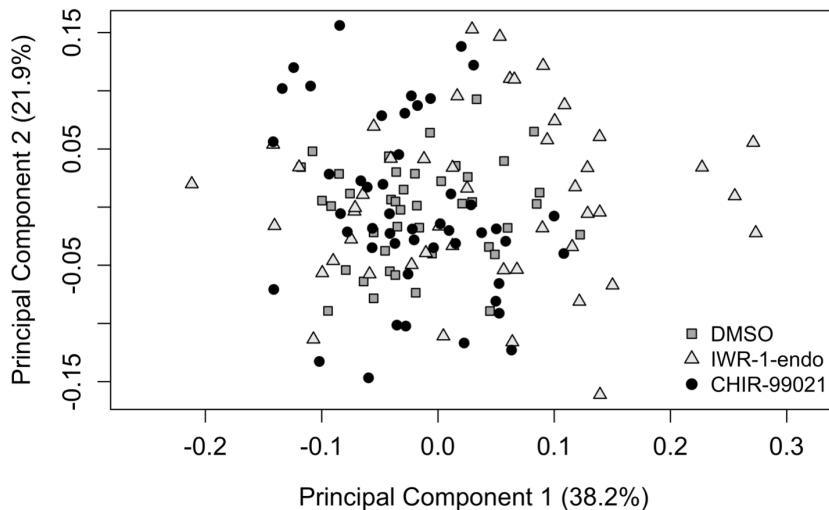


**Supplementary figure S1.** Sagittal section in situ hybridisation reveals a change in *bmp4* expression from bud stage (A) through to cap stage (B) and late-morphogenesis (C). *bmp4* is expressed throughout the dental epithelium and mesenchyme throughout all stages of tooth development, although its expression becomes restricted at the apical tip of the tooth during cap stage (B). The extent of this apical restriction increases during late morphogenesis (C). Images A-C are false coloured. *bmp4* expression is in magenta. DAPI is in grey. White dotted lines depict columnar basal epithelial cells of the dental lamina and dental epithelium. Images A'-C' are original bright field images of A-C. Scale bars are 50 $\mu$ m.

Well No.	Sample	A <sub>230</sub>	A <sub>260</sub>	A <sub>280</sub>	A <sub>260:280</sub>	A <sub>260:230</sub>	RNA conc (ng/ul)
1	0.1% DMSO (S1)	1.794	4.144	2.317	1.79	2.31	120
2	0.1% DMSO (S2)	1.619	3.173	1.502	2.11	1.96	55
3	0.1% DMSO (S3)	1.399	2.797	1.415	1.98	2	82.6
4	2μM CHIR-99021 (S1)	0.498	1.151	0.707	2.14	2.31	25.2
5	2μM CHIR-99021 (S2)	0.915	2.068	1.188	1.74	2.26	52.2
6	2μM CHIR-99021 (S3)	1.378	2.977	1.666	1.79	2.16	64.4
7	1μM IWR-1-endo (S1)	1.102	2.293	1.303	1.76	2.08	44
8	1μM IWR-1-endo (S2)	1.449	3.232	1.616	2	2.23	166
9	1μM IWR-1-endo (S3)	0.535	1.1981	1.247	1.59	2.24	27



**Supplementary figure S2.** RNA sample quality and concentration used for RT-qPCR. Gel electrophoresis shows integrity of RNA samples. Gel numbers 1-9 refer to the sample in the table. L = 100bp ladder.



**Supplementary figure S3.** Scatter plot illustrating all individual tooth data points from principle component analysis illustrated in Figure 6. There is an increase in the variation of dental shapes across the PC1 axis following Wnt downregulation with IWR-1-endo relative to DMSO control teeth (pairwise F-test:  $F_{41,47} = 0.277, p < 0.001$ ).

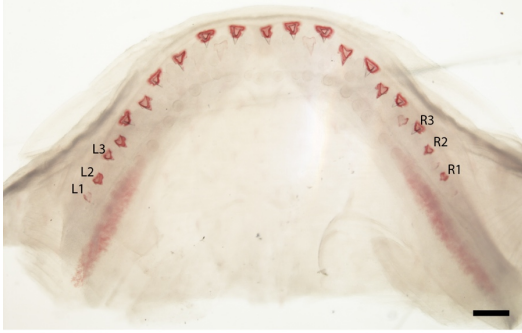
Egr==0.0220000	Boy==0.1000000
Mgr==200.0000000	Dff==0.0004500
Rep==1.0000000	Bgr==1.0000000
Swi==0.0000000	Abi==15.0000000
Adh==0.0010000	Pbi==14.0000000
Act==0.2000000	Bbi==1.0000000
Inh==1.5000000	Lbi==1.0000000
Sec==0.0300000	Rad==2.0000000
Da==0.2000000	Deg==0.0600000
Di==0.1700000	Dgr==15000.0000000
Ds==0.2000000	Ntr==0.0000100
Int==0.1500000	Bwi==0.8000000
Set==0.9500000	Ina==5.0000000

**Supplementary figure S4.** Baseline ToothMaker parameters set for catshark. Parameters were developed through modification of parameters used for the seal dentition (Salazar-Ciudad and Jernvall, 2010).

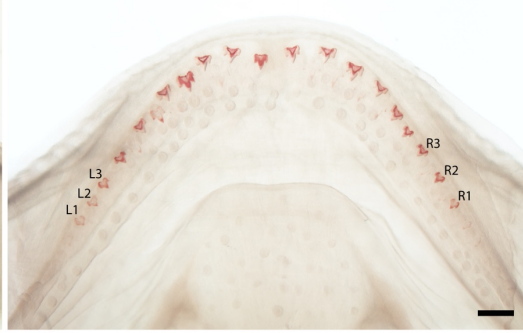
Gene	Forward Primer	Reverse Primer
<i>lef1</i>	CATGCACTCTACAGGGATCCC	TCTGGATCAGAGTCTTGCTGC
<i><math>\beta</math>-catenin</i>	AGTGGTTAAGCTACTGCACCC	AAGCTAGCATCATCTGGACGG
<i>wnt11</i>	TCTGACATGAGGTGGAAGTGC	TCTCTTGAGTTCGGTTGGAGC
<i>dkk1</i>	TGCCTCTACAATGTCGTGAGC	GTGCAGCCTCGAATTCTTGC
<i>sfrp3</i>	CCGTCATGAGGAGGTACAACC	TTCTGTTCCCTCTGCTTCGACG
<i>fgf3</i>	CTTGTTGCTGAGTCTTCTGGC	AACTCTTCAGCAGGTTCTCCC
<i>fgf10</i>	TGGATACTGACAAAGGGTGCC	GACATCGTGTCTCACCCTATTGG
<i>bmp4</i>	GGAGCACAGGTCTATGGAAAGG	GGAGCACAGGTCTATGGAAAGG
<i>smad1</i>	GGAATCCGAGACACTCTTGGC	TTCAACAACCAGCTCTTCGCG
<i>smad3</i>	TAGTCACCATGAGCTTCGAGC	CCAATGTGCCTTCTTGTCAGC
<i>smad7</i>	TCCTTGCCGGTACTGATATGC	GTGTGAAATCGTGGTTCGTTGG
<i>bambi</i>	GCATCTAACTGTGTGGCAACG	TCCAAGTCTAACTTCGCCACC
<i>mdk</i>	GACAGGGTCTCTGAAGCTG	TTAGGGTTCATTGCGAGTC
<i>shh</i>	TGACTCCCAATTACAACCCGG	TCAGGTCCTTCACTGACTTGC
<i>isl1</i>	ATTGTTTCGGACTAAATGCGC	TGCAGCGTTTGTCTGAAACC
<i>axin2</i>	GACGGACAGTAGCGTAGATGG	TGGTGGATGTGATGATGGTGG

**Supplementary figure S5.** List of forward and reverse primers used in the synthesis of probes for *in situ* hybridisation.

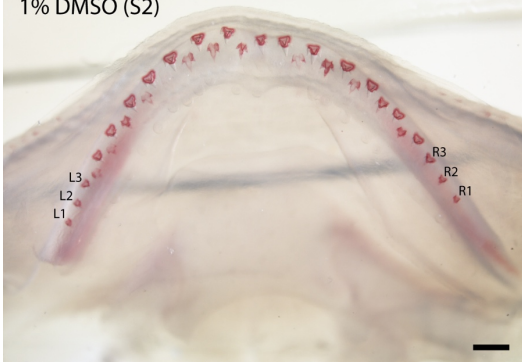
1% DMSO (S1)



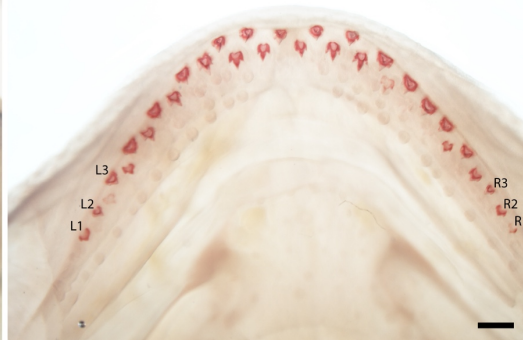
1% DMSO (S5)



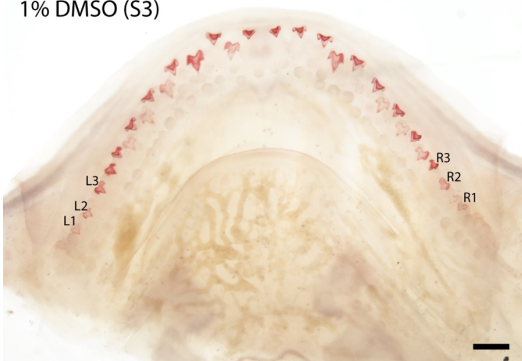
1% DMSO (S2)



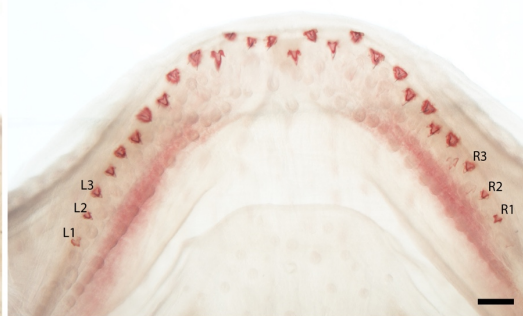
1% DMSO (S6)



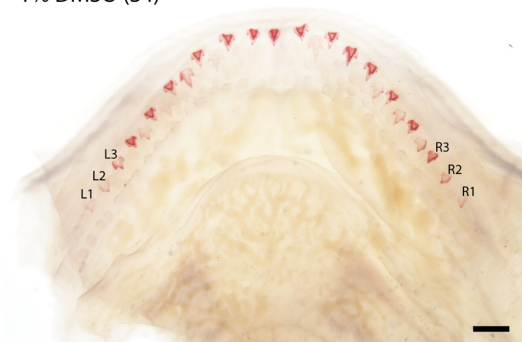
1% DMSO (S3)



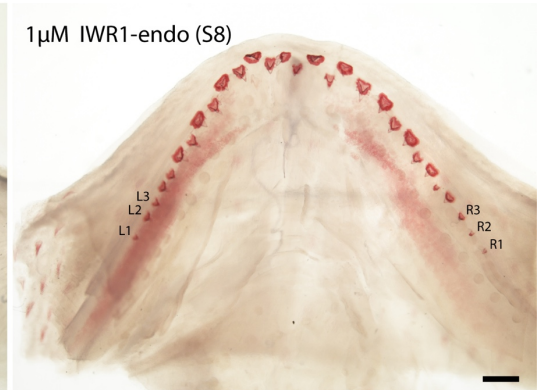
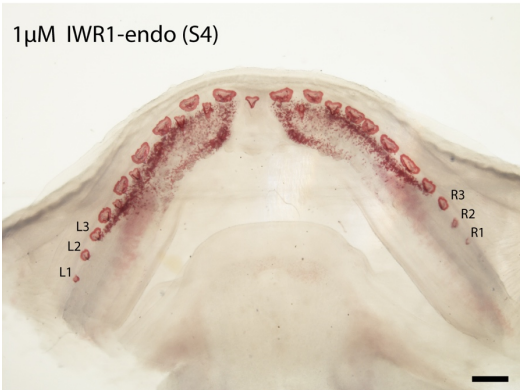
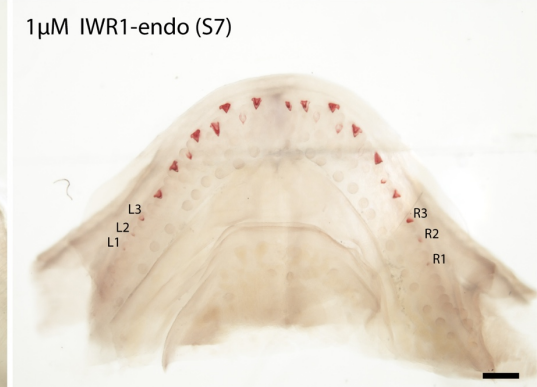
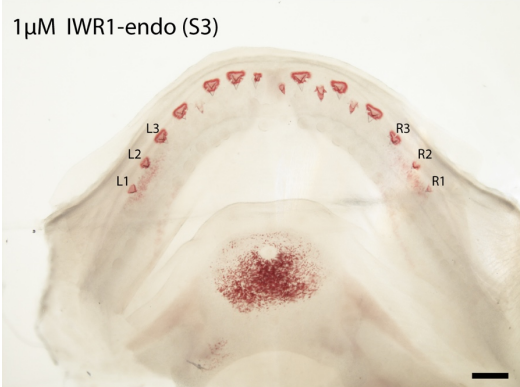
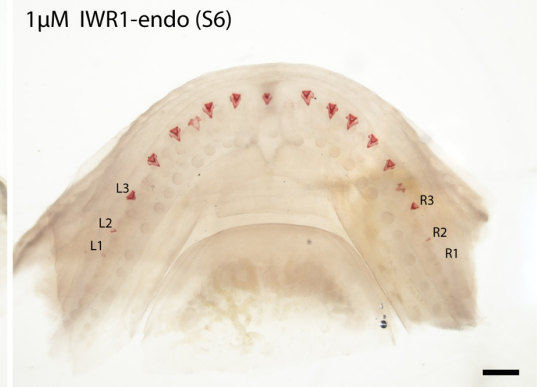
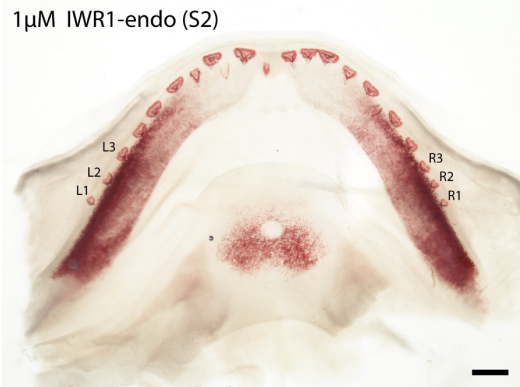
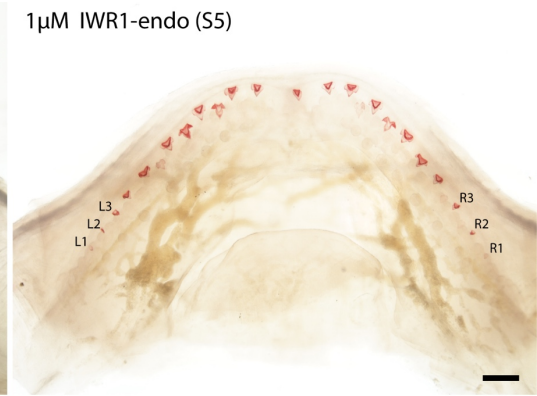
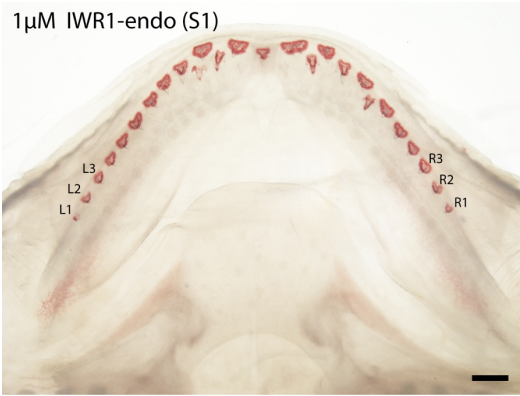
1% DMSO (S7)

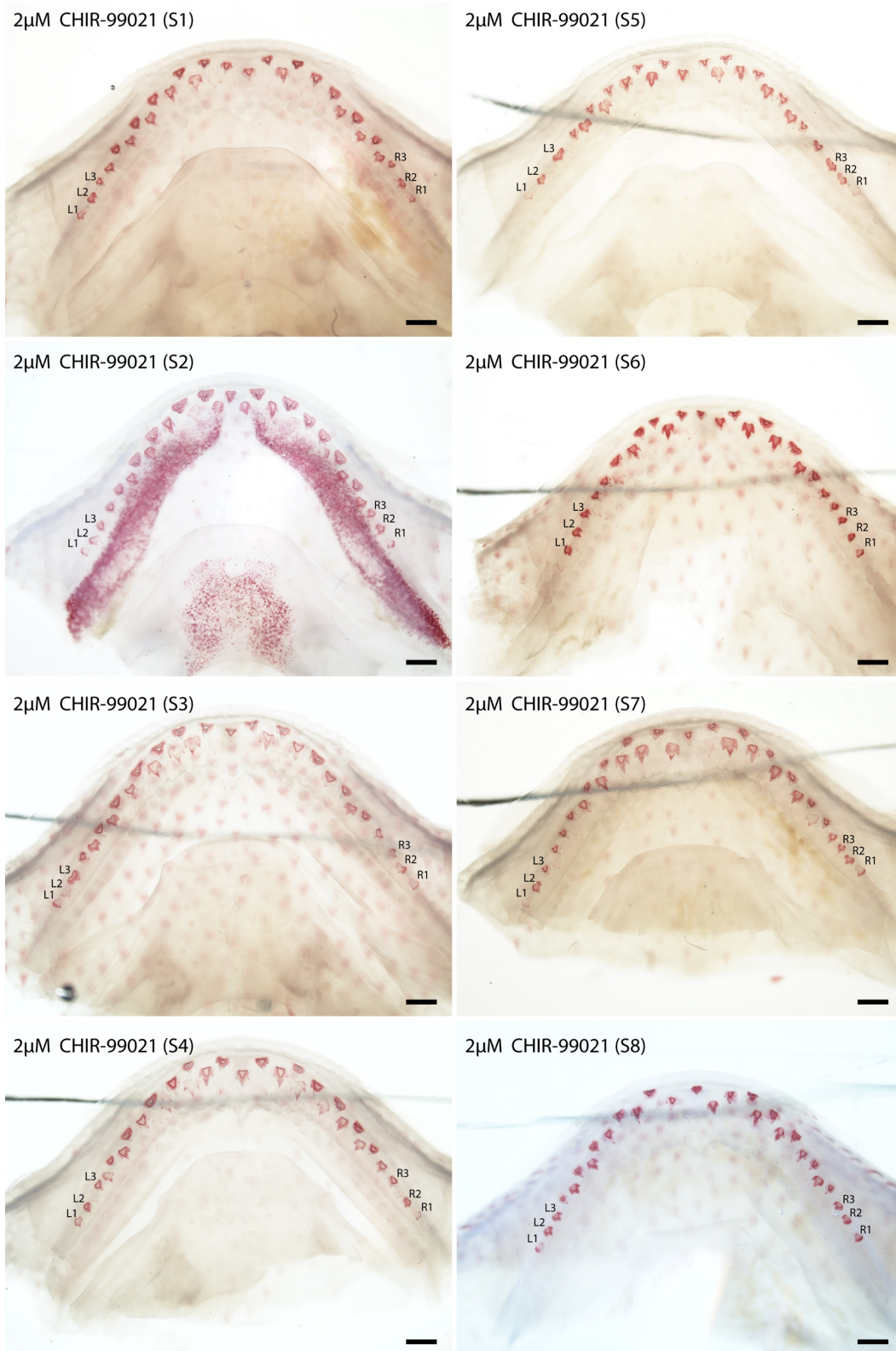


1% DMSO (S4)

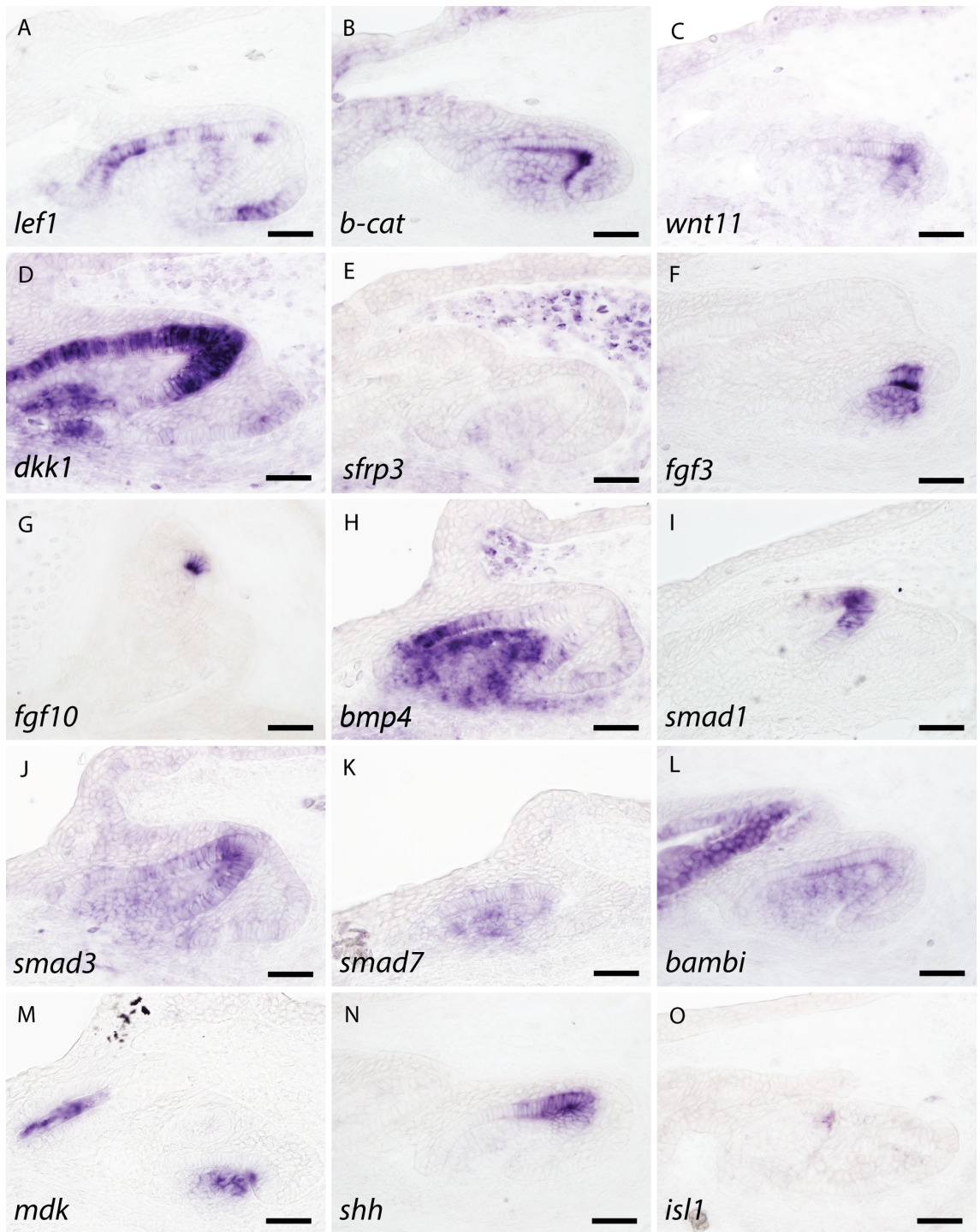




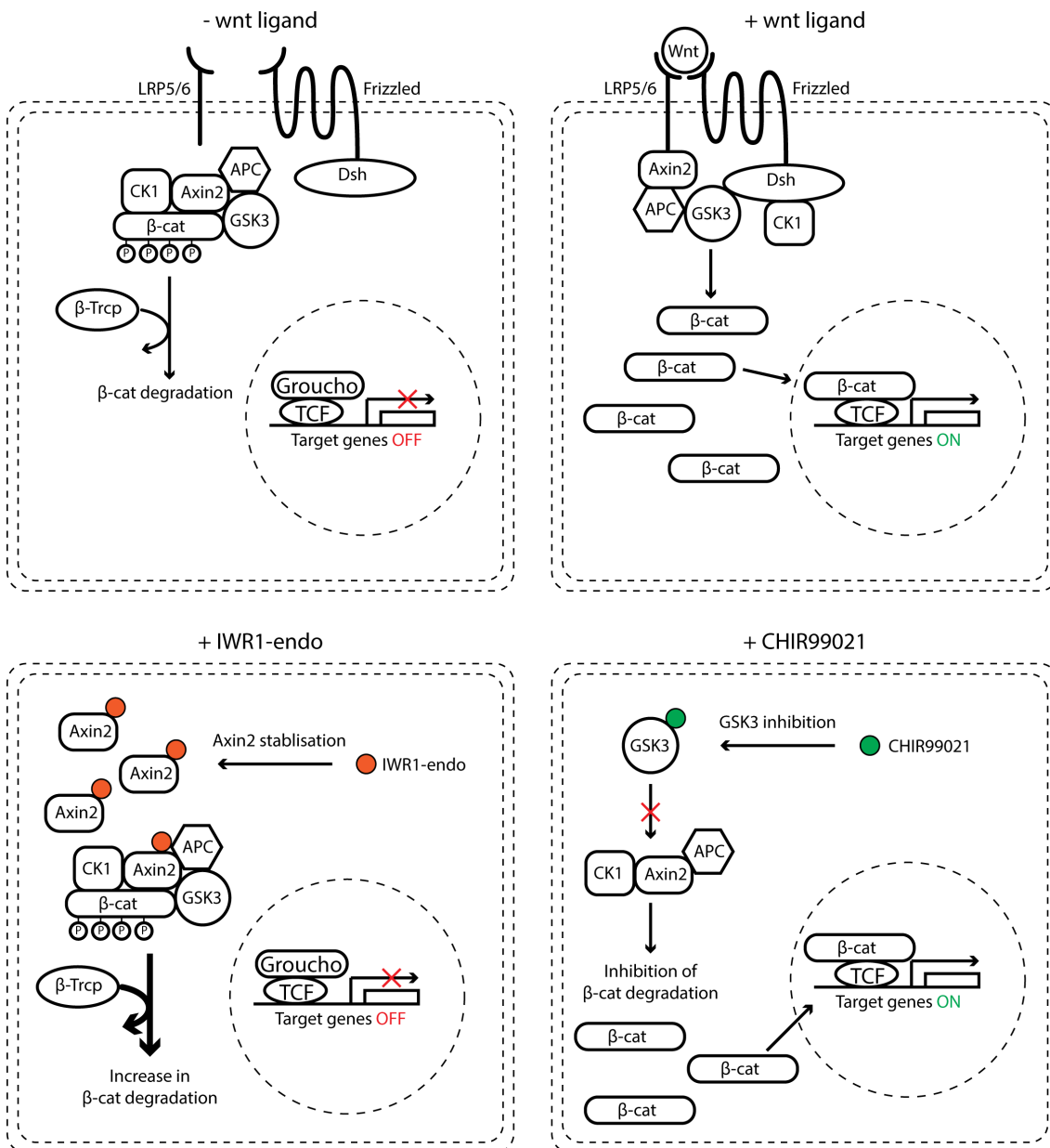




**Supplementary figure S6.** Images of all lower jaws following small molecule treatment with 0.1% DMSO, 1µM IWR-1-endo and 2µM CHIR9902.



**Supplementary figure S7.** Raw *in situ* hybridisation data false coloured in Fig 2. Scale bars are 50µm.



**Supplementary figure S8.** Schematic of canonical Wnt signalling showing translocation of cytoplasmic  $\beta$ -catenin to the nucleus in the presence of Wnt ligands adapted from (Komiya and Habas, 2008). Under the influence of small molecule canonical Wnt inhibitor, IWR1-endo, cytoplasmic Axin2 is stabilised and there is an increase in  $\beta$ -catenin degradation (Chen *et al.*, 2009a). In contrast, CHIR99021 selectively inhibits GSK3 kinase activity, leading to an upregulation of cytoplasmic  $\beta$ -catenin and subsequent canonical Wnt signalling (Ring *et al.*, 2003).

## Chapter 5

### General Discussion

#### *Research summary*

Vertebrate beaked feeding structures have convergently evolved in teleost fish, birds and mammals. The keratin beaks of birds and mammals (platypus and echidna) develop following a loss of the oral dentition (Davit-Béal *et al.*, 2009) and thus differ from the beak-like dentitions of the teleost parrotfish and pufferfish which are composed primarily of dentine and enamel (Andreucci *et al.*, 1982; Fraser *et al.*, 2012; Marcus *et al.*, 2017). Previous research has indicated that pufferfish form their beaks through the development of elongated tooth bands, which accumulate and fuse together over the course of successive rounds of dental regeneration. These bands develop following a developmental shift from the unicuspid first dental generation (Fraser *et al.*, 2012). However, it was unknown whether these bands form through the fusion of multiple individual tooth units or a loss of dental regeneration.

In order to identify which changes to the ancestral bauplan take place during the development of the pufferfish beak, we further investigated the regulation of dental regeneration during this process. Our results reveal that this shift in morphology is enabled as a result of a loss of dental regeneration at all but four tooth sites and an elongation of the dental unit during dental morphogenesis. Although we observe changes in the regulation of dental regeneration between ancestral and derived dental

morphologies, the underlying molecular network regulating this process is highly conserved.

Simultaneous study of morphological novelty, as well as the ancestral form, provides an unparalleled understanding of the evolutionary changes, which have taken place during the evolution of such derived morphologies. This same logic can be extended to understanding the secondary loss of polyphyodonty in mammals. If we are able to understand how polyphyodonty is regulated in a basal vertebrate lineage, we can comparatively analyse dental development in other vertebrate groups and gain insight as to the critical molecular components required for successional regeneration. During the evolution of teeth, true teeth are defined from their odontode counterparts, by their ability to successionaly regenerate (Martin *et al.*, 2016). It is previously known that canonical Wnt signalling plays a critical role in the regulation of Sox2+ dental epithelial stem cells located within the dental lamina throughout vertebrates (Gaete and Tucker, 2013; Juuri *et al.*, 2013; Martin *et al.*, 2016). Furthermore, degradation of the dental lamina has been implicated in the loss of mammalian polyphyodonty (Buchtová *et al.*, 2012).

Whereas research has developed a detailed understanding of mammalian hair and intestinal crypt regeneration (Greco *et al.*, 2009; van der Flier *et al.*, 2009), our understanding of successional dental regeneration remains somewhat limited. We aimed to identify novel dental stem cell markers and the key molecular signalling pathways regulating dental stem cells through whole transcriptome sequencing of dental sub-regions. We developed a framework for identifying novel markers from such datasets,

through the use of predictive gene regulatory network tools in combination with prior system knowledge. This approach led to the identification of *mycn*, a novel stem cell candidate co-expressed with Sox2 within the successional lamina. We also describe the expression of numerous other markers at the site of dental initiation, including Pitx3, which is yet to be described during dental regeneration. Further research is required to investigate the function of these genes during dental regeneration. Future endeavours in this area could build upon our results, as they provide a large dataset obtained from a polyphyodont model.

Finally, given the shifts in tooth shape observed during pufferfish beak development, we sought to investigate the conservation of dental morphogenesis throughout vertebrates. Tooth shape is primarily regulated by the enamel knot, a transient signalling centre located at the apical tip of developing cusps which regulates differential proliferation of the dental epithelium. We observe the restricted expression of *fgf3* and *fgf10* within both primary and secondary (accessory) putative enamel knots in the catshark. Furthermore, we reveal a lack of cellular proliferation within this region. Chemical manipulation of the canonical Wnt signalling pathway, which has been implicated in upstream enamel knot signalling, results in a shift in tooth shape, size and cusp number. These results suggest the presence of an epithelial signalling centre in sharks. Although there are clear differences in the expression of certain enamel knot genes between shark and mammals, our results identify the components of a conserved signalling centre regulating tooth shape. We suggest that the differences in gene expression observed in mammals are merely lineage specific modifications of this

ancestral signalling centre and cannot alone be used to refute the presence of an enamel knot in other vertebrate species.

### *The bigger picture*

Vertebrate dental development is a highly dynamic process, which encompasses numerous developmental processes including cell migration, tissue regeneration, stem cell regulation, cell specification, tissue morphogenesis and cell differentiation. Each of these processes has been individually investigated at depth in the mouse, advancing our understanding of dental development. However, in order to understand the developmental programme underpinning vertebrate dental development and regeneration, we must identify developmental processes regulating species specific characteristics and separate these from fundamental dental developmental processes conserved throughout vertebrates. For example, understanding the difference between dental renewal (e.g. continuous growth of the rodent incisor, which is a mammalian specific modification) and successional dental regeneration (the ancestral gnathostome condition (Martin *et al.*, 2016)), or redefining developmental processes such as EK signalling based on evolutionary homology criteria instead of functional characteristics (which are often species dependent and less relevant in an evolutionary context).

This thesis has demonstrated the use of alternative models in order to take a comparative approach to addressing these questions. For the study of dental regeneration and dental morphogenesis we use a basal gnathostome which provides an ancestral reference point for the comparative study with other vertebrate species. For the



study of morphological diversity, we use a derived teleost lineage in the pufferfish, which represents an extreme case of morphological adaptation. This allows us to separate which developmental processes are conserved and which remain flexible to lineage specific change.

Our results reveal that the process of dental development is conserved in the face of evolutionary change. Subtle shifts to the ancestral developmental framework enable drastic modification of the dentition, both in terms of dental initiation and dental morphogenesis, whilst the underlying organisation of dental cell types within a dental unit remains intact. For example, simple restriction of an epithelial cellular input into the dental cavity appears to drive spatial specific loss in dental regeneration, whereas modifications to dental morphogenetic elongation (hypothesised to be driven by modified Notch signalling) and matrix secretion lead to the fusion of tooth units. In the face of these drastic morphological shifts, the underlying dental framework appears robust to change; tissue layers including oral epithelium, inner and outer dental epithelium and dental mesenchyme, retain a core signalling network. This is highly conserved and gives rise to conserved cell types including odontoblasts and ameloblasts which are found across vertebrate lineages.

Furthermore, the process of dental regeneration appears to remain relatively unchanged, even in the face of morphological diversification. In both our models, Sox2 is a clear marker of dental regenerative competence within the DL. This link between Sox2 expression and dental regeneration has been documented across vertebrates, with the loss of Sox2 in mammals (following degradation of the dental lamina) thought to

underpin the loss of successional dental regeneration. This link has previously been described, however our research reveals that dental morphology is also intimately linked to regenerative capacity. The pufferfish develops a simplistic first generation dentition (Fraser *et al.*, 2012), and only through successive rounds of regeneration is it able to modify its dental morphological complexity.

This phenomenon has been described in other species and appears to be common throughout most vertebrates. For example, both cichlids (which have experienced explosive dental morphological radiation (Streelman and Albertson, 2006)) and catshark (a basal gnathostome) exhibit an increase in cusp number and regional specification of tooth shape across the jaw, which arises following numerous rounds of dental regeneration (Fraser *et al.*, 2013). Interestingly, although the ability to regenerate the dentition appears linked to an increase in morphological complexity in most vertebrates, the inverse is true in mammals. Mammals have rapidly evolved a morphologically diverse dentition, with closely related species identifiable from their dentitions alone (Gingerich and Schoeninger, 1979). Despite this rapid diversification in shape, mammalian teeth show high levels of occlusion (David Polly, 2012). It is thought that successional regeneration has been lost in favour of this precise occlusion (Jernvall and Thesleff, 2012; Tucker and Fraser, 2014), with the fossil record supporting this correlation (Kielan-Jaworowska *et al.*, 2004).

Our research reveals conservation in dental development between vertebrate species despite initial observed morphological variation, whilst also highlighting differences

with mammalian vertebrates. This reveals the necessity to diversify the range of developmental models used for the study of dental development.

### *New models, new questions*

Given the recent explosion in experimental, sequencing and imaging technologies, the range of developmental models accessible for study is rapidly increasing. The use of diverse models has clear advantages for the study of evolutionary development. However, an understanding of evolution is also critical for the comparative developmental study between any species, although this is often overlooked. A clear example of this importance can be seen in the zebrafish, which due to its short generation time and ease of genetic manipulation, is increasingly being used as a biomedical developmental model. However, teleost fish have undergone an independent whole genome duplication relative to humans (Meyer and Schartl, 1999). As a result, detailed understanding of zebrafish evolutionary genetics and mapping of the zebrafish and human genomes has been necessary in order to uncover gene orthology and allow for cross species genetic comparisons (Howe *et al.*, 2013).

Large scale genome sequencing projects, such as the 10k genome project (which aims to sequence the genome of 10,000 species (Koepfli *et al.*, 2015)) are making it possible to pick a range of developmental models based on the biological question of interest. This is in contrast to classic developmental research, which up until recently had depended heavily upon a limited group of animal models. The benefits of this shift in approach are clear in the field of regenerative dentistry. Given the lack of successional

dental regenerative ability in chick, mouse and zebrafish, the use of models which regenerate their dentitions throughout life is required in order to elucidate the underlying developmental mechanism regulating this process (Tucker and Fraser, 2014).

As a result of the lack of comparative study of dental development, there remain numerous unanswered questions which can now be addressed using new vertebrate models. One of the question of primary focus remains: ‘how is dental regeneration developmentally regulated’? In order to understand the process of dental regeneration in more depth, we need to address a series of more fundamental questions. This requires us rethink how we view the process of dental regeneration. For instance, if a new dental generation develops from a stem cell population within the oral epithelium, with little/no cellular contribution from the preceding tooth generation, do we define this as regeneration? If so, this raises the question as to how this process is different from normal development? It also suggests that the fundamental difference between the development of a first- and second-generation tooth is purely based on the cyclical re-activation of a resident stem cell population. The following question is therefore, how is cyclicity in stem cell regulation regulated? Is cyclicity regulated through dynamic proliferation of the dental lamina which then leads to new space created between preceding teeth whereby a new tooth is able to develop? If so, does this represent a modified form of ectodermal appendage patterning which continues to arise dynamically through time? In sharks for example, this could explain the similarity in patterning between teeth and denticles, with the latter previously shown to develop through Turing reaction-diffusion patterning (Cooper *et al.*, 2018).

The conveyor belt-like many-for-one replacement pattern observed in sharks, where teeth are staggered in their developmental initiation and are highly organised in their emergence, suggests a close link between dental patterning and dental regeneration. However, other species regenerate their teeth one-for-one. For example, in the alligator, regeneration of the dental unit is closely linked with loss of the preceding tooth; physical extraction of the tooth is sufficient to trigger the re-activation of dental initiation within the dental lamina (Wu *et al.*, 2013). Could the preceding tooth be providing inhibitory signals to surrounding epithelium, thereby preventing the formation of a new tooth? Or have dental regeneration and patterning become uncoupled? There remain many unanswered questions. However, the study of dental patterning, dental initiation and dental morphogenesis in a range of species will help us achieve a clearer picture as to both, how development of the dentition is regulated and how it has evolved and diversified throughout vertebrates. Finally, in order to understand the regulation of the dynamism and cyclicity underlying the regenerative process, it is critical that we study dental development over time to ensure that the developmental links between patterning, regeneration and morphogenesis can be fully understood.

#### *Future project directions*

Our results indicate significant conservation of the odontogenetic process throughout vertebrates and highlight how subtle modifications to this ancestral bauplan can lead to the development of unusual phenotypes. The primary purpose of studying the evolution

of vertebrate dental development in the present study is to provide a new polyphyodont reference point for future comparative research. The catshark is phylogenetically well placed to become a reference species in this area of research, and in so doing, answer a number of fundamental questions.

The staggered developmental timing of adjacent tooth families is an interesting feature of the catshark dentition as it allows for the simultaneous comparative developmental analysis of multiple odontogenic stages. However, a three dimensional view of gene expression is required in order to accurately compare between tooth families. The catshark dental lamina is embedded deep within the oral tissue. Chromogenic whole mount *in situ* hybridisation methods presented in this thesis, offer insight only into superficial gene expression on the oral surface. The CLARITY method clears the tissue of interest, reducing light scattering during imaging post *in situ* hybridisation (Sylwestrak *et al.*, 2016). Developing fluorescent *in situ* hybridisation techniques, alongside the use of CLARITY would allow for deep tissue imaging following *in situ* hybridisation. Using these techniques, it would be possible to investigate the expression of novel gene candidates identified from follow up transcriptome datasets, together with Sox2 and other new stem cell candidates such as Mycn. Comparing the co-expression of these markers between the successional lamina of adjacent tooth families, would allow us to investigate subtle fluctuations in co-expression between initiation and pre-initiation stages. Ultimately, this would provide a deeper insight into the regulation of epithelial dental stem cells during cyclical dental regeneration.

Although we have developed a transcriptome dataset of five dental sub-regions, there is still significant avenue for further RNAseq experiments in order to further explore the process of successional regeneration. It is known that the co-expression of activated  $\beta$ -catenin together with Sox2 is dependent upon the stage of the developing tooth (Martin *et al.*, 2016). As a result, the activation and subsequent proliferation of these cells is also temporally variable. Fluorescence activated cell sorting (FACS), allows for the separation of cells based on monoclonal antibody labelling (Herzenberg *et al.*, 2000). RNAseq of five distinct FACS sorted cell populations ((i) Sox2+/  $\beta$ -catenin-/ PCNA- (ii) Sox2+/  $\beta$ -catenin+/ PCNA- (iii) Sox2+/  $\beta$ -catenin+/ PCNA+ (iv) Sox2-/  $\beta$ -catenin+/ PCNA+ (v) Sox2-/  $\beta$ -catenin-/PCNA+) from within the successional lamina would allow for differential expression analysis of distinct stem cell sub-populations. This dataset would be ideally suited for expression-based gene regulatory network inference (e.g. GENIE3 (Huynh-Thu *et al.*, 2010)), given the lack of contamination from surrounding tissues. These experiments would allow for the development of testable gene regulatory networks and subsequently provide deep insight into the regulation of dental stem cell sub-populations.

### *Limitations*

Despite the major strengths of the catshark system, there are limited techniques available for functional manipulation. Samples are not bred in captivity; instead, eggs are collected from pregnant females. This, coupled with their long generation time, renders transgenic modification unrealistic. The potential use of CRISPR is also limited as it is not possible to collect samples at the first cell stage. A further limitation is both

the large size of the catshark embryos and their slow embryonic development. This means that the use of morpholinos or RNAi is prohibitively expensive. Nevertheless, there are other options for functional manipulation. Small molecule chemical targeting of molecular signalling pathways is effective, as demonstrated by our results in both shark and pufferfish. However, there are often unforeseen off-target effects which need to be considered when conducting these experiments. The discovery of new and more targeted small molecules will enable further, more precise functional manipulation. Finally, slice culture of oral tissue has proved successful in the snake, another polyphyodont species (Gaete and Tucker, 2013). Developing slice culture in the catshark would open up the possibility of highly targeted functional manipulation via electroporation, RNAi and morpholino treatment.

### *Conclusion*

We are entering an exciting period in the study of successional dental regeneration; previous barriers to investigating non-traditional developmental models are being broken down by rapid advances in RNA sequencing, imaging techniques and experimental methodology. The study of a range of vertebrate models will provide novel insights into the evolution of the vertebrate dentition, whilst simultaneously elucidating the mechanisms through which diversification and morphological novelty arise. Ultimately, this research could help bridge the gap between evolutionary and medical based research fields, as research projects take a systems biology approach to addressing questions on odontogenesis and regeneration.



# Appendix

## Abbreviations

ARACNE	Algorithm for the Reconstruction of Accurate Cellular Networks (Margolin <i>et al.</i> , 2006)
bHLH	Basic helix-loop-helix transcription factor
BHTB	Basi-hyal taste buds
CDS	Coding sequence
DAPI	4',6-diamidino-2-phenylindole
DAVID	Database for Annotation, Visualization and Integrated Discovery
ddCT	Delta Delta cycle threshold
DE	Dental epithelium
DEPC	Diethyl pyrocarbonate
DIG	Digoxigenin
DL	Dental lamina
DMSO	Dimethyl sulfoxide
edgeR	Empirical Analysis of Digital Gene Expression Data in R (Robinson <i>et al.</i> , 2009)
EK	Enamel knot
ET	Early tooth
FC	Fold change
FDR	False discovery rate
FPKM	Fragments Per Kilobase Million
GENIE3	GEne Network Inference with Ensemble of trees (Huynh-Thu <i>et al.</i> , 2010)
GO	Gene ontology

GTR	General Time Reversible substitution model (Waddell and Steel, 1997)
KEGG	Kyoto Encyclopedia of Genes and Genomes
LBN	Local Bayesian network (Liu <i>et al.</i> , 2016)
LG	Le and Gascuel substitution model (Le and Gascuel, 2008)
LT	Late tooth
MDE	Middle dental epithelium
MS-222	Tricaine mesylate
MUSCLE	Multiple sequence comparison by log-expectation (Edgar, 2004)
NARROMI	Noise and redundancy (NAR)-reduction technology by combining ordinary differential equation (ODE)-based recursive optimization (RO) and information-theory based MI (Zhang <i>et al.</i> , 2013)
ORegAnno	Open Regulatory Annotation Database
ORF	Open reading frame
PHYML	Phylogeny reconstruction by maximum likelihood (Guindon and Gascuel, 2003)
RNEA	Regulatory Network Enrichment Analysis (Chouvardas <i>et al.</i> , 2016)
SL	Successional lamina
TB	Taste bud
TMM	Trimmed mean of M values (edgeR (Robinson <i>et al.</i> , 2009))
TRED	Transcriptional Regulatory Element Database
TRRUST	Transcriptional regulatory relationships unravelled by sentence-based text-mining
TTJ	Taste tooth junction
ZPA	Zone of polarising activity

## Solutions

ddH <sub>2</sub> O	double distilled water
DEPC-ddH <sub>2</sub> O	500µl C <sub>6</sub> H <sub>10</sub> O <sub>5</sub> (diethyl pyrocarbonate) in 1L ddH <sub>2</sub> O; autoclave
10xPBS	80g (1.37M) NaCl; 2g (27mM) KCl; 17.2g (100mM) Na <sub>2</sub> HPO <sub>4</sub> ·2H <sub>2</sub> O; 2.4g (18mM) KH <sub>2</sub> PO <sub>4</sub> ; ddH <sub>2</sub> O to 1L; pH 7.6 with 1M HCl; autoclave
DEPC-PBS	100ml 10xPBS in 900ml DEPC-ddH <sub>2</sub> O
0.5M EDTA	186.1g (0.5M) C <sub>10</sub> H <sub>18</sub> N <sub>2</sub> Na <sub>2</sub> O <sub>10</sub> (disodium edetate dihydrate); 20g (0.5M) NaOH; DEPC-ddH <sub>2</sub> O to 800ml; pH 8 with 5M NaOH; DEPC-ddH <sub>2</sub> O to 1L; autoclave
4% paraformaldehyde	4g paraformaldehyde in 100ml pre-heated (70°C) DEPC-PBS; add 2M NaOH until PFA dissolves; pH 7.6 with 1M HCl; store at -20°C
20xSSC	175.3g (3M) NaCl; 88.2g (0.3M) Na <sub>3</sub> C <sub>6</sub> H <sub>5</sub> O <sub>7</sub> ·2H <sub>2</sub> O (trisodium citrate dihydrate); ddH <sub>2</sub> O to 1L; autoclave
1% RBR	1g roche blocking reagent (Roche 11096176001); 100ml MAB; microwave until dissolved
MAB	11.6g (100mM) Maleic Acid; 8.76g (150mM) NaCl; 8g (0.2M) NaOH; ddH <sub>2</sub> O to 1L; pH 7.5 with 5M NaOH; autoclave
NTMT	10ml 5M NaCl; 25ml 1M MgCl <sub>2</sub> ; 50ml 1M Tris pH 9.5; 500µl Tween-20; 0.241g (2mM) tetramisole hydrochloride; ddH <sub>2</sub> O to 500ml
0.1% KOH	1g KOH in 1L ddH <sub>2</sub> O
0.02% alizarin red in 0.1% KOH	0.02g alizarin red S in 100ml 0.1% KOH
1M sodium citrate	29.4g Na <sub>3</sub> C <sub>6</sub> H <sub>5</sub> O <sub>7</sub> (trisodium citrate); DEPC-ddH <sub>2</sub> O to 100ml; pH 6 with 1M HCl
0.01M sodium citrate buffer	10ml 1M sodium citrate in 1L ddH <sub>2</sub> O
Pre-hybridisation solution	250ml deionised-formamide; 125ml 20xSSC; 5ml 1M sodium citrate; 500µl Tween-20; 119.7ml DEPC-ddH <sub>2</sub> O; pH 6 with 1M HCl



## References

- Adams, D., Collyer, M. and Kaliontzopoulou, A. (2018) 'Geomorph: Software for geometric morphometric analyses. R package version 3.0.6.', <https://cran.r-project.org/package=geomorph>.
- Ahtiainen, L. *et al.* (2014) 'Directional Cell Migration, but Not Proliferation, Drives Hair Placode Morphogenesis', *Developmental Cell*, 28(5), pp. 588–602.
- Albertson, R. C. *et al.* (2009) 'Evolutionary mutant models for human disease', *Trends in Genetics*, 25(2), pp. 74–81.
- Andl, T. *et al.* (2002) 'WNT signals are required for the initiation of hair follicle development', *Developmental Cell*, 2(5), pp. 643–653.
- Andreucci, R. D., Britski, H. A. and Carneiro, J. (1982) 'Structure and evolution of tetraodontoid teeth: An autoradiographic study (pisces, Tetraodontiformes)', *Journal of Morphology*, 171(3), pp. 283–292.
- Arnold, K. *et al.* (2011) 'Sox2 + adult stem and progenitor cells are important for tissue regeneration and survival of mice', *Cell Stem Cell*, 9(4), pp. 317–329.
- Aulehla, A. *et al.* (2003) 'Wnt3a plays a major role in the segmentation clock controlling somitogenesis', *Developmental Cell*, pp. 395–406.
- Ballard, W. W., Mellinger, J. and Lechenault, H. (1993) 'A series of normal stages for development of *Scyliorhinus canicula*, the lesser spotted dogfish Chondrichthyes: Scyliorhinidae', *Journal of Experimental Zoology*, 267(3), pp. 318–336.
- Barker, N. *et al.* (2007) 'Identification of stem cells in small intestine and colon by marker gene *Lgr5*', *Nature*, 449(7165), pp. 1003–1007.
- Bei, M. (2009) 'Molecular genetics of tooth development.', *Current opinion in genetics & development*, 19(5), pp. 504–10.
- Bely, A. E. (2010) 'Evolutionary loss of animal regeneration: Pattern and process', *Integrative and Comparative Biology*, pp. 515–527.
- Bely, A. E. and Nyberg, K. G. (2010) 'Evolution of animal regeneration: re-emergence of a field', *Trends in Ecology & Evolution*, 25(3), pp. 161–170.
- Biehs, B. *et al.* (2013) 'BMI1 represses *Ink4a/Arf* and *Hox* genes to regulate stem cells in the rodent incisor.', *Nature cell biology*, 15(7), pp. 846–52.
- Bloomquist, R. F. *et al.* (2015) 'Coevolutionary patterning of teeth and taste buds', *Proceedings of the National Academy of Sciences*, p. 201514298.

- Brainerd, E. L. and Patek, S. N. (1998) 'Vertebral Column Morphology, C-Start Curvature, and the Evolution of Mechanical Defenses in Tetraodontiform Fishes', *Copeia*, (4), p. 971.
- Britski, H. A., Andreucci, R. D. and Menezes, J. A. (1985) 'Coalescence of teeth in fishes', *Revista Brasileira de zoologia*, 2(8), pp. 459–482.
- Brockes, J. F. and Kumar, A. (2005) 'Appendage regeneration in adult vertebrates and implications for regenerative medicine', *Science*, pp. 1919–1923.
- Buchtová, M. *et al.* (2008) 'Initiation and patterning of the snake dentition are dependent on Sonic hedgehog signaling.', *Developmental biology*, 319(1), pp. 132–45.
- Buchtová, M. *et al.* (2012) 'Early regression of the dental lamina underlies the development of diphyodont dentitions.', *Journal of dental research*, 91(5), pp. 491–8.
- Chen, B. *et al.* (2009) 'Small molecule-mediated disruption of Wnt-dependent signaling in tissue regeneration and cancer', *Nature Chemical Biology*, 5(2), pp. 100–107.
- Chen, E. Y. *et al.* (2014) 'Glycogen synthase kinase 3 inhibitors induce the canonical WNT/ -catenin pathway to suppress growth and self-renewal in embryonal rhabdomyosarcoma', *Proceedings of the National Academy of Sciences*, 111(14), pp. 5349–5354.
- Chen, J.-Y. *et al.* (2016) 'Spliceosomal protein eftud2 mutation leads to p53-dependent apoptosis in zebrafish neural progenitors', *Nucleic Acids Research*, 45(6), pp. 3422–3436.
- Chen, S. *et al.* (2009) 'Runx2, Osx, and Dspp in Tooth development', *J Dent Res*, 88(10), pp. 904–909.
- Cheng, H., Cao, Y. and Olson, L. (1996) 'Spinal Cord Repair in Adult Paraplegic Rats: Partial Restoration of Hind Limb Function', *Science*, 273.
- Cheng, H. and Leblond, C. P. (1974) 'Origin, differentiation and renewal of the four main epithelial cell types in the mouse small intestine V. Unitarian theory of the origin of the four epithelial cell types', *American Journal of Anatomy*, 141(4), pp. 537–561.
- Chouvardas, P., Kollias, G. and Nikolaou, C. (2016) 'Inferring active regulatory networks from gene expression data using a combination of prior knowledge and enrichment analysis', *BMC Bioinformatics*, 17(S5), p. 181.
- Cobourne, M. T. and Sharpe, P. T. (2010) 'Making up the numbers: The molecular control of mammalian dental formula.', *Seminars in cell & developmental biology*, 21(3), pp. 314–24.
- Cooper, R. L. *et al.* (2017) 'Developing an ancient epithelial appendage: FGF signalling regulates early tail denticle formation in sharks', *EvoDevo*, 8(1), pp. 1–19.
- Cooper, R. L. *et al.* (2018) 'An ancient Turing-like patterning mechanism regulates skin

denticle development in sharks', *Science Advances*, 4(11), pp. 1–11.

Corn, K. A. *et al.* (2016) 'Modelling tooth–prey interactions in sharks: The importance of dynamic testing', *Royal Society Open Science*, 3(8), p. 160141.

Cotsarelis, G. *et al.* (1999) 'Epithelial stem cells in the skin: definition, markers, localization and functions.', *Experimental dermatology*, 8(1), pp. 80–8.

Cotsarelis, G., Sun, T. T. and Lavker, R. M. (1990) 'Label-retaining cells reside in the bulge area of pilosebaceous unit: implications for follicular stem cells, hair cycle, and skin carcinogenesis.', *Cell*, 61(7), pp. 1329–37.

Cuvier, G. L. (1805) *Leçons d'Anatomie Comparee: La première partie des organes de la digestion*. Paris, Crochard.

Dassule, H. R. *et al.* (2000) 'Sonic hedgehog regulates growth and morphogenesis of the tooth.', *Development*, 127(22), pp. 4775–4785.

David Polly, P. (2012) 'Movement adds bite to the evolutionary morphology of mammalian teeth', *BMC Biology*, p. 69.

Davit-Béal, T., Tucker, A. S. and Sire, J. Y. (2009) 'Loss of teeth and enamel in tetrapods: Fossil record, genetic data and morphological adaptations', *Journal of Anatomy*, 214(4), pp. 477–501.

Debiais-Thibaud, M. *et al.* (2015) 'Tooth and scale morphogenesis in shark: an alternative process to the mammalian enamel knot system.', *BMC evolutionary biology*, 15(1), p. 292.

Dhouailly, D. (2009) 'A new scenario for the evolutionary origin of hair, feather, and avian scales', *Journal of Anatomy*, 214(4), pp. 587–606.

Di-Poï, N. and Milinkovitch, M. C. (2016) 'The anatomical placode in reptile scale morphogenesis indicates shared ancestry among skin appendages in amniotes', *Science Advances*, 2(6).

Dinsmore, C. (1991) *A History of Regeneration Research: Milestones in the Evolution of a Science*. Cambridge: Cambridge University Press.

Donoghue, P. C. J. and Rücklin, M. (2016) 'The ins and outs of the evolutionary origin of teeth', *Evolution & Development*, 18(1), pp. 19–30.

Donoghue, P. C. J. and Sansom, I. J. (2002) 'Origin and early evolution of vertebrate skeletonization', *Microscopy Research and Technique*, 59(5), pp. 352–372.

Edgar, R. C. (2004) 'MUSCLE: Multiple sequence alignment with high accuracy and high throughput', *Nucleic Acids Research*, 32(5), pp. 1792–1797.

van der Flier, L. G. *et al.* (2009) 'Transcription Factor Achaete Scute-Like 2 Controls Intestinal Stem Cell Fate', *Cell*, 136(5), pp. 903–912.

- Fraser, G. J. *et al.* (2006) 'Gene deployment for tooth replacement in the rainbow trout (*Oncorhynchus mykiss*): a developmental model for evolution of the osteichthyan dentition.', *Evolution & development*, 8(5), pp. 446–57.
- Fraser, G. J. *et al.* (2010) 'The odontode explosion: The origin of tooth-like structures in vertebrates', *BioEssays*, 32(9), pp. 808–817.
- Fraser, G. J. *et al.* (2012) 'Replacing the first-generation dentition in pufferfish with a unique beak.', *Proceedings of the National Academy of Sciences of the United States of America*, 109(21), pp. 8179–84.
- Fraser, G. J., Bloomquist, R. F. and Streelman, J. T. (2008) 'A periodic pattern generator for dental diversity.', *BMC biology*, 6, p. 32.
- Fraser, G. J., Bloomquist, R. F. and Streelman, J. T. (2013) 'Common developmental pathways link tooth shape to regeneration.', *Developmental biology*, 377(2), pp. 399–414.
- Fraser, G. J., Graham, A. and Smith, M. M. (2004) 'Conserved deployment of genes during odontogenesis across osteichthyans.', *Proceedings of the Royal Society B*, 271(1555), pp. 2311–7.
- G. Brodeur, R. Seeger, M. Schwab, H. V. J. (1984) 'Amplification of N-myc in untreated human neuroblastomas correlates with advanced disease stage', *Science*, 224(4653), pp. 1121–1124.
- Gaete, M. and Tucker, A. S. (2013) 'Organized Emergence of Multiple-Generations of Teeth in Snakes Is Dysregulated by Activation of Wnt/Beta-Catenin Signalling', *PLoS ONE*, 8(9), p. e74484.
- Gillis, A. and Donoghue, P. (2007) 'The Homology and Phylogeny of Chondrichthyan Tooth Enameloid', *Journal of morphology*, 268, pp. 33–49.
- Gingerich and Schoeninger (1979) 'Patterns of tooth size variability in the dentition of primates', *American Journal of Physical Anthropology*, 51(3), pp. 457–465.
- Grabherr, M. G. *et al.* (2011) 'Full-length transcriptome assembly from RNA-Seq data without a reference genome.', *Nature biotechnology*, 29(7), pp. 644–52.
- Greco, V. *et al.* (2009) 'A Two-Step Mechanism for Stem Cell Activation during Hair Regeneration', *Cell Stem Cell*, 4(2), pp. 155–169.
- Greco, V. and Guo, S. (2010) 'Compartmentalized organization: a common and required feature of stem cell niches?', *Development*, 137(10), pp. 1586–1594.
- Guindon, S. and Gascuel, O. (2003) 'A simple, fast, and accurate algorithm to estimate large phylogenies by maximum likelihood.', *Systematic biology*, 52(5), pp. 696–704.
- Haegebarth, A. and Clevers, H. (2009) 'Wnt signaling, Lgr5, and stem cells in the intestine and skin', *American Journal of Pathology*, 174(3), pp. 715–721.



- Handrigan, G. R., Leung, K. J. and Richman, J. M. (2010) 'Identification of putative dental epithelial stem cells in a lizard with life-long tooth replacement.', *Development*, 137(21), pp. 3545–9.
- Handrigan, G. R. and Richman, J. M. (2010a) 'A network of Wnt, hedgehog and BMP signaling pathways regulates tooth replacement in snakes.', *Developmental biology*, 348(1), pp. 130–41.
- Handrigan, G. R. and Richman, J. M. (2010b) 'Autocrine and paracrine Shh signaling are necessary for tooth morphogenesis, but not tooth replacement in snakes and lizards (Squamata).', *Developmental biology*, 337(1), pp. 171–86.
- Harada, H. *et al.* (1999) 'Localization of putative stem cells in dental epithelium and their association with Notch and FGF signaling', *Journal of Cell Biology*, 147(1), pp. 105–120.
- Harada, H. *et al.* (2002) 'FGF10 maintains stem cell compartment in developing mouse incisors.', *Development*, 129(6), pp. 1533–41.
- Hardcastle, Z. *et al.* (1998) 'The Shh signalling pathway in tooth development: defects in Gli2 and Gli3 mutants.', *Development*, 125(15), pp. 2803–2811.
- Herzenberg, L. A., De Rosa, S. C. and Herzenberg, L. A. (2000) 'Monoclonal antibodies and the FACS: complementary tools for immunobiology and medicine', *Immunology Today*, 21(8), pp. 383–390.
- Van der heyden, C., Wautier, K. and Huyseune, a (2001) 'Tooth succession in the zebrafish (*Danio rerio*)', *Archives of Oral Biology*, 46(11), pp. 1051–1058.
- Holliday, J. A. and Stepan, S. J. (2004) 'Evolution of hypercarnivory: the effect of specialization on morphological and taxonomic diversity', *Paleobiology*, 30(1), pp. 108–128.
- Howe, K. *et al.* (2013) 'The zebrafish reference genome sequence and its relationship to the human genome', *Nature*, 496, p. 498.
- Huang, D. W., Sherman, B. T. and Lempicki, R. A. (2009) 'Bioinformatics enrichment tools: paths toward the comprehensive functional analysis of large gene lists', *Nucleic Acids Research*, 37(1), pp. 1–13.
- Huang, D. W., Sherman, B. T. and Lempicki, R. A. (2009) 'Systematic and integrative analysis of large gene lists using DAVID bioinformatics resources', *Nature Protocols*, 4(1), pp. 44–57.
- Huelsken, J. *et al.* (2001) ' $\beta$ -Catenin Controls Hair Follicle Morphogenesis and Stem Cell Differentiation in the Skin', *Cell*, 105(4), pp. 533–545.
- Huynh-Thu, V. A. *et al.* (2010) 'Inferring Regulatory Networks from Expression Data Using Tree-Based Methods', *PLoS ONE*, 5(9), p. e12776.

- Huysseune, A. and Thesleff, I. (2004) 'Continuous tooth replacement: the possible involvement of epithelial stem cells.', *BioEssays : news and reviews in molecular, cellular and developmental biology*, 26(6), pp. 665–71.
- IUCN (2018) *The IUCN Red List of Threatened Species. Version 2018-1*.
- Jansen, S. R. *et al.* (2015) 'Prostaglandin E2 promotes MYCN non-amplified neuroblastoma cell survival via  $\beta$ -catenin stabilization', *Journal of Cellular and Molecular Medicine*, 19(1), pp. 210–226.
- Jarvinen, E. *et al.* (2006) 'Continuous tooth generation in mouse is induced by activated epithelial Wnt/beta-catenin signaling', *Proceedings of the National Academy of Sciences*, 103(49), pp. 18627–18632.
- Järvinen, E. *et al.* (2018) 'Mesenchymal Wnt/ $\beta$ -catenin signaling limits tooth number', *Development*, p. dev.158048.
- Järvinen, E., Tummers, M. and Thesleff, I. (2009) 'The role of the dental lamina in mammalian tooth replacement.', *Journal of experimental zoology. Part B, Molecular and developmental evolution*, 312B(4), pp. 281–91.
- Jeffery, W. R. (2005) 'Adaptive Evolution of Eye Degeneration in the Mexican Blind Cavefish', *Journal of Heredity*, 96(3), pp. 185–196.
- Jernvall, J. *et al.* (1994) 'Evidence for the role of the enamel knot as a control center in mammalian tooth cusp formation: Non-dividing cells express growth stimulating Fgf-4 gene', *International Journal of Developmental Biology*, 38(3), pp. 463–469.
- Jernvall, J. *et al.* (1998) 'The life history of an embryonic signaling center: BMP-4 induces p21 and is associated with apoptosis in the mouse tooth enamel knot.', *Development*, 125(2), pp. 161–169.
- Jernvall, J., Keranen, S. V. E. and Thesleff, I. (2000) 'Evolutionary modification of development in mammalian teeth: Quantifying gene expression patterns and topography', *Proceedings of the National Academy of Sciences*, 97(26), pp. 14444–14448.
- Jernvall, J. and Thesleff, I. (2012) 'Tooth shape formation and tooth renewal: evolving with the same signals', *Development*, 139(19), pp. 3487–3497.
- Jheon, A. H. *et al.* (2016) 'Inhibition of Notch Signaling during Mouse Incisor Renewal Leads to Enamel Defects', *Journal of Bone and Mineral Research*, 31(1), pp. 152–162.
- Jho, E. -h. *et al.* (2002) 'Wnt/  $\beta$ -Catenin/Tcf Signaling Induces the Transcription of Axin2, a Negative Regulator of the Signaling Pathway', *Molecular and Cellular Biology*, 22(4), pp. 1172–1183.
- Jia, S. *et al.* (2016) 'Bmp4-Msx1 signaling and Osr2 control tooth organogenesis through antagonistic regulation of secreted Wnt antagonists', *Developmental Biology*, 420(1), pp. 110–119.

- Jussila, M., Crespo Yanez, X. and Thesleff, I. (2014) 'Initiation of teeth from the dental lamina in the ferret', *Differentiation*, 87(1–2), pp. 32–43.
- Jussila, M. and Thesleff, I. (2012) 'Signaling networks regulating tooth organogenesis and regeneration, and the specification of dental mesenchymal and epithelial cell lineages.', *Cold Spring Harbor perspectives in biology*, 4(4), p. a008425.
- Juuri, E. *et al.* (2012) 'Sox2+ stem cells contribute to all epithelial lineages of the tooth via Sfrp5+ progenitors.', *Developmental cell*, 23(2), pp. 317–28.
- Juuri, E. *et al.* (2013) 'Sox2 marks epithelial competence to generate teeth in mammals and reptiles.', *Development*, 140(7), pp. 1424–1432.
- Keränen, S. V. E. *et al.* (1999) 'Gene expression patterns associated with suppression of odontogenesis in mouse and vole diastema regions', *Development Genes and Evolution*, 209(8), pp. 495–506.
- Kettunen, P. *et al.* (2000) 'Associations of FGF-3 and FGF-10 with signaling networks regulating tooth morphogenesis', *Developmental Dynamics*, 219(3), pp. 322–332.
- Kettunen, P., Karavanova, I. and Thesleff, I. (1998) 'Responsiveness of developing dental tissues to fibroblast growth factors: Expression of splicing alternatives of FGFR1, -2, -3, and of FGFR4; and stimulation of cell proliferation by FGF-2, -4, -8, and -9', *Developmental Genetics*, 22(4), pp. 374–385.
- Kielan-Jaworowska, Z., Cifelli, R. L. and Luo, Z. X. (2004) 'Mammals from the Age of Dinosaurs. Origins, Evolution and Structure', *New York: Columbia University Press*.
- Klingenberg, C. P. (2016) 'Size, shape, and form: concepts of allometry in geometric morphometrics', *Development Genes and Evolution*, pp. 113–137.
- Knoepfler, P., Cheng, P. F. and Eisenman, R. N. (2002) 'N-myc is essential during neurogenesis for the rapid expansion of progenitor cell populations and the inhibition of neuronal differentiation', *Genes and Development*, 16(20), pp. 2699–712.
- Koepfli, K.-P., Paten, B. and O'Brien, S. J. (2015) 'The Genome 10K Project: A Way Forward', *Annual Review of Animal Biosciences*, 3(1), pp. 57–111.
- Komiya, Y. and Habas, R. (2008) 'Wnt signal transduction pathways', *Organogenesis*, 4(2), pp. 68–75.
- Kratochwil, K. *et al.* (2002) 'FGF4, a direct target of LEF1 and Wnt signaling, can rescue the arrest of tooth organogenesis in Lef1(-/-) mice.', *Genes & development*, 16(24), pp. 3173–85.
- Le, S. Q. and Gascuel, O. (2008) 'An Improved General Amino Acid Replacement Matrix', *Molecular Biology and Evolution*, 25(7), pp. 1307–1320.
- Lee, M. J. *et al.* (2016) 'Sox2 contributes to tooth development via Wnt signaling', *Cell and Tissue Research*, pp. 1–8.

- Lethbridge, R. C. and Potter, I. C. (1981) 'The Development of Teeth and Associated Feeding Structures During the Metamorphosis of the Lamprey, *Geotria australis*', *Acta Zoologica*, 62(4), pp. 201–214.
- Li, Y. H. *et al.* (2010) 'Progranulin A-mediated MET signaling is essential for liver morphogenesis in zebrafish', *Journal of Biological Chemistry*, 285(52), pp. 41001–41009.
- Lin, C. *et al.* (2017) 'YAP is essential for mechanical force production and epithelial cell proliferation during lung branching morphogenesis', *eLife*, 6, p. e21130.
- Lin, C. M. *et al.* (2006) 'Molecular signaling in feather morphogenesis', *Current Opinion in Cell Biology*, 18(6), pp. 730–741.
- Lin, C. R. *et al.* (1999) 'Pitx2 regulates lung asymmetry, cardiac positioning and pituitary and tooth morphogenesis.', *Nature*, 401(6750), pp. 279–282.
- Lin, S.-J. *et al.* (2013) 'Feather regeneration as a model for organogenesis', *Development, growth and differentiation*, 55(1), pp. 139–148.
- Liu, F. *et al.* (2008) 'Wnt/beta-catenin signaling directs multiple stages of tooth morphogenesis.', *Developmental biology*, 313(1), pp. 210–24.
- Liu, F. *et al.* (2016) 'Inference of Gene Regulatory Network Based on Local Bayesian Networks.', *PLoS computational biology*, 12(8), p. e1005024.
- Liu, L. *et al.* (2012) 'Na<sup>+</sup>/H<sup>+</sup>exchanger regulatory factor 1 (NHERF1) directly regulates osteogenesis', *Journal of Biological Chemistry*, 287(52), pp. 43312–43321.
- Livak, K. J. and Schmittgen, T. D. (2001) 'Analysis of Relative Gene Expression Data Using Real-Time Quantitative PCR and the 2<sup>-</sup> $\Delta\Delta$ CT Method', *Methods*, 25(4), pp. 402–408.
- Logan, C. Y. and Nusse, R. (2004) 'The Wnt signaling pathway in development and disease.', *Annual review of cell and developmental biology*, 20, pp. 781–810.
- Maderson, P. F. A. 197. (1972) 'When? Why? and How? Some Speculations on the Evolution of the Vertebrate Integument', *Source: American Zoologist*, 12(1)(1), pp. 159–171.
- Madison, B. B. *et al.* (2009) 'FoxF1 and FoxL1 link Hedgehog signaling and the control of epithelial proliferation in the developing stomach and intestine', *Journal of Biological Chemistry*, 284(9), pp. 5936–5944.
- Mansukhani, A. *et al.* (2005) 'Sox2 induction by FGF and FGFR2 activating mutations inhibits Wnt signaling and osteoblast differentiation.', *The Journal of cell biology*, 168(7), pp. 1065–76.
- Mao, A. S. and Mooney, D. J. (2015) 'Regenerative medicine: Current therapies and future directions', *Proceedings of the National Academy of Sciences*, 112(47), pp.

14452–14459.

Marcus, M. A. *et al.* (2017) ‘Parrotfish Teeth: Stiff Biominerals Whose Microstructure Makes Them Tough and Abrasion-Resistant to Bite Stony Corals’, *ACS Nano*, 11(12), pp. 11856–11865.

Margolin, A. A. *et al.* (2006) ‘ARACNE: An Algorithm for the Reconstruction of Gene Regulatory Networks in a Mammalian Cellular Context’, *BMC Bioinformatics*, 7(Suppl 1), p. S7.

Martin, K. J. *et al.* (2016) ‘Sox2+ progenitors in sharks link taste development with the evolution of regenerative teeth from denticles’, *Proceedings of the National Academy of Sciences*, 113(51), pp. 14769–14774.

Massagué, J. (2012) ‘TGF $\beta$  signalling in context’, *Nature Reviews Molecular Cell Biology*, 13(10), pp. 616–630.

Matalova, E. *et al.* (2006) ‘Molar tooth development in caspase-3 deficient mice’, *International Journal of Developmental Biology*, 50(5), pp. 491–497.

Meyer, A. and Schartl, M. (1999) ‘Gene and genome duplications in vertebrates: the one-to-four (-to-eight in fish) rule and the evolution of novel gene functions’, *Current Opinion in Cell Biology*, 11(6), pp. 699–704.

Mitsiadis, T. a *et al.* (2010) ‘BMPs and FGFs target Notch signalling via jagged 2 to regulate tooth morphogenesis and cytodifferentiation.’, *Development (Cambridge, England)*, 137(18), pp. 3025–35.

Mitsiadis, T. a, Regaudiat, L. and Gridley, T. (2005) ‘Role of the Notch signalling pathway in tooth morphogenesis.’, *Archives of oral biology*, 50(2), pp. 137–40.

Moustakas, J. E., Smith, K. K. and Hlusko, L. J. (2011) ‘Evolution and development of the mammalian dentition: insights from the marsupial *Monodelphis domestica*.’, *Developmental dynamics : an official publication of the American Association of Anatomists*, 240(1), pp. 232–9.

Munne, P. M. *et al.* (2010) ‘Splitting placodes: effects of bone morphogenetic protein and Activin on the patterning and identity of mouse incisors.’, *Evolution & development*, 12(4), pp. 383–392.

Murdock, D. J. E. *et al.* (2013) ‘The origin of conodonts and of vertebrate mineralized skeletons.’, *Nature*, 502(7472).

Musser, J. M., Wagner, G. P. and Prum, R. O. (2015) ‘Nuclear  $\beta$ -catenin localization supports homology of feathers, avian scutate scales, and alligator scales in early development’, *Evolution & Development*, 17(3), pp. 185–194.

Ohe, S. *et al.* (2015) ‘Maintenance of sweat glands by stem cells located in the acral epithelium’, *Biochemical and Biophysical Research Communications*, 466, pp. 333–338.

Okubo, T., Pevny, L. H. and Hogan, B. L. M. (2006) 'Sox2 is required for development of taste bud sensory cells', *Genes and Development*, 20(19), pp. 2654–2659.

Owen, R. (no date) *Odontography*. London, Hippolyte Bailliere.

Paus, R. and Cotsarelis, G. (1999) 'The Biology of Hair Follicles', *N Engl J Med*, 341(7), pp. 491–497.

Pearson, B. J. and Alvarado, A. S. (2008) 'Regeneration, stem cells, and the evolution of tumor suppression.', *Cold Spring Harbor symposia on quantitative biology*, 73, pp. 565–572.

Perez, S. I., Bernal, V. and Gonzalez, P. N. (2006) 'Differences between sliding semi-landmark methods in geometric morphometrics, with an application to human craniofacial and dental variation', *Journal of Anatomy*, 208(6), pp. 769–784.

Pispa, J. and Thesleff, I. (2003) 'Mechanisms of ectodermal organogenesis', *Developmental Biology*, 262, pp. 195–205.

Plikus, M. V. *et al.* (2008) 'Cyclic dermal BMP signalling regulates stem cell activation during hair regeneration', *Nature*, 451(7176), pp. 340–344.

Pokholkova, G. V *et al.* (2018) 'Tethering of CHROMATOR and dCTCF proteins results in decompaction of condensed bands in the *Drosophila melanogaster* polytene chromosomes but does not affect their transcription and replication timing', *PLOS ONE*, 13(4), p. e0192634.

Price, S. a *et al.* (2010) 'Functional innovations and morphological diversification in parrotfish.', *Evolution; international journal of organic evolution*, 64(10), pp. 3057–68.

Purnell, M. A. (1995) 'Microwear on conodont elements and macrophagy in the first vertebrates', *Nature*, 374(6525), pp. 798–800.

Rasch, L. J. *et al.* (2016) 'An ancient dental gene set governs development and continuous regeneration of teeth in sharks', *Developmental Biology*, 415(2), pp. 347–370.

Ratajczak, M. *et al.* (2012) 'Pluripotent and multipotent stem cells in adult tissues', *Advances in Medical Sciences*, 57(1), pp. 1–17.

Reif, W.-E. (1978) 'Wound healing in Sharks', *Zoomorphologie*, 90(2), pp. 101–111.

Reif, W. -E (1980) 'Development of dentition and dermal skeleton in embryonic *Scyliorhinus canicula*', *Journal of Morphology*, 166(3), pp. 275–288.

Renvoisé, E. and Michon, F. (2014) 'An Evo-Devo perspective on ever-growing teeth in mammals and dental stem cell maintenance', *Frontiers in Physiology*, 5(5).

Richman, J. M. and Handrigan, G. R. (2011) 'Reptilian tooth development.', *Genesis*, 49(4), pp. 247–60.

- Riddle, R. D. *et al.* (1993) 'Sonic hedgehog mediates the polarizing activity of the ZPA', *Cell*, 75(7), pp. 1401–1416.
- Ring, D. B. *et al.* (2003) 'Selective Glycogen Synthase Kinase 3 Inhibitors Potentiate Insulin Activation of Glucose Transport and Utilization In Vitro and In Vivo', *Diabetes*, 52(3), p. 588 LP-595.
- Robinson, M. D., McCarthy, D. J. and Smyth, G. K. (2009) 'edgeR: A Bioconductor package for differential expression analysis of digital gene expression data', *Bioinformatics*, 26(1), pp. 139–140.
- Robinson, M. D. and Oshlack, A. (2010) 'A scaling normalization method for differential expression analysis of RNA-seq data', *Genome Biology*, 11(3), p. R25.
- Rohlf (2009a) 'tpsDig'.
- Rohlf (2009b) 'tpsUtil'.
- Salazar-Ciudad, I. (2012) 'Tooth patterning and evolution.', *Current opinion in genetics & development*, 22(6), pp. 585–92.
- Salazar-Ciudad, I. and Jernvall, J. (2010) 'A computational model of teeth and the developmental origins of morphological variation', *Nature*, 464(7288), pp. 583–586.
- Sansom, I. J. *et al.* (1992) 'Presence of the earliest vertebrate hard tissues in conodonts', *Science*, 256(5061), pp. 1308–1311.
- Santini, F., Sorenson, L. and Alfaro, M. E. (2013) 'A new phylogeny of tetraodontiform fishes (Tetraodontiformes, Acanthomorpha) based on 22 loci', *Molecular Phylogenetics and Evolution*, 69(1), pp. 177–187.
- Sarkar, L. *et al.* (2000) 'Wnt/Shh interactions regulate ectodermal boundary formation during mammalian tooth development', *Proceedings of the National Academy of Sciences*, 97(9), pp. 4520–4524.
- Sarkar, L. and Sharpe, P. T. (1999) 'Expression of Wnt signalling pathway genes during tooth development', *Mechanisms of Development*, 85(1–2), pp. 197–200.
- Sasaki, T. *et al.* (2005) 'LEF1 is a critical epithelial survival factor during tooth morphogenesis', *Developmental Biology*, 278(1), pp. 130–143.
- Schartl, M. (2014) 'Beyond the zebrafish: diverse fish species for modeling human disease.', *Disease models & mechanisms*, 7(2), pp. 181–92.
- Seetah, K. *et al.* (2014) 'A geometric morphometric re-evaluation of the use of dental form to explore differences in horse ( *Equus caballus* ) populations and its potential zooarchaeological application', *Journal of Archaeological Science*, 41, pp. 904–910.
- Seidel, K. *et al.* (2017) 'Resolving stem and progenitor cells in the adult mouse incisor through gene coexpression analysis', *eLife*, 6.

- Semina, E. V *et al.* (1998) 'A novel homeobox gene PITX3 is mutated in families with autosomal- dominant cataracts and ASMD', *Nature Genetics*, 19(2), pp. 167–170.
- Sire, J.-Y. *et al.* (2002) 'First-generation teeth in nonmammalian lineages: evidence for a conserved ancestral character?', *Microscopy research and technique*, 59(5), pp. 408–34.
- Smith *et al.* (2009) 'Reiterative pattern of sonic hedgehog expression in the catshark dentition reveals a phylogenetic template for jawed vertebrates.', *Proceedings. Biological sciences / The Royal Society*, 276(1660), pp. 1225–33.
- Smith, M. *et al.* (2018) 'Development and evolution of tooth renewal in neoselachian sharks as a model for transformation in chondrichthyan dentitions', *Journal of Anatomy*, 232(6), pp. 891–907.
- Smith, M. M. *et al.* (2013) 'Pattern formation in development of chondrichthyan dentitions: A review of an evolutionary model', *Historical Biology*, 25(2), pp. 127–142.
- Smith, M. M. and Coates, M. I. (1998) 'Evolutionary origins of the vertebrate dentition: phylogenetic patterns and developmental evolution', *European Journal of Oral Sciences*, 106(S1), pp. 482–500.
- Smith, M. M., Fraser, G. J. and Mitsiadis, T. a (2009) 'Dental lamina as source of odontogenic stem cells: evolutionary origins and developmental control of tooth generation in gnathostomes.', *Journal of experimental zoology. Part B, Molecular and developmental evolution*, 312B(4), pp. 260–80.
- Soukup, V. *et al.* (2008) 'Dual epithelial origin of vertebrate oral teeth', *Nature*, 455(7214), pp. 795–798.
- St.amand, T. R. *et al.* (2000) 'Antagonistic signals between BMP4 and FGF8 define the expression of Pitx1 and Pitx2 in mouse tooth-forming anlage', *Developmental Biology*, 217(2), pp. 323–332.
- Stocum, D. L. (1984) 'The urodele limb regeneration blastema: Determination and organization of the morphogenetic field', *Differentiation*, pp. 13–28.
- Streelman, T. and Albertson, R. C. (2006) 'Evolution of Novelty in the Cichlid Dentition', *Journal of experimental zoology. Part B, Molecular and developmental evolution*, 306B, pp. 216–226.
- Sumigray, K. D., Terwilliger, M. and Lechler, T. (2018) 'Morphogenesis and Compartmentalization of the Intestinal Crypt', *Developmental Cell*, 45(2), p. 183–197.e5.
- Sun, N. *et al.* (2017) 'Inhibitory effect of dexamethasone on residual Lewis lung cancer cells in mice following palliative surgery', *Oncology Letters*, 13(1), pp. 356–362.
- Suomalainen, M. and Thesleff, I. (2010) 'Patterns of Wnt pathway activity in the mouse incisor indicate absence of Wnt/beta-catenin signaling in the epithelial stem cells.',



*Developmental dynamics : an official publication of the American Association of Anatomists*, 239(1), pp. 364–72.

Sylwestrak, E. L. *et al.* (2016) ‘Multiplexed Intact-Tissue Transcriptional Analysis at Cellular Resolution’, *Cell*, 164(4), pp. 792–804.

Szemes, M. *et al.* (2018) ‘Wnt Signalling Drives Context-Dependent Differentiation or Proliferation in Neuroblastoma’, *Neoplasia*, 20(4), pp. 335–350.

Tanaka, M. *et al.* (2005) ‘Developmental genetic basis for the evolution of pelvic fin loss in the pufferfish *Takifugu rubripes*’, *Developmental Biology*, 281(2), pp. 227–239.

Thesleff, I. (2003) ‘Epithelial-mesenchymal signalling regulating tooth morphogenesis.’, *Journal of cell science*, 116(Pt 9), pp. 1647–8.

Thesleff, I. (2009) ‘Tooth organogenesis and regeneration’, *StemBook*, pp. 1–12.

Thesleff, I., Keranen, S. and Jernvall, J. (2001) ‘Enamel Knots as Signaling Centers Linking Tooth Morphogenesis and Odontoblast Differentiation’, *Advances in Dental Research*, 15(1), pp. 14–18.

Thesleff, I. and Sharpe, P. (1997) ‘Signalling networks regulating dental development’, *Mechanisms of Development*, 67(2), pp. 111–123.

Thesleff, I., Vaahtokari, A. and Partanen, A. M. (1995) ‘Regulation of organogenesis. Common molecular mechanisms regulating the development of teeth and other organs.’, *The International journal of developmental biology*, 39(1), pp. 35–50.

Thiery, A. P. *et al.* (2017) ‘Spatially restricted dental regeneration drives pufferfish beak development’, *Proceedings of the National Academy of Sciences*, 114(22), pp. E4425–E4434.

Ting-Berrett, S. A. and Chuong, C. M. (1996) ‘Sonic hedgehog in feather morphogenesis: Induction of mesenchymal condensation and association with cell death’, *Developmental Dynamics*, 207(2), pp. 157–170.

Trapani, J. (2001) ‘Position of Developing Replacement Teeth in Teleosts’, *Copeia*, 2001(1), pp. 35–51.

Tsonis, P. A. (2000) ‘Regeneration in vertebrates’, *Developmental Biology*, pp. 273–284.

Tucker, A. S. *et al.* (1998) ‘Transformation of Tooth Type Induced by Inhibition of BMP Signaling’, *Developmental Dynamics*, 234(5391), pp. 1136–1138.

Tucker, A. S. *et al.* (2004) ‘The activation level of the TNF family receptor, Edar, determines cusp number and tooth number during tooth development’, *Developmental Biology*, 268(1), pp. 185–194.

Tucker, A. S. and Fraser, G. J. (2014) ‘Evolution and developmental diversity of tooth

- regeneration.’, *Seminars in cell & developmental biology*, 25–26, pp. 71–80.
- Tucker, A. and Sharpe, P. (2004) ‘The cutting-edge of mammalian development; how the embryo makes teeth.’, *Nature reviews. Genetics*, 5(7), pp. 499–508.
- Turingan, R. G. (1994) ‘Ecomorphological relationships among Caribbean tetraodontiform fishes’, *Journal of Zoology*, 233(3), pp. 493–521.
- Turner, S. *et al.* (2010) ‘False teeth: conodont-vertebrate phylogenetic relationships revisited’, *Geodiversitas*, 32(4), pp. 545–595.
- Tyler, J. C. (1980) *Osteology, phylogeny, and higher classification of the fishes of the order Plectognathi (Tetraodontiformes)*. Washington DC, U.S. Dept. of Commerce, National Oceanic and Atmospheric Administration, National Marine Fisheries Service.
- Uchibe, K. *et al.* (2012) ‘Identification of Novel Transcription-Regulating Genes Expressed During Murine Molar Development’, *Developmental Dynamics*, 241, pp. 1217–1226.
- Underwood, C. J. *et al.* (2015) ‘Development and Evolution of Dentition Pattern and Tooth Order in the Skates And Rays (Batoidea; Chondrichthyes)’, *PLOS ONE*, 10(4), p. e0122553.
- Vahtokari, A. *et al.* (1996) ‘The enamel knot as a signaling center in the developing mouse tooth’, *Mechanisms of Development*, 54(1), pp. 39–43.
- Vainio, S. *et al.* (1993) ‘Identification of BMP-4 as a signal mediating secondary induction between epithelial and mesenchymal tissues during early tooth development’, *Cell*, 75(1), pp. 45–58.
- Van Valkenburgh, B. (1989) ‘Carnivore Dental Adaptations and Diet: A Study of Trophic Diversity within Guilds’, *Carnivore Behavior, Ecology, and Evolution*, pp. 410–436.
- Vandenplas, S. *et al.* (2016) ‘Slow cycling cells in the continuous dental lamina of *Scyliorhinus canicula*: new evidence for stem cells in sharks’, *Developmental Biology*, pp. 1–11.
- Vivien, C. J., Hudson, J. E. and Porrello, E. R. (2016) ‘Evolution, comparative biology and ontogeny of vertebrate heart regeneration’, *npj Regenerative Medicine*, 1(1), p. 16012.
- Waddell, P. J. and Steel, M. A. (1997) ‘General Time-Reversible Distances with Unequal Rates across Sites: Mixing  $\Gamma$  and Inverse Gaussian Distributions with Invariant Sites’, *Molecular Phylogenetics and Evolution*, 8(3), pp. 398–414.
- Wagman, A., Johnson, K. and Bussiere, D. (2004) ‘Discovery and Development of GSK3 Inhibitors for the Treatment of Type 2 Diabetes’, *Current Pharmaceutical Design*, 10(10), pp. 1105–1137.

Wagner, G. P. and Lynch, V. J. (2010) 'Evolutionary novelties.', *Current biology : CB*, 20(2), pp. R48-52.

Wang, X.-P. *et al.* (2009) 'Apc inhibition of Wnt signaling regulates supernumerary tooth formation during embryogenesis and throughout adulthood.', *Development (Cambridge, England)*, 136(11), pp. 1939-49.

Wang, X.-P. and Fan, J. (2011) 'Molecular genetics of supernumerary tooth formation.', *Genesis*, 49(4), pp. 261-77.

Weeks, O., Bhullar, B.-A. S. and Abzhanov, A. (2013) 'Molecular characterization of dental development in a toothed archosaur, the American alligator *Alligator mississippiensis*', *Evolution & Development*, 15(6), pp. 393-405.

Whitenack, L. B. and Gottfried, M. D. (2010) 'Journal of Vertebrate Paleontology', *Journal of Vertebrate Paleontology*, 30(1), pp. 17-25.

Willert, K. and Nusse, R. (1998) 'β-catenin: a key mediator of Wnt signaling', *Current Opinion in Genetics & Development*, 8(1), pp. 95-102.

Wu, P. *et al.* (2004) 'Evo-Devo of amniote integuments and appendages.', *The International journal of developmental biology*, 48(2-3), pp. 249-70.

Wu, P. *et al.* (2013) 'Specialized stem cell niche enables repetitive renewal of alligator teeth.', *Proceedings of the National Academy of Sciences of the United States of America*, 110(22), pp. E2009-18.

Wu, P., Alibardi, L. and Chuong, C.-M. (2014) 'Regeneration of reptilian scales after wounding: neogenesis, regional difference, and molecular modules', *Regeneration*, 1(1), pp. 15-26.

Wu, X. *et al.* (2017) 'Spatiotemporal expression of Wnt/β-catenin signaling during morphogenesis and odontogenesis of deciduous molar in miniature pig', *International Journal of Biological Sciences*, 13(8), pp. 1082-1091.

Xavier, G. M. *et al.* (2015) 'Activated WNT signaling in postnatal SOX2-positive dental stem cells can drive odontoma formation', *Scientific Reports*, 5(April), p. 14479.

Xu, X. *et al.* (2003) 'Developmental expression of Smad1-7 suggests critical function of TGF-β/BMP signaling in regulating epithelial-mesenchymal interaction during tooth morphogenesis', *International Journal of Developmental Biology*, 47(1), pp. 31-39.

Yamanoue, Y. *et al.* (2008) 'A new perspective on phylogeny and evolution of tetraodontiform fishes (Pisces: Acanthopterygii) based on whole mitochondrial genome sequences: basal ecological diversification?', *BMC evolutionary biology*, 8(1), p. 212.

Yang, C. C. and Cotsarelis, G. (2010) 'Review of hair follicle dermal cells', *Journal of Dermatological Science*, pp. 2-11.

Yergeau, D. A. *et al.* (2005) 'bloodthirsty, an RBCC/TRIM gene required for

erythropoiesis in zebrafish', *Developmental Biology*, 283(1), pp. 97–112.

Yue, Z. *et al.* (2005) 'Mapping stem cell activities in the feather follicle', *Nature*, 438(7070), pp. 1026–1029.

Zahradnicek, O. *et al.* (2014) 'The development of complex tooth shape in reptiles', *Frontiers in Physiology*, pp. 1–7.

Zahradnicek, O., Horacek, I. and Tucker, A. S. (2008) 'Viperous fangs: Development and evolution of the venom canal', *Mechanisms of Development*, 125(9–10), pp. 786–796.

Zhang, J. T. *et al.* (2016) 'MycN Is critical for the maintenance of human embryonic stem cell-derived neural crest stem cells', *PLoS ONE*, 11(1), pp. 1–14.

Zhang, X. *et al.* (2013) 'NARROMI: A noise and redundancy reduction technique improves accuracy of gene regulatory network inference', *Bioinformatics*, 29(1), pp. 106–113.

Zhang, Y. D. *et al.* (2005) 'Making a tooth: growth factors, transcription factors, and stem cells.', *Cell research*, 15(5), pp. 301–16.

Zhou, B. *et al.* (2012) 'Interactions between  $\beta$ -catenin and transforming growth factor- $\beta$  signaling pathways mediate epithelial- mesenchymal transition and are dependent on the transcriptional co-activator cAMP-response element-binding protein (CREB)-binding protein (CBP)', *Journal of Biological Chemistry*, 287(10), pp. 7026–7038.

Zuo, Y. *et al.* (2017) 'Incorporating prior biological knowledge for network-based differential gene expression analysis using differentially weighted graphical LASSO', *BMC Bioinformatics*, 18(1), p. 99.